Bulletin of Natural Sciences Research

Vol. 14, N° 1-2, 2024.

BULLETIN OF NATURAL SCIENCES RESEARCH

Vol. 14, Nº 1-2, 2024.

CONTENTS

EVALUATING THE INFLUENCE OF TRYPANOSOMIASIS ON MURINE MODEL USING *Corchorus olitorius* LEAF EXTRACT AS A TRYPANOCIDAL AGENT

FATIMA M. MADAKI[1], ADAMU Y. KABIRU[1], OGUNROMBI D. CLINTON[1], SAKARIYAU A. WAHEED[2*], YUNUSA O. IBRAHIM[1]

[1]Department of Biochemistry, Faculty of Life Sciences, Federal University of Technology, Minna, Bosso, Nigeria
[2]Department of Chemistry and Biochemistry, College of Science, Old Dominion University, Norfolk, USA

ABSTRACT

Trypanosomiasis, a parasitic disease caused by trypanosomes, which are flagellate protozoa transmitted through the bite of the tsetse fly, manifests with symptoms including substantial weight loss, anemia, fever, edema, adenitis, dermatitis, and nervous disorders. This research investigated the impact of trypanosomiasis on a murine model while utilizing *Corchorus olitorius* leaf extract as a potential trypanocidal agent. An acute toxicity analysis was conducted following Lorke's method, and the antitrypanosomal efficacy was assessed in rats at doses of 100, 200, and 400 mg/kg over three weeks, monitoring changes in parasitemia count, body weight, and hematological parameters. Additionally, lipid profile, electrolyte concentration, and liver and kidney function were evaluated using standard techniques. The extract demonstrated potent antitrypanosomal activity at 400 mg/kg, significantly reducing the parasitemia count to 11.33±4.16 count/mL compared to the positive control at 2.5 mg/kg body weight doses. Furthermore, the 400 mg/kg dose notably increased packed cell volume and body weight in infected rats. Moreover, there were no significant discrepancies in numerous hematological parameters between the infected treated with diminazene aceturate and the extract's 400 mg/kg body weight. This study suggests that *Corchorus olitorius* extract exhibits significant antitrypanosomal, antilipidemic, and erythropoietic effects, mitigating parasitemia count, lipid levels, and oxidative damage by impeding the biochemical activities of trypanosomes through its active constituents. Thus, *Corchorus olitorius* extract may offer an alternative therapeutic approach for managing trypanosomal infections.

Keywords: *Corchorus olitorius*, Parasite, Phytochemical Analysis, *Trypanosoma brucei*, Trypanosomiasis.

INTRODUCTION

Trypanosomiasis, a persistent parasitic disease affecting both humans and animals (Mirshekar et al., 2019), stems from *Trypanosoma brucei*, a flagellate protozoan species within the *Trypanosomatidae* family and *Trypanosoma* genus (Sobhy et al., 2017; Ereqat et al., 2020). This single-celled parasite, transmitted by tsetse flies, is the causative agent of Human African Trypanosomiasis (HAT) (de Sousa et al., 2021). Globally, trypanosomiasis is prevalent in underprivileged and rural regions of sub-Saharan Africa, resulting in significant global losses and posing fatal risks if left undiagnosed and untreated (Ereqat et al., 2020). Manifesting through pronounced weight loss, intermittent fever, anemia, frequent diarrhea, adenitis, dermatitis, nervous disorders, and deteriorating health conditions, trypanosomiasis encompasses various diseases that often culminate in death (Field et al., 2017; Alanazi et al., 2018). Several ongoing studies are focused on the development of vaccines against Human African trypanosomiasis. Presently, chemotherapeutic agents like diminazene aceturate and isoethamidium chloride serve as common trypanocidal drugs for both preventive and curative purposes (WHO, 1998). Despite extensive disease control and prevention research, challenges such as inadequate clinical efficacy, drug toxicity, and resistance hinder progress (Fathabad et al., 2018). Trypanosomiasis compromises the immune system, rendering hosts incapable of eliminating the parasite (trypanosome) even after administering antitrypanosomal drugs (Zhou et al., 2017). Regrettably, these parasites have developed resistance to conventional treatment medications, underscoring the urgent need to explore highly effective and non-toxic remedies sourced from medicinal plants (Gao et al., 2019).

Corchorus olitorius, commonly known as 'Ewedu' in the Yoruba language, is a plant species belonging to the *Tiliaceae* family (Nasreen et al., 2022). This annual herb is valued for both its culinary and medicinal uses, with its leaves and roots being utilized in herbal medicine and consumed as vegetables (Becer et al., 2020). It is indigenous to regions such as East Malaysia, India, Egypt, and the Philippines, as well as various West African countries, notably Ghana, Nigeria, and Sierra Leone (Matsufuji et al., 2001). The leaves of *Corchorus olitorius* are particularly notable for their high antioxidant content, which has been documented to enhance metabolic and

---

* Corresponding author: waheedsackson@gmail.com
BIOLOGY

physiological processes within the human body (Airaodion et al., 2019). Additionally, they contain a diverse array of phytoconstituents, including flavonoids, phenols, fatty acids, minerals, vitamins, and mucilaginous polysaccharides, suggesting potential benefits such as anti-inflammatory, antimicrobial, antiplasmodial, and antitrypanosomal properties (Nasreen et al., 2022; Ogungbemi et al., 2019). Despite its various biological and medicinal attributes, research concerning its trypanocidal effects remains insufficient. Hence, this study aims to explore the antitrypanosomal activity of extracts derived from *Corchorus olitorius* against *Trypanosoma brucei* in male Wistar rats.

EXPERIMENTAL

Materials and methods

Chemicals

The chemicals used in this study are of analytical grade with 96% purity of the solvents.

Collection of plant materials

The fresh leaves of *Corchorus olitorius* were gathered from Kure Market in Minna, Nigeria, and subsequently verified and authenticated at the herbarium division of the Department of Biological Sciences, Federal University of Technology, Minna, Niger State, Nigeria.

Experimental animals

The experiment involved using thirty male Wistar rats weighing between 100-120 g. Male rats were used due to hormonal differences in female rats which might disrupt some of the biochemical parameters. These rats were sourced from the animal farm at the University of Jos in Plateau State, Nigeria. Upon acquisition, they underwent a two-week acclimatization period during which they were housed in well-ventilated plastic cages and provided with rat chow and water ad libitum. All procedures involving the animals adhered to stringent care protocols by established standards. The experimental protocols were conducted with utmost care, following established guidelines outlined in the Current Animal Care Regulations and Standards as approved by the Institute for Laboratory Animal Research (Guide for Care and Use of Laboratory Animals in Biomedical and Behavioral Research).

Trypanosome parasite

The *Trypanosoma brucei* parasite strain was procured from the National Institute for Research in Kaduna, Kaduna State, Nigeria, and then consistently preserved through asynchronous transfer within experimental rats in the Animal Housing Unit of the Department of Biochemistry.

Plant processing and extraction

The fresh leaves of *Corchorus olitorius* were detached from the stems, washed with distilled water, and subsequently air-dried to a consistent weight over seven (7) days at room temperature in the laboratory. Following this, the dried leaves were meticulously ground into a fine powder using an electric blender and then stored in an airtight container until the extraction process commenced (Gupta et al., 2015).

Preparation of Corchorus olitorius extract

The cold maceration extraction technique was employed to extract the plant sample. About 200 grams of the ground *Corchorus olitorius* sample were accurately weighed and immersed in 1600 mL of methanol (James & Dubery, 2011). The mixture was then placed in shade for 72 hours, undergoing constant agitation using a water bath shaker at the temperature of 37 degrees. Following this period, it was filtered using Whatman filter paper, with the resulting filtrate collected in a beaker. Subsequently, the water content was allowed to evaporate over a water bath (37 degrees), resulting in the concentration of the extract, as detailed by Abubakar & Haque, (2020).

Preparation of parasite

The *Trypanosoma brucei* parasite was sustained through asynchronous transfer within Wistar rats until required for experimentation. Blood samples were collected from the tail of a heavily infected rat using an EDTA-coated insulin syringe. Subsequently, 0.2 mL of blood from the infected Wistar rats was dissolved in 20 mL of 0.98% NaCl solution, and the resulting mixture was injected into healthy rats (Madaki et al., 2022).

Phytochemical Analysis

Preliminary quantitative phytochemical analysis of the *Corchorus olitorius* extract was conducted following standard methods utilized in comparable studies, as outlined by Abubakar & Haque, (2020) & Madhu et al., (2016).

Parasite inoculation

The parasites were intraperitoneally introduced into the acclimatized/healthy rats weighing 100-120 g, using 0.2 mL of infected blood containing *Trypanosoma brucei*, as described by (Madaki et al., 2016). This inoculum was prepared by diluting the blood with normal saline (20 mL 0.9% NaCl).

Parasitemia level determination

Blood obtained from the tail vein of the infected rat was examined under a microscope to assess the parasite load. A small volume of blood was applied to a slide using a ×40 objective lens. Parasitemia levels were evaluated 72 hours after parasite infection and subsequently monitored every

seven days until the conclusion of the treatment period, following the protocol outlined by (Madaki et al., 2016). The parasite count was measured in count/ml of blood sample.

In vivo antitrypanosomal activity

On the initial day (day 0), the parasites were intraperitoneally injected into the Wistar rats. After seventy-two hours post-infection, the rats were divided into five groups, each consisting of six rats. Groups, I-III received varying doses of *Corchorus olitorius* methanol extract orally (100, 200, and 400 mg/kg body weight), while group IV (the positive control) was administered 2.5 mg/kg body weight) of diminazene aceturate. Group V (the negative control) received an equivalent volume of distilled water. The administration of *Corchorus olitorius* and drugs began 72 hours post-parasite infection, with each administered at a single daily dose for three weeks, following the protocol outlined by (Madaki et al., 2016).

Biochemical/Hematological Analysis

The rats were weighed and euthanized through cervical dislocation 24 hours following the final administration. Each rat was secured on a dissecting board with twine, and blood samples were obtained for hematological analysis and assessment of biochemical markers. Hematological analysis, including the determination of red blood cell count (RBC) and white blood cell count (WBC), was conducted using the standard method outlined by Akhter et al., (2021) with an auto-hematological analyzer (Abacus Junior).

Biochemical parameters

ALT, AST, ALP, total protein, albumin, cholesterol, triglycerides, LDL, HDL, creatinine, urea, uric acid, sodium, potassium, and bicarbonate levels were determined using a commercial kit (AGAPE, Switzerland), and a UV-visible spectrophotometer at specified wavelengths, following established protocols (Nurudeen et al., 2023; Ojo et al., 2021). The multiplication factor was determined by the reagent manufacturer.

Alkaline phosphatase (ALP)

To each test tube, 1000 μL of reagent was dispensed, followed by the addition of 20 μL of each sample to its corresponding tube. The reaction mixture was thoroughly mixed and then incubated at 37 ºC for 1 minute. Subsequently, the absorbance (A) change per minute was assessed for 3 minutes at a wavelength of 405 nm.

$$ALP \text{ activity } (U/L) = (\text{change in absorbance x } 2750). \quad (1)$$

Alanine aminotransferase (ALT)

To each test tube, 1000 μL of reagent was dispensed, followed by the addition of 100 μL of each sample to its corresponding tube. The reaction mixture was thoroughly mixed and then incubated at 37 ºC for 1 minute. Subsequently, the absorbance change per minute was assessed for 3 minutes at a wavelength of 340 nm.

$$ALT \text{ activity } (U/L) = (\text{change in absorbance x } 1745). \quad (2)$$

Aspartate aminotransferase (AST)

An aliquot of the working reagent, measuring 1 μL, was dispensed into all test tubes, followed by the addition of 100 μL of each sample to their respective tubes. The reaction mixture was thoroughly mixed and then incubated at 37 ºC for 1 minute. Subsequently, the absorbance change per minute was assessed for 3 minutes at a wavelength of 340 nm.

$$AST \text{ activity } (U/L) = (\text{change in absorbance x } 1745). \quad (3)$$

Total protein

An aliquot of 1000 μL of reagent was added to blank, standard, and sample test tubes. Subsequently, 20 μL of standard reagent was added to the standard test tube, and 20 μL of each sample was added to their respective sample test tubes. The reaction mixture was thoroughly mixed and then incubated for 10 minutes at 37 ºC. Following incubation, the absorbance of the reaction mixtures was measured against a reagent blank at 546 nm.

$$Total \text{ Pr} otein \text{ conc. } (g/dL) = \frac{\text{Absorbance of sample}}{\text{Absorbance of standard}} \text{ x } 3. \quad (4)$$

Albumin

To each of the blank, standard, and sample test tubes, 1000 μL of reagent was dispensed. Following this, 20 μL of standard reagent was added to the standard test tube, while 20 μL of each sample was added to their respective sample test tubes. The reaction mixture was thoroughly mixed and then incubated for 10 minutes at 37 ºC. Subsequently, the absorbance of the reaction mixtures was measured against a reagent blank at 546 nm.

$$Albumin \text{ conc. } (g/dL) = \frac{\text{Absorbance of sample}}{\text{Absorbance of standard}} \text{ x } 6. \quad (5)$$

Cholesterol

The test tubes were labeled to correspond with each sample, with two additional tubes designated as standard and blank, respectively. To each tube, 1000 μL of working reagent was dispensed. Following this, 10 μL of the standard reagent was added to the tube labeled as standard, while 10 μL of the serum sample was added to the tubes designated for serum. The mixture was thoroughly mixed and then incubated at 37 ºC for 5 minutes. Subsequently, the absorbance of the sample and standard against the reagent blank was measured at 505 nm.

$$\textit{Total cholesterol} \text{ conc. } (mg/dL) = \frac{\text{Absorbance of sample}}{\text{Absorbance of standard}} \times 200. \quad (6)$$

Triglycerides

The test tubes were labeled according to the identity of each serum sample, and two additional tubes were designated as standard and reagent blank, respectively. To each tube, 1000 µL of the working reagent was added. Subsequently, 10 µL of standard reagent was added to the tube labeled as standard, and 10 µL of the serum sample was added to the corresponding sample tube. The reaction mixtures were thoroughly mixed and then incubated at 37 ℃ for 5 minutes. Following incubation, the absorbance of both the standard and sample against the reagent blank was measured at 546 nm.

$$\textit{Triglyceride} \text{ conc. } (mg/dL) = \frac{\text{Absorbance of sample}}{\text{Absorbance of standard}} \times 200. \quad (7)$$

Low-density lipoprotein (LDL)

The test tubes were labeled to correspond with the identity of each sample, with two additional tubes designated as calibrator and blank, respectively. To each tube, 270 µL of reagent R1 was dispensed. Subsequently, 3 µL of calibrator reagent was added to the tube labeled as the calibrator, and 3 µL of each serum sample was added to their corresponding sample tubes. The reaction mixtures were thoroughly mixed and then incubated at 37 ℃ for 5 minutes. Absorbance (OD1) was measured at 546 nm/660 nm. Following this, 90 µL of reagent R2 was added to all the tubes. The reaction mixtures were once again incubated at 37 ℃ for 5 minutes, and absorbance (OD2) was measured at 546 nm/660 nm.

$$\textit{LDL} \text{ conc. } (mg/dL) = \frac{(OD2\text{-}OD1)\,sample}{(OD2\text{-}OD1)\,calibrator} \times C.C. \quad (8)$$

Bicarbonate

To each of the blank, standard, and sample test tubes, 1000 µL of reagent was dispensed. Following this, 10 µL of standard reagent was added to the tube designated as the standard, while 10 µL of each sample was added to their respective sample test tubes. The reaction mixture was thoroughly mixed and then incubated for 1 minute at 37 ℃. Subsequently, the absorbance of the reaction mixtures was measured against a reagent blank at 505 nm.

$$\textit{Bicarbonate} \ (mEq/L) = \frac{\text{Absorbance of sample}}{\text{Absorbance of standard}} \times 100. \quad (9)$$

Bilirubin

The test tubes were labeled according to the identity of each serum sample, with one additional tube designated as blank. To all tubes, 200 µL of R1 and 1000 µL of R3 were added. Subsequently, 200 µL of each sample was added to their corresponding tubes, excluding the blank tube.

Additionally, 50 µL of R2 was added to each sample tube, while 50 µL of distilled water was added to the blank tube. The reaction mixtures were thoroughly mixed and then incubated at 25 ℃ for 10 minutes. Following this incubation period, 1000 µL of R4 was added to all tubes, mixed, and further incubated for 30 minutes at 25 ℃. The absorbance of each sample against the blank was measured at 578 nm.

$$\text{Total } \textit{bilirubin} \text{ conc. } (mg/dL) = 12.9 \times A\,(sample). \quad (10)$$

Urea

In each of the sample, blank, and standard tubes, 10 µL of each sample, distilled water, and standard were dispensed, followed by the addition of 100 µl of R1 to each test tube. The mixtures were thoroughly mixed and then incubated at 37 ℃ for 10 minutes. Subsequently, 2.5 ml of both reagents R2 and R3 was added to the tubes. The resulting mixtures were further incubated at 37 ℃ for 15 minutes. The absorbance of the samples and standard against the blank was measured at 578 nm.

$$\textit{Urea} \text{ conc. } (mg/dL) = \frac{A\,(sample)}{A\,(standard)} \times \text{Standard curve.} \quad (11)$$

Creatinine

The test tubes were labeled to correspond with the identity of each serum sample, with two additional tubes designated as standard and blank, respectively. To all tubes, 1000 µL of working reagent was dispensed. Subsequently, 100 µL of standard reagent was added to the tube labeled as standard, and 100 µL of each serum sample was added to their corresponding tubes. The reaction mixtures were thoroughly mixed, and the absorbance (A1 and A2) of both the standard and serum samples against the blank was measured at 492 nm.

$$\textit{Creatinine}\,(mg/dL) = \frac{\Delta A\,(sample)}{\Delta A\,(standard)} \times \text{Standard curve.} \quad (12)$$

Uric acid

The test tubes were labeled according to the identity of each sample, with two additional tubes designated as standard and blank, respectively. To all tubes, 1000 µL of uric acid reagent was added. Subsequently, 25 µL of the standard solution was added to the tube labeled as standard, while 25 µL of each sample was added to their corresponding tubes. The reaction mixtures were thoroughly mixed and then incubated at 37 ℃ for 5 minutes. Following incubation, the absorbance of the standard and each sample against the reagent blank was measured at 546 nm.

$$\textit{Creatinine}\,(mg/dL) = \frac{\Delta A\,(sample)}{\Delta A\,(standard)} \times \text{Standard.} \quad (13)$$

Sodium

To each of the blank, standard, and sample test tubes, 1000 μL of reagent was dispensed. Subsequently, 10 μL of standard reagent was added to the tube designated as the standard, while 10 μL of each sample was added to their respective sample test tubes. The reaction mixture was thoroughly mixed and then incubated for 5 minutes at 37 ℃. Following incubation, the absorbance of the reaction mixtures was measured against a reagent blank at 630 nm.

$$Na \text{ conc.}(mEq/L) = \frac{A(sample)}{A(standard)} \times 150. \quad (14)$$

Potassium

To each of the blank, standard, and sample (test) tubes, 1000 μL of R1 reagent was added. Following this, 25 μL of standard reagent was added to the tube designated as the standard, while 25 μL of each sample (test) was added to their respective sample test tubes. The reaction mixture was thoroughly mixed and then incubated for 5 minutes at 37 ℃. Subsequently, 250 μL of R2 reagent was added to all tubes. The reaction mixtures were further incubated for 1 minute at 37 ℃, and the absorbance (A1) was measured against the blank at 405 nm. Following this, the reaction mixtures were again incubated for 3 minutes at 37 ℃, and the absorbance (A2) was measured against the blank at 405 nm.

$$K \text{ conc.}(mEq/L) = \frac{A2\text{-}A1(sample)}{A2\text{-}A1(standard)} \times 150. \quad (15)$$

Glucose

To each of the blank, standard, and sample test tubes, 1000 μL of glucose reagent was dispensed. Following this, 10 μL of standard reagent was added to the tube designated as the standard, while 10 μL of each sample (test) was added to their respective sample test tubes. The reaction mixtures were then incubated at 37 ℃ for 10 minutes, after which the absorbance was measured against the reagent blank.

$$Glucose \text{ conc.}(mg/dL) = \frac{A(sample)}{A(standard)} \times Standard \text{ conc.} \quad (16)$$

Statistical Analysis

Statistical analysis was conducted using a statistical software package (IBM SPSS version 21.0), and the data are presented as mean ± standard error of the mean (SEM). The differences between groups were assessed using a one-way analysis of variance followed by Duncan's test. A significance level of $p \leq 0.05$ was considered statistically significant.

NUMERICAL RESULTS

Phytochemical analysis of Corchorus olitorius extract

Table 1 below presents the phytochemical constituents of the *Corchorus olitorius* extract. The findings indicate a notable disparity between phenol and the other constituents, with polyphenol exhibiting the highest value (540.60±0.24) and alkaloids showing the lowest value (12.50±0.16).

Table 1. Quantitative phytochemicals analysis of *Corchorus olitorius*.

Constituents (mg/g)					
Samples	Polyphenol	Flavonoids	Tannins	Saponins	Alkaloids
Amount (mg/g)	540.60±0.24[c]	45.51± 0.17[c]	89.85±0.18[c]	27.71±0.17[c]	12.50±0.16[c]

*Values mean ± standard deviation of three replicates. Values with different superscripts (a, b, c, d, e…) are significant at p<0.05. The joined letter signifies how close the values are, while single letters show differences in the values.

Antitrypanosomal activities of the extract

Parasitemia level

The parasitemia levels of rats infected with *Trypanosoma brucei* were monitored across all experimental groups, as depicted in Figure 1. A notable rise in parasitemia was observed in infected rats that did not receive treatment (P<0.05). Among the studied groups, the 400 mg/kg group demonstrated a significant substantial reduction in parasitemia compared to others. The parasite was measured in count/ml of the sample collected.
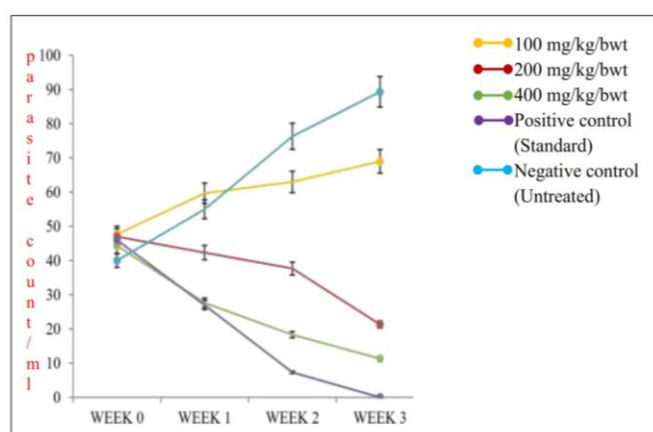

Figure 1. Effects of *Corchorus olitorius* methanolic extract on parasitemia in rats infected with *Trypanosoma brucei*.

Changes in packed cell volume

Figure 2 illustrates the packed cell volume (PCV) levels of infected rats. A decline in PCV levels was observed in the infected rats that did not receive treatment. Conversely, the groups treated with doses of 100, 200, and 400 mg/kg

exhibited a notable increase in their PCV levels compared to the negative control group.
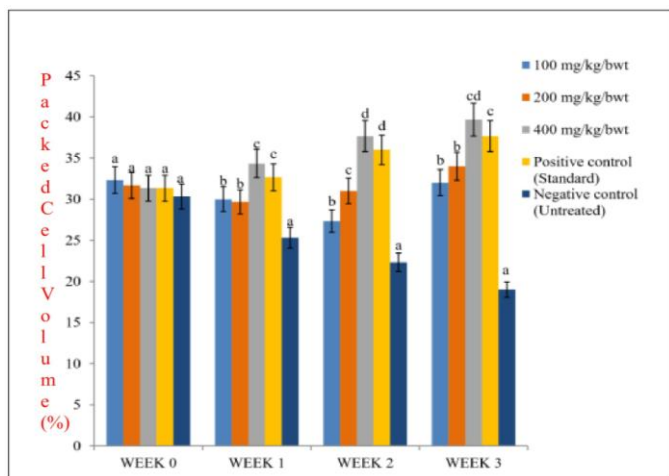

Figure 2. Effects of *Corchorus olitorius* methanolic extract on PCV levels in rats infected with *Trypanosoma brucei*.

Changes in body weight

Figure 3 depicts alterations in the body weight of rats infected with *Trypanosoma brucei*. A statistically significant decrease was observed in the body weights of the infected rats that did not receive treatment. Additionally, notable differences were observed in the body weights of the treated groups, with a significant increase noted in the rats treated with doses of 100, 200, and 400 mg/kg of the *Corchorus olitorius* methanolic extract compared to those in the negative control group ($P<0.05$).
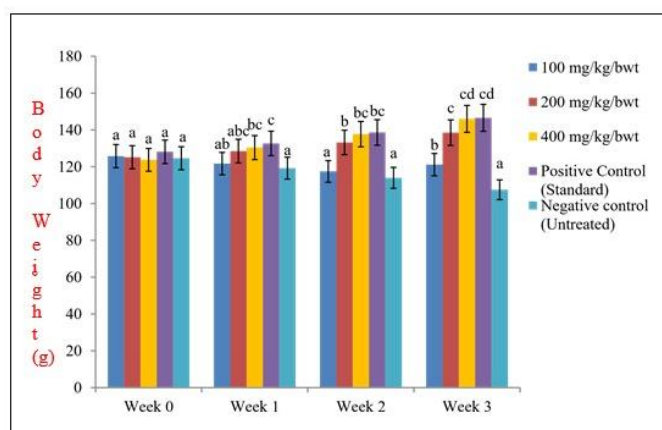
Figure 3. Effects of *Corchorus olitorius* methanolic extract on the body weight of rats infected with *Trypanosoma brucei*.

Hematological parameters

Table 2 below illustrates the impact of *Corchorus olitorius* extract on the hematological parameters of rats infected with *Trypanosoma brucei*. Administration of the extract to trypanosome-infected rats exhibited significant antitrypanosomal activity at the highest dose of 400 mg/kg, comparable to that observed in the positive control when compared to the infected but untreated group ($P<0.05$). Platelet count did not display significant differences ($P>0.05$) among rats treated with any extract concentrations. Similarly, no significant differences were observed in PCV and RBC at 200 mg/kg of the extract and in the positive control group. However, the PCV, mean corpuscular hemoglobin concentration (MCHC), platelet count (PLT), and lymphocyte levels were significantly higher in the positive control compared to those documented for the group administered 400 mg/kg of the extract (Table 2).

Table 2. Effect of *Corchorus olitorius* methanolic extract on hematological parameters.

PARAMETERS									
Sample	**Hb (g/dL)**	**PCV (%)**	**MCV (fi)**	**MCH (pg)**	**MCHC(g/dL)**	**PLT (10^6/L)**	**RBC (10^{12}/L)**	**TWBC (10^9/L)**	**L (10^9/L)**
100mg/kg bwt	3.98± 0.04[b]	35.50±1.50[b]	42.00±2.00[abc]	36.00±1.00[bc]	43.50±1.50[c]	145.00±2.00[a]	5.25±0.23[b]	9.73±0.61[c]	30.00±2.00[c]
200 mg/kg bwt	5.09±0.58[c]	39.00±1.00[c]	43.50±1.50[bc]	34.00±2.00[b]	40.00±2.00[ab]	142.50±2.50[a]	7.49±0.36[c]	9.11±0.36[bc]	26.50±1.50[ab]
400 mg/kg bwt	7.96± 0.38[d]	41.00±1.00[d]	44.50±1.50[c]	39.50±0.50[d]	37.50±1.50[a]	144.00±2.00[a]	9.00±0.75[d]	8.05±0.69[ab]	25.00±1.00[ab]
Positive control	8.93± 0.61[d]	38.50±0.50[c]	39.50±0.50[a]	40.00±2.00[d]	41.00±2.00[bc]	150.50±1.50[b]	8.06±0.24[c]	6.53±0.57[a]	27.50±1.50[bc]
Negative control	2.92±0.53[a]	25.00±1.00[a]	47.50±1.50[d]	30.00±2.00[a]	47.00±2.00[d]	165.00±2.00[c]	3.17±0.19[a]	12.05±1.81[d]	33.50±1.50[d]

*Values mean ± standard deviation of three replicates. Values with different superscripts (a, b, c, d, e…) are significant at p<0.05. The joined letter signifies how close the values are, while single letters show differences in the values.

Biochemical parameters

The *Corchorus olitorius* extract, administered at concentrations of 100, 200, and 400 mg/kg, led to an increase in total serum proteins from 6.30±0.92 mg/dl (in the infected but untreated group) to 6.85±0.73, 6.73±1.12, and 11.55±0.79 mg/dl, respectively, in comparison with the positive control group (Table 3). Concurrently, at the same concentrations, the extract caused a decrease in albumin concentrations from 4.18±0.99 mg/dl (in the infected but untreated group) to 4.63±0.53, 3.79±0.61, and 8.29±1.06 mg/dl, respectively. Additionally, AST activities decreased from 45.06±1.77 U/l (in the infected but untreated group) to 35.25±1.34, 32.19±1.96, and 28.80±1.32 U/l in rats treated with 100, 200, and 400 mg/kg of the extract, respectively.

Table 3. Effect of *Corchorus olitorius* methanolic extract on Liver function and Lipid profile of rats infected with *Trypanosoma brucei.*

PARAMETERS										
Sample	TP (g/L)	ALB (g/L)	ALP (U/L)	ALT (U/L)	AST (U/L)	CHO (mmol/L)	LDL (mmol/L)	HDL (mmol/L)	TRIG (mmol/L)	TB (mg/dL)
100 mg/kg bwt	6.85±0.73[a]	4.63±0.53[a]	64.87±2.48[c]	28.50±1.07[b]	35.25±1.34[d]	352.27±2.08[d]	111.61±1.87[c]	74.83±1.89[b]	148.29±1.95[b]	0.68±0.01[d]
200 mg/kg bwt	6.73±1.12[a]	3.79±0.61[a]	56.14±1.80[b]	25.23±1.74[a]	32.19±1.96[c]	350.08±1.86[cd]	107.74±2.40[c]	80.28±1.85[c]	154.78±1.94[c]	0.63±0.03[bc]
400 mg/kg bwt	11.55±0.79[b]	8.29±1.06[bc]	47.59±1.65[a]	26.08±1.13[ab]	28.80±1.32[b]	348.07±2.13[c]	101.03±2.45[b]	86.20±1.38[d]	146.38±1.57[b]	0.66±0.02[cd]
Positive control	10.71±1.14[b]	8.08± 0.35[b]	50.36±2.04[a]	24.55±1.45[a]	34.23±1.38[cd]	339.87±2.06[b]	109.86±2.52[c]	80.31±1.88[c]	151.81±2.04[c]	0.61±0.03[b]
Negative control	6.30±0.92[a]	4.18±0.99[a]	81.34±1.89[d]	32.76±1.53[c]	45.06±1.77[e]	370.78±1.94[e]	127.32±1.91[d]	59.10±1.33[a]	166.07±1.78[d]	0.89±0.02[e]

*Different values (a, b, c, d, e…) on the same columns were significant at P< 0.05. The joined letter signifies how close the values are, while single letters show differences in the values.

Table 4. Effect of *Corchorus olitorius* methanolic extract on Kidney function and Electrolytes of rats infected with *Trypanosoma brucei.*

PARAMETERS						
Sample	Creatinine (mg/dL)	Urea (mg/dL)	Uric acid (mg/dL)	Na (mEq/l)	K (mEq/L)	Bicarbonate (mg/dL)
100 mg/kg bwt	7.76±0.64[c]	25.04±1.55[b]	6.20±0.52[b]	146.92±1.76[d]	4.69±0.46[b]	21.90±1.95[a]
200 mg/kg bwt	7.23±0.22[c]	25.84±1.33[bc]	6.48±0.45[b]	139.74±2.20[c]	6.34±0.37[c]	24.59±1.10[b]
400 mg/kg bwt	6.28±0.31[b]	21.92±1.57[a]	5.15±0.20[b]	143.09±2.52[c]	7.28±0.57[d]	25.76±1.46[b]
Positive control	7.41±0.46[c]	28.10±1.52[c]	6.25±0.53[b]	146.76±1.59[d]	6.18±0.54[c]	26.40±0.95[b]
Negative control	10.09±0.24[d]	35.56±1.61[d]	10.05±0.82[c]	154.26±2.08[e]	3.98±0.06[a]	30.74±1.40[c]

*Values mean ± standard deviation of three replicates. Values with different superscripts (a, b, c, d, e…) are significant at p<0.05. The joined letter signifies how close the values are, while single letters show differences in the values.

Trypanosoma brucei

All doses of the extract tested significantly increased the cholesterol and HDL levels in the treated rats compared to those in the infected but untreated group. Conversely, triglyceride and LDL concentrations significantly decreased among rats treated at doses of 100, 200, and 400 mg/kg of the extract compared to those for the infected but untreated group (Table 3). Moreover, at the same extract concentrations, total serum bilirubin, ALP, and ALT levels (Table 3), as well as creatinine, urea, and uric acid concentrations (Table 4), exhibited significant decreases in experimental rats from the control group to the 100, 200, and 400 mg/kg concentrations of the extract, respectively.

Furthermore, the extract at the same concentrations decreased the sodium concentrations from 154.26±2.08 mEq/l (in the infected but untreated group) to 146.92±1.76, 139.74±2.20, and 143.09±2.52 mEq/l, respectively. Additionally, potassium activities increased from 3.98±0.06 mEq/l (in the infected but untreated group) to 4.69±0.46, 6.34±0.37, and 7.28±0.57 mEq/l in rats treated with 100, 200, and 400 mg/kg of the extract, respectively. However, there

was no significant difference (P>0.05) in the bicarbonate concentration of the extract compared with the infected but untreated group (Table 4).

DISCUSSION

The quantitative phytochemical analysis of *Corchorus olitorius* extract revealed the presence of tannin, saponin, and flavonoids, with alkaloids exhibiting the lowest concentration at 45.67 mg/100 g, while polyphenol appeared to be the most concentrated among the other parameters. Significant differences (P<0.05) were observed in all analyzed parameters. This finding is consistent with the study by (Ogungbemi et al., 2019), which reported polyphenols as having the highest quantitative phytochemical concentration. Similarly, in research conducted by Waheed et al., (2021), flavonoids were found to have a high concentration (276.15±134.57 mg/100 g) in *Jatropha gossypifolia* extract which is in contrast with this study where the flavonoid concentration is 45.51 ± 0.17^c mg/g. The variation in these constituents could be attributed to factors such as the method of sample preparation, environmental conditions, and/or pest infestation affecting the plants (Ogungbemi et al., 2019).

The antitrypanosomal efficacy of the *Corchorus olitorius*methanol extract exhibited significant differences (p<0.05) in parasitemia counts between the treated groups and both control groups (positive and negative). Notably, the negative control group displayed a consistent increase in parasite levels until week 3, culminating in mortality, consistent with the findings of Obi et al., (2023), where all untreated rats succumbed to the infection. While complete parasite clearance was not achieved in the 400 mg/kg bw group and the standard group, both managed to substantially reduce parasite levels. Conversely, the 100 mg/kg-weight group experienced an initial increase in parasite levels until week 3; however, they successfully contained the parasites until the conclusion of the treatment period. This observation aligns with the findings of Madaki et al., (2022). who reported dose-dependent antitrypanosomal activity of *Allium sativum*. In a study conducted by Zhou et al., (2021). *G. Kobayashi* plant extract showed 100% antiparasitic activity at 10 mg/L and recorded a therapeutic index (TI, LC_{50}/EC_{50}) of 5.26. The incomplete clearance of parasites may be attributed to factors such as delayed initiation of treatment in infected rats and the development of resistance, possibly involving lipopolysaccharides, by the parasitic organisms against the activity of the extract and standard drugs (Madaki et al., 2022).

Hematological parameters, including RBC, PCV, Hb, MCH, MCHC, and RDW, serve as valuable indicators of circulatory erythrocyte levels, reflecting the bone marrow's capacity to produce RBCs in response to drug, toxin, or plant extract administration (Obi et al., 2023). The significant increases observed in hemoglobin, packed cell volume, red blood cells, and MCHC following treatment with 400 mg/kg of *Corchorus olitorius* methanolic extract suggest its potential to stimulate erythropoiesis. The extract likely enhances erythropoietin synthesis and release in the kidneys, the humoral regulator of RBC production (Abdeta et al., 2020). In this study, hematological analysis of surviving animals revealed significant differences (p<0.05) between the 100 and 200 mg/kg body weight groups compared to the positive control group in PCV, MCV, RBC, lymphocytes, and RDW. However, in the 400 mg/kg body weight group, most parameters analyzed did not show significant differences (p>0.05). The highest dose (400 mg/kg body weight) exhibited more promising values in hematological assays than the standard group. Notably, values for RBC and PCV at 400 mg/kg body weight fell within a more favorable range compared to those of the positive control group (Table 2), indicating the potential utility of the extract in managing anemia. Similar observations have been reported in rats treated with extracts of *T. occidentalis* (Obi et al., 2023). and *Allium sativum* (Madaki et al., 2022). The observed effects on white blood cell and lymphocyte counts suggest that the extract may exert leucopoietic and potentially immunomodulatory effects on treated animals (Madaki et al., 2022; Maikai et al., 2008). In another study by Akah et al., (2009), *Vernonia amygdalina* fraction at doses of 160 and 320 mg/kg significantly (p<0.05) increased lymphocyte levels from 50.4±4.69 in diabetic control rats to 60.1±2.05 and 60.6±3.42, respectively, in treated diabetic rats, while other hematological indices were not significantly altered.

Concentrations of total serum proteins, albumin, bilirubin, urea, creatinine, and electrolytes serve as informative markers of the liver and kidneys secretory, synthetic, and excretory functions (Madaki et al., 2022; Obi et al., 2023). The observed increases in total serum proteins and decreases in bilirubin suggest a compromised synthetic capacity of the liver due to *Corchorus olitorius* methanolic extract administration. The extract may have enhanced liver function by disturbing the equilibrium in synthesis and degradation, as well as removal or clearance of total proteins and bilirubin in the animals. This finding aligns with an earlier study on the hepatoprotective effects of leaf extracts of *V. amygdalina* in mice (Iwalokun et al., 2006). A similar outcome was previously reported in rats administered snail hemolymph (Obi et al., 2023). However, the elevation in total serum proteins could potentially lead to dehydration, adversely affecting cellular homeostasis and metabolic liver activities, thereby impacting animal health negatively.

Urea and creatinine tend to accumulate in urine when glomerular function is compromised. Hence, the preserved concentrations of urea and creatinine in rats treated with *Corchorus olitorius* methanolic extract indicate maintained glomerular function (Obi et al., 2023; Lorke, 1983).

Additionally, Akah et al., (2009) demonstrated that diabetic control rats exhibited elevated serum levels of urea (13.3±1.60 mmol/L) and creatinine (94.3±1.91 mmol/L), while 80 and 160 mg/kg of *Vernonia amygdalina* fraction significantly (p<0.05) reduced these indices. Literature suggests that ingestion of medicinal compounds or drugs can disrupt the normal range of hematological parameters (Ajagbona et al., 1999).

CONCLUSION

The extract derived from *Corchorus olitorius* showcases properties that are antitrypanosomal, antilipidemic, and erythropoietic. It effectively addresses parasitemia, extends the lifespan of infected rats, and mitigates trypanosomal infections, potentially due to its active metabolites disrupting metabolic pathways within trypanosomes. Furthermore, the extract demonstrates relative safety at concentrations of 400 mg/kg in rats, particularly concerning liver and kidney functions following three weeks of daily administration. Hence, it emerges as a promising option for managing trypanosomal infections, addressing challenges associated with current chemotherapeutic agents and drug resistance. There is encouragement for further exploration of the ethnobotanical aspects of *Corchorus olitorius*. Additionally, prompt adoption of early treatment strategies utilizing *Corchorus olitorius* extract is advocated to prevent the progression of trypanosome infections to chronic stages.

LIST OF ABBREVIATIONS

HAT- Human African trypanosomiasis; EDTA- Ethylene diamine tetra acetic acid; RBC- Red blood cell; WBC- White blood cell; ALT- Alanine transaminase; AST- Aspartate transaminase; ALP- Alanine phosphatase; LDL- Low-density lipoprotein; HDL- High-density lipoprotein; UV- Ultraviolet; OD- Optical density; A- Absorbance; SEM- Standard error mean; PCV- Packed cell volume; PLT- platelet count; MCHC- Mean corpuscular hemoglobin concentration; MCH- Mean corpuscular hemoglobin; RDW- Red cell distribution width; TWBC- Total white blood cell count; ALB- Albumin; TP- Total protein; CHO- Carbohydrate; TRIG- Triglyceride; TB- Total bilirubin; K- Potassium; Na- Sodium; C.C-Calibration concentration.

REFERENCES

Abdeta, D., Kebede, N., Giday, M., Terefe, G. & Abay, S. M. 2020. In vitro and in vivo antitrypanosomal activities of methanol extract of *Echinops kebericho* roots. Evidence-Based Complementary and Alternative Medicine, 2020(1),p.8146756. doi: 10.1155/2020/8146756

Abubakar, A. R. & Haque, M. 2020. Preparation of medicinal plants: Basic extraction and fractionation procedures for experimental purposes. Journal of Pharmacy and Bio allied Sciences, 12(1), pp. 1-10. doi: 10.4103/jpbs.JPBS_175_19

Ajagbonna, O. P., Onifade, K. I. & Suleiman, U. 1999. Hematological and biochemical changes in rats given an extract of *Calotropis procera*. Sokoto Journal of Veterinary Sciences, 1(1), pp. 36-42.

Akah, P. A., Alemji, J. A., Salawu, O. A., Okoye, T. C. & Offiah, N. V. 2009. Effects of Vernonia amygdalina on biochemical and hematological parameters in diabetic rats. Asian Journal of Medical Science, 1(3), pp. 108-113.

Akhter, M. J., Aziz, F. B., Hasan, M. M., Islam, R., Parvez, M. M. M., Sarkar, S. & Meher, M. M. 2021. Comparative effect of papaya (Carica papaya) leaves extract and Toltrazuril on growth performance, hematological parameter, and protozoal load in Sonali chickens infected by mixed Eimeria spp. Journal of Advanced Veterinary and Animal Research, 8(1), p.91. doi: 10.5455/javar.2021.h490

Alanazi, A. D., Puschendorf, R., Salim, B., Alyousif, M. S., Alanazi, I. O. & Al-Shehri, H. R. 2018. Molecular detection of equine trypanosomiasis in the Riyadh Province of Saudi Arabia. Journal of Veterinary Diagnostic Investigation, 30(6), pp. 942-945. doi: 10.1177/1040638718798688

Airaodion, A. I., Ogbuagu, E. O., Ewa, O., Ogbuagu, U., Awosanya, O. O. & Adekale, O. A. 2019. Ameliorative efficacy of phytochemical content of Corchorus olitorius leaves against acute ethanol-induced oxidative stress in Wistar rats. Asian Journal of Biochemistry, Genetics and Molecular Biology, 2(2), pp. 1-10. doi: 10.9734/AJBGMB/2019/v2i230054

Becer, E., Soykut, G., Kabadayi, H., Mammadov, E., Çaliş, İ. & Vatansever, S. 2020. Obtaining stem cell spheroids from foreskin tissue and the effect of *Corchorus olitorius* L. on spheroid proliferation. Turkish Journal of Pharmaceutical Sciences, 17(3), p.265. doi: 10.4274/tjps.galenos.2019.05658

de Sousa, N. F., Scotti, L., Rodrigues, G., de Moura, É. P., Costa Barros, R. P. B., Sessions, Z. L., Muratov, E. N. & Scotti, M. T. 2021. Recent studies on neglected drug design. Current topics in medicinal chemistry, 21(21), pp. 1943-1974. doi: 10.2174/1568026621666210920155939

Ereqat, S., Nasereddin, A., Al-Jawabreh, A., Al-Jawabreh, H., Al-Laham, N. & Abdeen, Z. 2020. Prevalence of Trypanosoma evansi in livestock in Palestine. Parasites & vectors, 13, pp. 1-8. doi: 10.1186/s13071-020-3894-9

Fathabad, A. E., Shariatifar, N., Moazzen, M., Nazmara, S., Fakhri, Y., Alimohammadi, M., Azari, A. & Khaneghah, A. M. 2018. Determination of heavy metal content of processed fruit products from Tehran's market using ICP-OES: a risk assessment study. Food and chemical toxicology, 115, pp. 436-446. doi: 10.1016/j.fct.2018.03.044

Field, M. C., Horn, D., Fairlamb, A. H., Ferguson, M. A., Gray, D. W., Read, K. D., De Rycker, M., Torrie, L. S., Wyatt, P. G., Wyllie, S. & Gilbert, I. H. 2017. Anti-

trypanosomatid drug discovery: an ongoing challenge and a continuing need. Nature Reviews Microbiology, 15(4), pp. 217-231. doi: 10.1038/nrmicro.2016.193

Gao, F., Zhang, X., Wang, T. & Xiao, J. 2019. Quinolone hybrids and their anti-cancer activities: An overview. European Journal of Medicinal Chemistry, 165, pp. 59-79. doi: 10.1016/j.ejmech.2019.01.017

Gupta, S., Kapur, S., D V. P. & Verma, A. 2015. Garlic: An Effective Functional Food to Combat the Growing Antimicrobial Resistance. Pertanika Journal of Tropical Agricultural Science, 38(2).

Iwalokun, B. A., Efedede, B. U., Alabi-Sofunde, J. A., Oduala, T., Magbagbeola, O. A. & Akinwande, A. I., 2006. Hepatoprotective and antioxidant activities of Vernonia amygdalina on acetaminophen-induced hepatic damage in mice. Journal of medicinal food, 9(4), pp. 524-530.

James, J. & Dubery, I. 2011. Identification and quantification of triterpenoid centelloids in *Centella asiatica* (L.) Urban by densitometric TLC. Jpc-Journal of Planar Chromatography-Modern Tlc, 24(1), pp. 82-87. doi: 10.1556/JPC.24.2011.1.16

Lorke, D. 1983. A new approach to practical acute toxicity testing. Archives of toxicology, 54, pp.275-287. doi: 10.1007/BF01234480

Madaki, F. M., Adio, S. W., Busari, M. B., Kabiru, A. Y., MANN, A. & Ogbadoyi, E. O. 2022. Antioxidant and Anti-trypanosomal Activities of the Allium sativum (Garlic) Bulb Aqueous Extract on Trypanosoma congolense Infected Mice. Iranian Journal of Toxicology, 15(3), pp. 153-162. doi: 10.32598/IJT.16.3.746.1

Madaki, F. M., Kabir, A. Y., Ogbadoyi, E. O., Busari, M. B. & Maishera, H. 2016. Antitrypanosomal activity of methanol extract of *Chamaecristamimosoides* leaf in *Trypanosoma brucei* infected. Journal of American Society, 5(6), pp. 196-203. doi: 10.20959/wjpps20166-6960

Madhu, M., Sailaja, V., Satyadev, T. N. V. S. S. & Satyanarayana, M. V. 2016. Quantitative phytochemical analysis of selected medicinal plant species by using various organic solvents. Journal of Pharmacognosy and Phytochemistry, 5(2), pp. 25-29.

Maikai, V. A., Nok, J. A., Adaudi, A. O. & Alawa, C. B. I. 2008. In vitro antitrypanosomal activity of aqueous and methanolic crude extracts of stem bark of Ximenia americana on Trypanosoma congolense. Journal of Medicinal Plants Research, 2(3), pp. 55-58.

Matsufuji, H., Sakai, S., Chino, M., Goda, Y., Toyoda, M. & Takeda, M. 2001. Relationship between cardiac glycoside contents and color of Corchorus olitorius seeds. Journal of Health Science, 47(2), pp. 89-93.

Mirshekar, F., Yakhchali, M. & Shariati-Sharifi, F. 2019. Molecular evidence of *Trypanosoma evansi* infection in Iranian dromedary camel herds. Annals of parasitology, 65(2). doi: 10.17420/ap6502.196

Nasreen, M. A., Ahmed, Z. & Ali, M. M. 2022. Determination of β-carotene in jute leaves by spectrophotometry and thin layer chromatography. World Journal of Biology Pharmacy and Health Sciences, 9(2), pp. 011-020.

Nurudeen, Q., Lambe, M. O., Adedo, A. I. & Elemosho, A. O. 2023. Effects of *Moringa oleifera* Tea Supplement on the Biochemical Indices of Diabetes and Hypertension Co-Morbidity Patients. ABUAD International Journal of Natural and Applied Sciences, 3(2), pp. 56-61. doi: 10.53982/aijnas.2023.0302.08-j

Obi, C. F., Okpala, M. I., Anyogu, D. C., Onyeabo, A., Aneru, G. E., Ezeh, I. O. & Ezeokonkwo, R. C. 2023. Comparative pathogenicity of single and mixed drug-resistant *Trypanosoma brucei brucei* and Trypanosoma congolense infections in rats. Research in Veterinary Science, 162, p.104946. doi: 10.1016/j.rvsc.2023.104946

Ogungbemi, K., Ilesanmi, F. F., Odeniyi, T. A., Ilori, A. O., Oke, O. A., Ogungbemi, A. M., Balogun, B. & Ogunremi, O. B. 2019. Comparative study of long-term consumption of *Corchorus olitorius* (Ewedu) and *Ocimumgratissimum* (Efirin) Diet-inclusion on male Wistar rat. Academia Journal of Medicinal Plants, 7(7), pp. 165-168. doi: 10.15413/ajmp.2019.0146

Ojo, R. J., Enoch, G. A., Adeh, F. S., Fompun, L. C., Bitrus, B. Y. & Kugama, M. A. 2021. Comprehensive analysis of oral administration of Vitamin E on the early stage of *Trypanosoma brucei* brucei infection. Journal of Parasitic Diseases, 45, pp. 512-523. doi: 10.1007/s12639-020-01322-5

Sobhy, H. M., Barghash, S. M., Behour, T. S. & Razin, E. A. 2017. Seasonal fluctuation of trypanosomiasis in camels in North-West Egypt and effect of age, sex, location, health status, and vector abundance on the prevalence. Beni-Suef University Journal of Basic and Applied Sciences, 6(1), pp. 64-68. doi: 10.1016/j.bjbas.2017.01.003

Waheed, S. A. & Benjamin, L. Y. 2021. Comparative studies on in vitro anti-diabetic activities of saponin and flavonoid extracts of *Jatropha gossypifolia*. International Journal of Applied Chemical and Biological Sciences, 2(5), pp.30-38.

WHO Expert Committee on the Control and Surveillance of African Trypanosomiasis, 1998. Control and surveillance of African Trypanosomiasis: report of a WHO Expert Committee (No. 881-884). World Health Organization.

Zhou, B., Bentham, J., Di Cesare, M., Bixby, H., Danaei, G., Cowan, M.J., Paciorek, C.J., Singh, G., Hajifathalian, K., Bennett, J.E. & Taddei, C. 2017. Worldwide trends in blood pressure from 1975 to 2015: a pooled analysis of 1479 population-based measurement studies with 19· 1 million participants. The Lancet, 389(10064), pp. 37-55. doi:10.1016/S0140-6736(16)31919-5

THE INHIBITION OF ACNE PROTEASE BY SOME FLAVONES: DFT, SWISSADMET AND MOLECULAR DOCKING

DAYO LATONA[1], ABIODUN TAIWO[1], YEMISI ASIBOR[1], FUNKE OLARINOYE[1], BANJO SEMIRE[2]

[1]Departmentof Pure & Applied Chemistry, Osun State University, Osogbo, Nigeria
[2]Department of Pure & Applied Chemistry, Ladoke Akintola University, Ogbomoso, Nigeria

ABSTRACT

This research sought to find a potent drug for the treatment of acne from six (6) flavones. DFT-B3LYP method was used to determine the molecular descriptors like HOMO, LUMO, Dipole moment, and volume of the ligands and standard drugs. SWISSADMET was employed to ascertain the pharmacokinetic properties of the ligands, and molecular docking was achieved by using PyRx and discovery studiosoft wares. It was observed that the six flavones showed better inhibition against acne main protease than the standard drugs, and from the binding affinity results, 5-hydroxy-2-phenylchromen-4-one best inhibited acne protease. The choice of flavones was based on the fact that they have good antibacterial properties because acne thrives in the presence of bacteria.

Keywords: Acne, Flavones, Molecular Docking, Spartan, DFT.

INTRODUCTION

Flavones are a subclass of flavonoids with biological activities. They are stable to hydrolysis and metabolically stable and can be found in flowers, leaves, and fruits of plants (Schmitz-Hoerner & Weissenbock, 2016). The anti-inflammatory, antimicrobial, and anticancer properties of flavones have received great attention over the years (Duarte et al., 2013; Akura et al., 2001). The anti-inflammatory properties are due to their ability to inhibit both cyclooxygenase and lipoxygenase, and their anticarcinogenic activity promotes apoptosis of cancer cells (Robak & Gryglweski, 1996).

Acne is a very common skin condition mostly found on the face, forehead, chest, shoulders, and upper back. The cause has been attributed to hormonal imbalance leading to fluctuation in hormonal levels, stress, high humidity, and the use of oily or greasy personal care products. Acne commonly affects teenagers and can affect other age groups (Mohuiddin, 2019).

It is a common skin condition involving the blockage of skin pores by hair, sebum (an oily substance), bacteria, and dead skin cells. Which consequently leads to blackheads, whiteheads, nodules, and other types of pimples. Statistics show that about 80% of human beings between the ages of 11 and 30 suffer from at least a mild form of acne, and most people are affected by it at some point in their lives (Bhate & Williams, 2013).

Treatment of acne depends upon its severity, and presently, various medications are being used for its treatment. This includes: Benzoyl peroxide, which targets surface bacteria, Salicylic acid is used as a cleanser or lotion which helps to remove the top layer of damaged skin. Azelaic acid, which is a natural acid found in grains, helps to kill microorganisms on the skin. Retinoids help break up blackheads and whiteheads and prevent clogged pores. While Antibiotics like Clindamycin, tetracycline, and Erythromycin help to control surface bacteria that facilitate the swelling of acne.Dapzone is a topical gel that contains some antibacterial properties, and Isotretinin has been reported to be the most effective drug for the treatment of acne as it shrinks the size of oil glands. However, one major common effect of Isotretinoin is that it causes dryness of the skin and can also lead to birth defects. Other therapies include: Steroids and Lasers (Zaenglein et al., 2016).

However, this research sought to investigate the efficacy of flavones as good inhibitors for acne.

EXPERIMENTAL

Materials and methods

The following softwares were used in this study: Spartan 14, Pubchem, Protein data bank, SWISSADMET, Discovery studio, and PyRx.

A Dell computer system with 8.00 GB installed RAM and 7.77 GB of usable memory was utilized for the computational study. Docking of the ligands with the protease was investigated by using discovery studio and PyRx software. The molecular descriptors of the compounds were optimized and calculated using density functional theory with B3LYP/6-31+G* via Spartan 14.

The acne inhibitory activities of the six ligands against the crystal structure of acne (PDB: 7LBU) were obtained. Dapsone, Isotretinoin, Benzyl Peroxide, and Doxycycline were

---

used as the standard drugs. The 3D SDF conformer of the ligands and standard drugs were downloaded from the PubChem Database (https://pubchem.ncbi.nlm.nih.gov).

The protein crystal structure of acne (PDB: 7LBU) was downloaded in PDB format from the protein data bank (RCSB)

Frontier molecular features, HOMO and LUMO, were employed to calculate the band gap (BG). Hardness (η), softness (s), chemical potential (μ), electronegativity (χ), and electrophilicity index (ω) and values were obtained from the below equations:

$$BG = E_{LUMO} - E_{HOMO}. \tag{1}$$

$$EA = -E_{LUMO} \cdot (eV). \tag{2}$$

$$IP = -E_{HOMO} \cdot (eV). \tag{3}$$

$$\eta = \frac{(IP - EA)}{2} = \frac{E_{LUMO} - E_{HOMO}}{2}(eV). \tag{4}$$

$$s = \frac{1}{\eta}(eV). \tag{5}$$

$$\eta = \frac{(IP - EA)}{2} = -\chi(eV). \tag{6}$$

$$\omega = \frac{\mu^2}{2\eta} = \frac{(IP - EA)^2}{4(IP - EA)} = \frac{E_{LUMO} + E_{HOMO}}{4(E_{LUMO} - E_{HOMO})}(eV). \tag{7}$$

$$\chi = -\mu = -\frac{(IP - EA)}{2} = \frac{(E_{LUMO} + E_{HOMO})}{2}(eV). \tag{8}$$

$$\omega^+ = \frac{(IP - 3EA)^2}{16(IP - EA)} = \frac{(E_{LUMO} + E_{HOMO})^2}{16\eta}(eV). \tag{9}$$

$$\omega^- = \frac{(3IP - EA)^2}{16(IP - EA)} = \frac{(3E_{LUMO} + E_{HOMO})^2}{16\eta}(eV). \tag{10}$$

$$\Delta\omega^\pm = \omega^+ - (-\omega^-) = \omega^+ + \omega^-. \tag{11}$$

Molecular docking and binding affinity scores of the ligands and the standard drugs against the Crystal structure of acne (PDB: 7LBU) were obtained using PyRx and Discovery studio software. The inhibition constants (Ki) μM were calculated from Equations (12), (13) and (14).

$$\Delta G = -nRT \ln K_{eq}. \tag{12}$$

$$K_{eq} = e^{-\frac{\Delta G}{nRT}}. \tag{13}$$

$$K_i = \frac{1}{K_{eq}}. \tag{14}$$

DISCUSSION

The six ligands and the standard drugs employed are listed in Table 1.

Table 1. Flavones and Standard Drugs.

S/N	Ligand Code	Ligand
1.	A1	2-phenylchromen-4-one
2.	A2	7,8-dihydroxy-2-phenylchromen-4-one
3.	A3	3-hydroxy-2-phenylchromen-4-one
4.	A4	5-hydroxy-2-phenylchromen-4-one
5.	A5	7-hydroxy-2-phenylchromen-4-one
6.	A6	2-phenylbenzo(h)chromen-4-one
7.	S1	Dapsone
8.	S2	Isotretinoin
9.	S3	Benzoyl peroxide
10.	S4	Doxycycline

Molecular Descriptors

The calculated molecular descriptors such as hydrophobicity (Log P), volume (V), Polar surface area (PSA), dipole moment (DM), HOMO, and LUMO energies obtained for the six flavones and the standard drugs are shown in Table 2. The HOMO and LUMO are vital descriptors that offer realistic qualitative facts about the excitation properties of molecules (Semire et al., 2012). The calculated electronic descriptors band gaps are 4.56eV for A1, 4.24eV for A2, 4.14eV for A3, 4.02eV for A4,4.59eV for A5, 4.29eV forA6.The band gap is in the order S3>S1>A5>A1>A2>A3>A4>S4>S2. The lower the band gap, the easier the excitation of electrons within the molecule and the better the ability of the molecule to donate electrons to its surroundings. The band gap plays an important role in protein-ligand interaction. S3, with the highest band gap, shows the greatest stability, and S2, with the least band gap is the least stable among the ligands and the standard drugs, implying S2 is the most chemically active standard drug while S3 is the least chemically active standard drug. The calculated Log p tells about the compound's ability to dissolve into non-aqueous solutions. The need for the compounds to permeate through the various biological membranes is very crucial. Lipophilicity is a measure of the distribution of the compound between non-aqueous and aqueous phases, and it reveals the biological activity of ligands (Abass et al., 2001). Furthermore, Log P estimates a compound's overall lipophilicity properties, it influences the behavior of compounds in biological membranes such ashepatetic clearance, lack of selectivity, and non-specific toxicity (Hughes et al., 2008). The acceptable log P value should not be higher than 5 (Meanwell, 2011). The calculated Log P values for the compounds are 3.18 for A1,

2.84 for A2, 2.93 for A3, 2.50 for A4, 4.09 for A5, 4.01 for A6, therefore the compounds have good lipophilicity properties. Furthermore, dipole moment, which is the product of the magnitude of the charge and the distance of separation between the charges, were 4.19 debye for A1, 5.63debye for A2, 5.08debye for A3, 5.00debye for A4,3.25debye for A5, 4.60debye for A6. Moreover, large values of dipole moment have been attributed to the anomalous property of individual molecules (Debendetti, 2003), therefore, the compounds are desirable in terms of dipole moment values because they have moderate values of dipole moment.

The electrophilicity index is in the order: S4>S2>A4>S3>A1>A2>A5>A6>S1as shown in Table 3. Ligand S4 with the highest electrophilicity index shows excellent character of an electrophile. While S1, with the least electrophilicity value possesses nucleophilicity character. S4 also gave the highest EA, which suggests readiness to accept electrons to form bonds. Furthermore, S2 and S4 showed good chemical softness properties, showing their good reactivity and drug stability properties (Asogwa et al., 2022).

Table 2. Geometries of a calculated molecular description of the ligands.

ID	HOMO (eV)	LUMO (eV)	BG	DM (Debye)	HBA	HBD	MW (amu)	Log P	V (A^3)	PSA (A^2)
A1	-6.36	-1.80	4.56	4.19	2	0	222.24	3.18	434	30.21
A2	-6.03	-1.79	4.24	5.63	3	1	238.24	2.84	434	50.44
A3	-5.87	-1.73	4.24	5.08	2	0	224.25	2.93	434	26.30
A4	-5.99	-1.97	4.02	5.00	5	2	284.26	2.50	434	79.90
A5	-6.31	-1.72	4.59	3.25	2	0	272.30	4.09	434	30.21
A6	-6.01	-1.72	4.29	4.60	2	0	272.30	4.01	434	30.21
S1	-5.67	-0.67	5.00	5.95	2	2	248.30	1.55	434	94.56
S2	-5.19	-2.07	3.12	2.60	2	1	300.44	1.55	302	37.30
S3	-7.42	-1.73	5.69	3.61	4	0	242.23	2.91	434	52.60
S4	-5.64	-2.43	3.21	3.89	9	6	444.43	-0.24	302	181.62

*BG: band gap($E_L - E_H$), DM: Dipole Moment, MW: Molecular Weight, HBA: Hydrogen bond acceptor, HBD: Hydrogen bond donor, PSA: Polar Surface Area, V: Volume.

Table 3. Global reactivity descriptor values.

Ligand	Hardness (η)	Softness (s)	Chemical Potential (μ)	Electrophilicity index (ω)	ω^+	ω^-	$-\Delta\omega^\pm$
A1	2.28	0.44	4.08	3.65	1.90	3.34	1.44
A2	2.12	0.47	3.91	3.61	1.92	5.83	3.91
A3	2.29	0.44	3.80	3.49	1.85	5.65	3.80
A4	2.01	0.50	3.98	3.94	2.20	6.18	3.98
A5	2.30	0.44	4.02	3.51	1.79	5.81	4.02
A6	2.15	0.47	3.87	3.48	1.82	5.68	3.86
S1	2.50	0.40	3.17	2.01	0.74	3.91	3.17
S2	1.56	0.64	3.63	4.22	2.60	6.23	3.63
S3	2.85	0.35	4.58	3.68	1.75	6.32	4.58
S4	1.61	0.62	4.04	5.07	3.26	7.29	4.04

CHEMISTRY

ADMET studies of the flavones

The ligands were subjected to an ADMET study using SWISSADMET server to predict their pharmacokinetic properties shown in Table 4. It was revealed that all six flavones have high GI Absorption (Gastrointestinal absorption) properties; this shows that the flavones will be able to be absorbed through the biological membranes. The Blood-brain barrier is the specialized system of the brain microvascular endothelial cells that shields the brain from toxic substances in the blood and filter harmful substances from the brain back to the bloodstream; with the exception of A4 others have good BBB permeant properties. All the ligands have no P-gp substrate property and are good inhibitors of CYP1A2, suggesting good drug candidates with good absorption and oral bioavailability. The basic enzymes for drug biotransformation are the cytochrome P450 (CYP) enzymes which include: CYP1A2, inhibitor, CYP2C19 inhibitor, CYP2C9 inhibitor, CYP2D6 inhibitor, and CYP3A4 inhibitor. Consequently, those ligands having an inhibitory effect on CYP3A4 enzymes may cause an increase in concentration and overdose of drugs. While, those ligands with no inhibitory effect on CYP3A4 enzyme will be easily converted after oral treatment. The more negative the log Kp, the less skin permeant property of the ligand, and the recommended value of log Kp being -9.63 cm/s suggests that all the flavones under investigation have good skin permeant properties.

Molecular docking analysis

The molecular docking method was validated by docking the six ligands into the active sites of the protein crystal structure of Acne protease (PDB: 7LBU). This was done in order to obtain binding affinities and the inhibition constants of the ligands and the standard drug. The docking results are shown in Table 5.

The 2D-structures of the interactions of ligands/standard drugs with aminoacids residues are shown in Figure 1.

Table 4. Pharmacokinetic properties.

Ligand	GI Absorption	BBB Permeant	P-gp Substrate	CYP1A2 Inhibitor	CYP2C19 Inhibitor	CYP2C9 Inhibitor	CYP2D6 Inhibitor	CYP3A4 Inhibitor	LogKp (cm/s)
A1	High	Yes	No	Yes	Yes	No	No	No	-5.13
A2	High	Yes	No	Yes	Yes	No	Yes	Yes	-5.34
A3	High	Yes	No	Yes	No	No	No	No	-5.44
A4	High	No	No	Yes	No	Yes	Yes	Yes	-5.66
A5	High	Yes	No	Yes	Yes	No	No	No	-4.55
A6	High	Yes	No	Yes	Yes	No	No	No	-4.82

Table 5. Amino acid residues of the ligands.

Ligand/Standard Drug	Amino Acid Residue	Binding Affinty(Kcal/mol)	Inhibition Constant/10^{-6}
A1	H- bonding: VAL A: 348. Pi-Alky Bonding: ARG A:289, PRO A:292, ILE A:184, ILE A:288, ALA A:347, VAL A:110, ALA A:46, LEU A:10	-9.5	0.108
A2	H - bonding: VAL A:348, THR A:47. Pi-Alkyl bonding: PRO A:292, ILE A:288, ALA A:347, ALA A:46, LEU A:10, ILE A:184, ARG A:289	-9.7	0.077
A3	H-bonding: ARG A:289, VAL A:348. Pi-Alkyl bonding: ILE A:184, PRO A:292, ALA A:347, ALA A:46, LEU A:10, VAL A:110, ILE A:288	-9.7	0.077
A4	H-bonding: VAL A:348. Pi-Alkyl bonding: ALA A:46, VAL A:110, ALA A:347, LEU A:10, PRO A:292, ILE A:184, ARG A:289	-9.8	0.065
A5	H-bonding: VAL A:348 Pi-Alkyl bonding: ARG A:289, ILE A:184,ILE A:288, PRO A:292, ALA A:347, LEU A:10. Unfavorable donor-donor: THR A:47	-9.7	0.770
A6	Pi-Alkyl bonding: ILE A:184, ARG A:289, PRO A:292, LEU A:10, ILE A:288, ALA A:347, VAL A:110, ALA A:46	-9.6	0.091
S1	H-bonding: THR A: 47, ARG A: 289 GLU A:238. Pi-Alkyl bonding: LEU A:10, ILE A: 184, PRO A:292	-8.2	0.970

S2	H-bonding: ARG A: 249, ARG A:41, Unfavorable donor-donor: ARG A:315	-.6.4	0.201
S3	H-bonding: THR A: 47. Pi-Donor hydrogen bond: VAL A: 348. Carbon Hydrogen Bonding: ALA A:46. Pi-Alkyl bond: ALA A:347, PRO A:292, LEU A:10, ILE A:288	-8.0	1.358
S4	H-bonding: ARG A:315, ARG A:41, ASP A:66. Unfavorable Donor-donor bonding: ARG A:249	-8.8	0.352

Docking with A1

The compound interacted with hydrogen bonds with VAL A:348 and Pi-Alky Bonding with ARG A:289, PRO A:292, ILE A:184, ILE A:288, ALA A:347, VAL A:110, ALA A:46, and LEU A:10. The binding affinity and the inhibition constant (Ki) were -9.5 Kcal/mol and 0.108×10^{-6} respectively. The binding affinity result of A1 is better than each of the standard drugs under investigation.

Docking with A 2

The ligand interacted with H – bonding with VAL A:348, THR A:47, Pi-Alkyl bonding with PRO A:292, ILE A:288, ALA A:347, ALA A:46, LEU A:10, ILE A:184, and ARG A:289. The interaction gave a better binding affinity of -9.7Kcal/mol and a lower inhibition constant (Ki) of 0.077×10^{-6} as compared to A1.

Docking with A3

A3 interacted with H-bonding with ARG A:289, VAL A:348 and Pi-Alkyl bonding with ILE A:184, PRO A:292, ALA A:347, ALA A:46, LEU A:10, VAL A:110, ILE A:288. The values of the binding affinity and the inhibition constant were the same as that of A2.

Docking with A4

Ligand A4 interacted with H-bonding with VAL A: 348, Pi-Alkyl bonding with ALA A:46, VAL A:110, ALA A:347, LEU A:10, PRO A:292, ILE A:184 and ARG A:289. The binding affinity of -9.8 Kcal/mol for ligand A4 is the best among the ligands and the standard drugs. Furthermore, the calculated inhibition constants of 0.065×10^{-6} were the least compared to the other ligands and the standard drugs.

Docking with A5

Ligand A5 showed interaction with H-bonding with VAL A:348, Pi-Alkyl bonding with ARG A:289, ILE A:184, ILE A:288, PRO A:292, ALA A:347, LEU A:10 and Unfavorable donor-donor with THR A:47. The binding affinity and inhibition constant results were the same for A2 and A3.

Docking with

*A6*A6 interacted with Pi-Alkyl bonding with ILE A:184, ARG A:289, PRO A:292, LEU A:10, ILE A:288, ALA A:347, VAL A:110, ALA A:46. The values of the binding affinity and calculated inhibition constants for the interaction were -9.6 Kcal/ mol and 0.091×10^{-6} respectively.

Docking with standard drug S1

The standard drug, S1 interacted with H-bonding with THR A: 47, ARG A: 289 GLU A:238, and Pi-Alkyl bonding with LEU A:10, ILE A: 184, PRO A:292. The binding affinity of -8.2 Kcal/mol is poor with high inhibition constant compared to those of A1, A2, A3, A4, A5, and A6.

Docking with standard drug S2

The second standard drug S2 interacted with H-bonding with ARG A:249, ARG A:41, Unfavorable donor-donor with ARG A:315. The binding affinity of -6.4 Kcal/mol is poor compared to A1, A2, A3, A4, A5, A6 and S1. The calculated inhibition constant 0f 0.201×10^{-6} is better than those of A4, A5, and S1.

Docking with standard drug S3

The third standard drug, S3 interacted with H-bonding with THR A:47, Pi-Donor hydrogen bond with VAL A:348, Carbon -Hydrogen Bonding with ALA A:46 and Pi-Alkyl bond with ALA A:347, PRO A:292, LEU A:10, ILE A:288. The binding affinity of -8.0 Kcal/mol is far better than that of S2 and it gave the poorest (highest) inhibition constant of 1.358×10^{-6} compared to all the ligands and the standard drugs under investigation.

Docking with standard drug S4

The standard drug, S4 interacted with H-bonding with ARG A: 315, ARG A:41, ASP A:66 and Unfavorable Donor-donor bonding with ARG A:249. It gave the best binding affinity of -8.8 Kcal/mol compared to all the standard drugs under study. It has an inhibition constant 0f 0.352×10^{-6}, which is second best after S2 in comparison to the standard drugs.
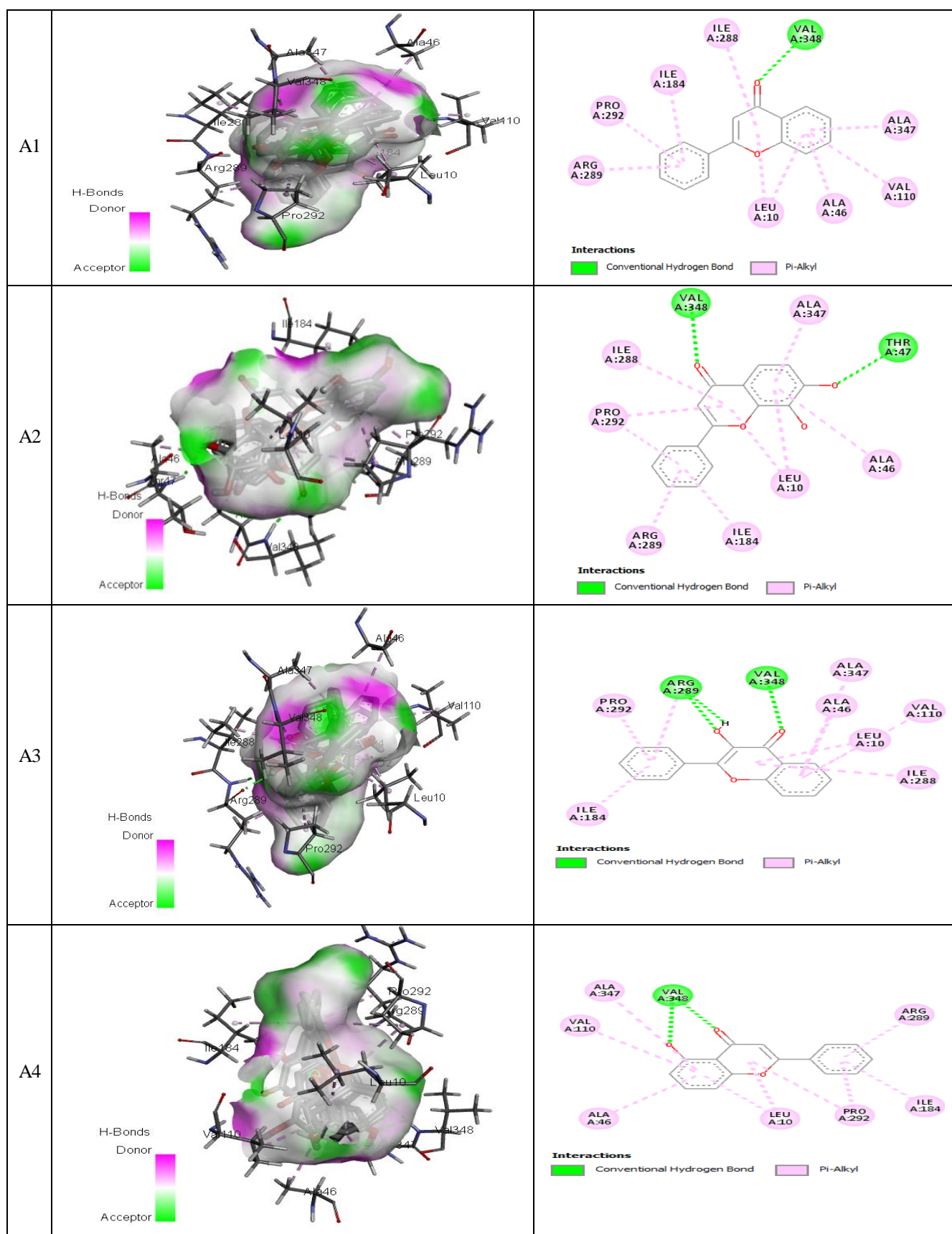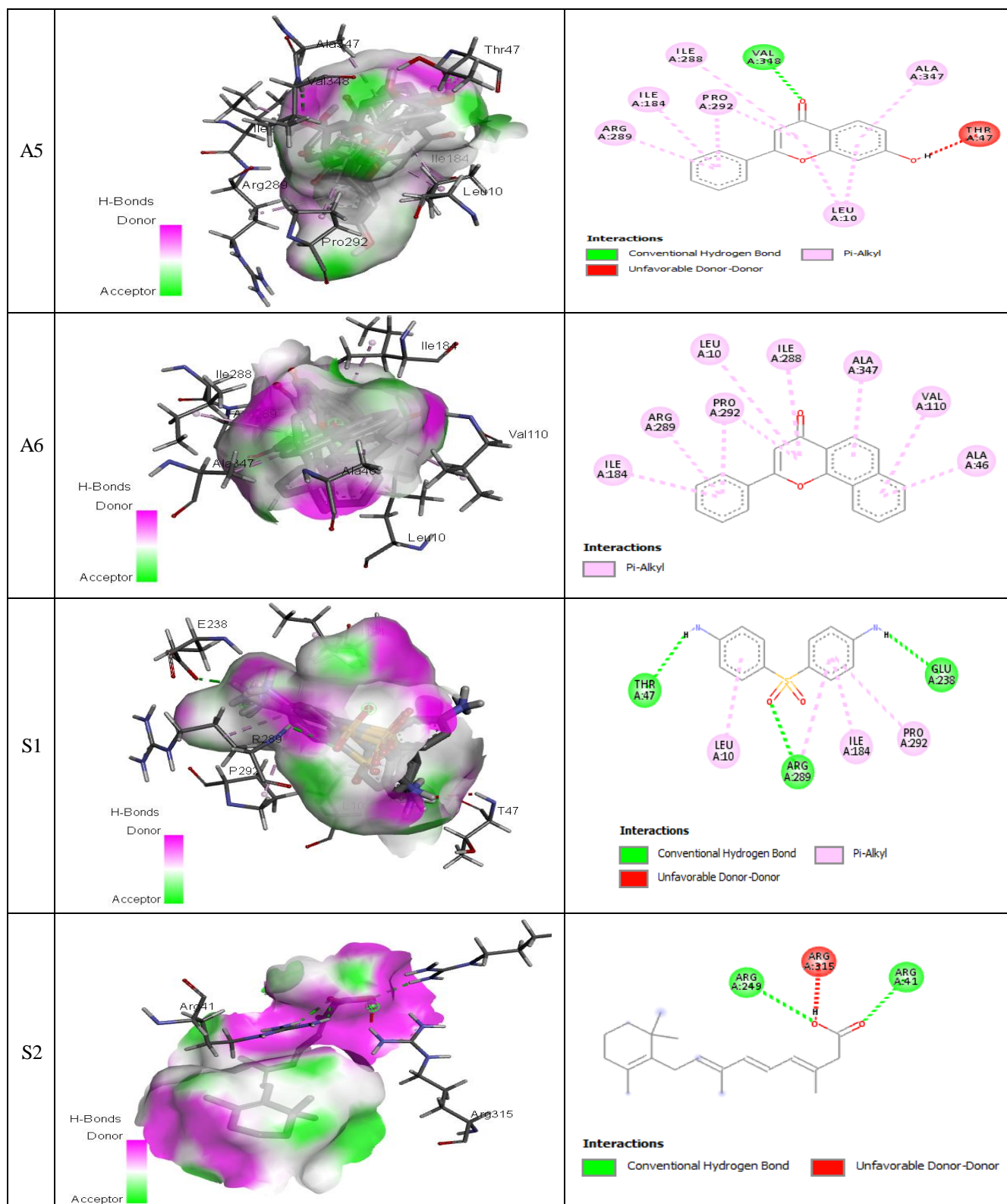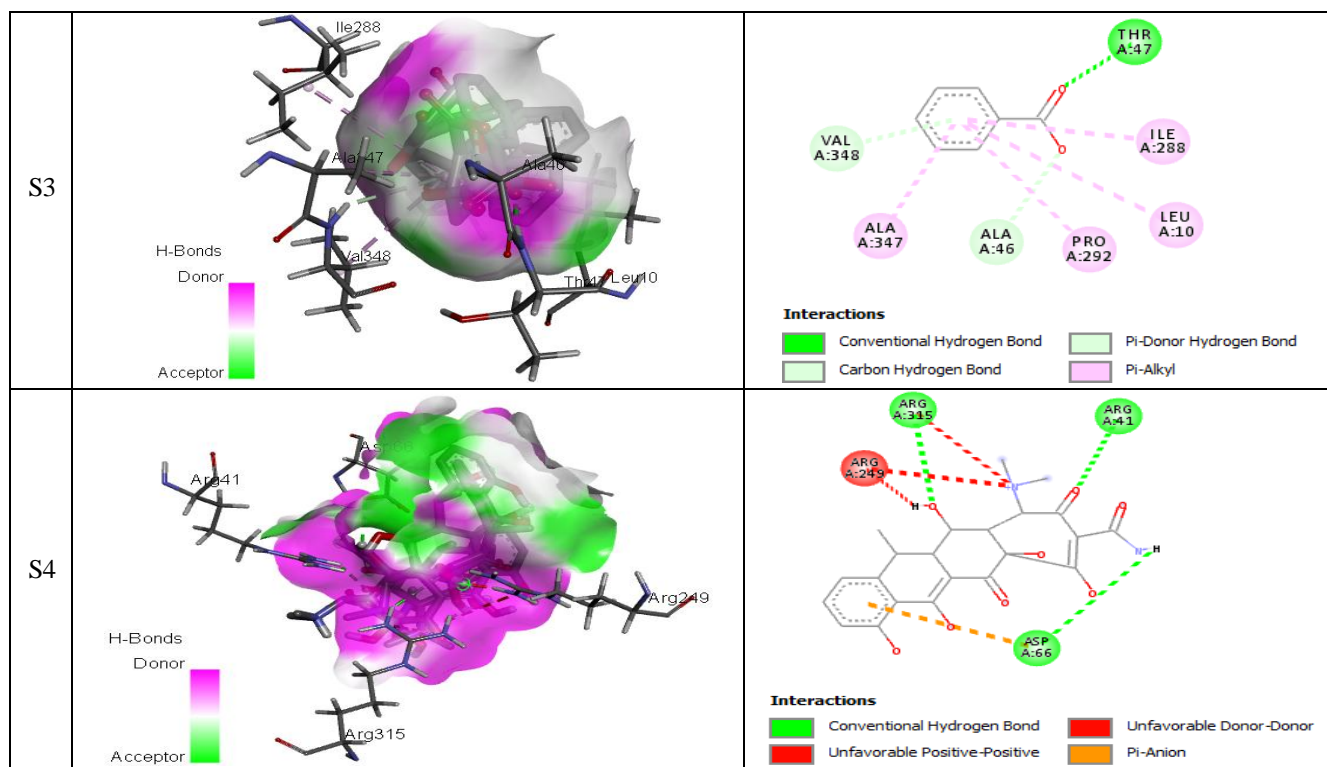
Figure 1. Interaction of ligands/standard drugs with respective amino-acid residues.

CONCLUSION

The molecular binding results revealed that all the flavones under investigation gave better binding affinities than the standard drugs, with A4 being the most preferred and having the least inhibition constant. However, S4 is the best among the standard drugs studied, with the highest electrophilicity index, ionization potential, and softness properties. The skin permeant properties of all the flavones are good and have minimal toxicity. All the flavones have good absorption and oral bioavailability properties. Ligands A1, A3, A5, and A6 are not CYP450 Inhibitors and therefore accessible after oral treatment. Flavones have antibacterial properties and can be employed to combat acne, which is a disease promoted by bacteria. The relatively good lipophilicity property of the flavones makes them good cosmetic products.

ACKNOWLEDGMENTS

REFERENCES

Abass, K., Reponen, P., Mattila, S. & Pelkonen, O. 2001. Metabolism of α-Thujone in human hepatic preparations in vitro, Xenobiotical. 41(2), pp. 101-111. Doi:10.3109/00498254.2010.528066

Akura, S., Takeda, K., & Kaisho, T. 2001. Toll-Like Receptors; Critical Proteins Linking Innate and Acquired Immunity, Nat. Immunol. 2(8), pp. 675-680. Doi:10.1038/90609

Asogwa, F. G., Ogechi, E. G., Louis, H., Izuchukwu, U. D., Apende, C. G., Florence, E. U., Ekeleme, M. G., James, E. A., Ikenyirimba, O. J., Ikeube, A. I., Owen, A. E. & Chris, O. U. 2022. Synthesis, Characterization, DFT Studies and Molecular Docking Investigation of 2-Oxo-Ethyl Piperidine Pentanamide-Derived Sulfonamides as Anti-Diabetic Agents, Results in Chemistry. 4, p.100672. doi.org/10.1016/j.rechem.2022.100672

Bhate, K. & Williams, H. C. 2013. Epidemiology of acnevulgaris, Brit. J Dermatol. 168(3), pp. 474-485. https://doi.org/10.1111/bjd.12149

Debendetti, P. 2003. Condensed Matter, Journal of Physics. 15, pp. 1669-1670.

Duarte, C. M., Losada, I. J., Hendriks, I. E., Mazarrasa, I. & Marba, N. 2013. The role of Coastal Plant Communities for Climate Change Mitigation and Adaptation, Nature Climate Change. 3, pp. 961-968. https://doi.org/10.1038/nclimate1970

Hughes, J. D., Blagg, J., Price, D. A., Bailey, S., Decrescenzo, G. A., Devraj, R. V., Ellsworth, E., Fobian, Y. M., Gibbs, M. E., Gibbs, R. W., Greene, N., Huang, E., Krieieger-Burke, T., Loesel, J., Wager, T., Whiteley, L. & Zheng, Y. 2008. Physicochemical drug properties associated with in vivo toxicological outcomes, Bioorg. Med Chem Lett. 18(17), pp. 4872-5. Doi:10.1016/j.bmcl.2008.07.071

Meanwell, N. A. 2011. Synopsis of some recent tactical application of biostereses in drug design, Journal of medicinal chemistry. 54(8), pp. 2529-2591. https://doi.org/10.1021/jm1013693

Mohuiddin, A. K. 2019. A comprehensive review of Acne Vulgaris, Clin Res Dermatol. 6(2), pp. 1-34. http://dx.doi.org/10.15226/2019/2378-1726/6/6/00186

Robak, J. & Gryglewski, R. J. 1996. Bioactivity of Flavonoids, Pol J Pharmacol. 48(6), pp. 555-564.

Schmitz-Hoerner, R. & Weissenbock, G. 2016. Contribution of Phenolic Compounds to the UV-B Screening Capacity of Developing Barley Primary Leaves in Relation to DNA Damage and Repair under Elevated UV-B Levels, Phytochemistry. 64(1), pp. 243-255. Doi: 10.1016/s0031-9422(03)00203-6

Semire, B., Oyebamiji, A. & Ahmad, M. 2012. Theoretical Study on Structure and Electronic Properties of 2,5-Bis [4-N,N-Dietylaminostyryl] Thiophene and Its Furan and Pyrrole Derivatives Using Density Functional Theory, Pakistan Journal of Chemistry. 2(4), pp. 166-173. Doi:10.15228/2012.v02.i04.p02

Zaenglein, A. L., Pathy, A. L., Schlosser, B. J., Alikhan, A., Baldwin, H. E. & Berson, D. S. 2016. Guildelines of care for the management of acne vulgaris, J. Am. Acad Dermatol. 74(5), pp. 945-973. Doi:10.1016/j.jaad.2015.12.037

ANALYSIS OF THE SELF-SUFFICIENCY OF WHEAT PRODUCTION IN BOSNIA AND HERZEGOVINA

MARKO IVANIŠEVIĆ[1], TATJANA POPOV[1], DIJANA GVOZDEN SLIŠKO[2]

[1]Faculty of Natural Sciences and Mathematics, University of Banja Luka, Banja Luka, Bosnia and Herzegovina
[2]Republic Institute for the Protection of Cultural, Historical and Natural Heritage, Banja Luka, Bosnia and Herzegovina

ABSTRACT

Wheat is recognized as a crucial staple food across nearly all countries. Achieving a specific level of self-sufficiency in primary food products is a common objective for nations, aimed at safeguarding domestic production, minimizing dependency on imports, and mitigating disruptions in global and regional supply chains. This study provides an analysis of wheat production and yields in Bosnia and Herzegovina, with the goal of evaluating the self-sufficiency of wheat production. The analysis covers the period from 2010 to 2019. The study places particular emphasis on spatial analysis, including production, yield, and self-sufficiency at the level of local administrative units. The findings indicate that Bosnia and Herzegovina's self-sufficiency in wheat production stands at 54%, with significant variability in production quantities across different local government units. These insights offer a foundation for future research that could delve deeper into the spatial-temporal, economic, and food security dimensions of wheat production.

Keywords: Wheat, Production and yields, Self-sufficiency, Bosnia and Herzegovina.

INTRODUCTION

Wheat (Triticum) is an annual plant and represents one of the most significant and widespread agricultural crops in the world. In human nutrition, wheat plays an irreplaceable role and is a main ingredient in staple food products such as bread and similar items (Kovačević & Rastija, 2014). Additionally, wheat is of great importance to the milling industry, the food processing industry, the pharmaceutical industry, and livestock feed production. It is characterized by a large distribution area due to its nature and polymorphism. The most favorable conditions for its cultivation are in the zone between 30 and 60° north latitude and 27 and 40° south latitude (Oleson, 1996; Nuttonson, 1955). The optimal temperature for wheat development is around 25°C, while the average temperature minima and maxima range from 3 to 4°C, and 30 to 32°C, respectively (Briggle, 1980).

Wheat has a high degree of adaptation when it comes to water availability. Although three-quarters of the world's land where wheat is grown receives between 375 and 875 mm of precipitation annually, it can be cultivated in most areas where the average annual precipitation ranges from 250 to 1750 mm (Leonard & Martin, 1963). According to Todorović and colleagues, the northern limit for cultivating winter wheat is at 67° north latitude, while in the southern hemisphere, this limit extends to the southern parts of South America, Africa, and Australia (Todorović et al., 2003). In terms of vertical distribution, wheat is grown up to 4000 meters above sea level in Asia, while in Europe it thrives up to an altitude of 1100 meters. Winter wheat provides higher and more stable yields compared to spring wheat, making it more economically significant. On the other hand, spring wheat produces higher quality grain and flour and is significantly more resistant to drought and high temperatures (Jablonskyté-Raščé et al., 2013).

The three most important cereals on a global level are wheat, rice, and corn. These cereals are fundamental elements of human nutrition and account for nearly half of the calories in global diets, as well as two-fifths of global protein intake. Wheat alone provides one-fifth of the calories and protein in the global diet and is the most widely cultivated crop, grown on over 217 million hectares annually (Ernstein et al., 2022). In this context, it can be concluded that wheat plays a crucial role in ensuring global food security due to its significant presence in the diets of the world's population (Dixon, 2007; Shiferaw et al., 2013). Wheat production has varied globally from 200 to 240 million tons from 1961 to the present, with a peak in production recorded during the 1980s. The area sown with wheat globally has not significantly fluctuated, but over the past fifty years, there has been a noticeable trend of increasing wheat yields. Wheat yields have nearly quadrupled in the past fifty years (Ernstein et al., 2022).

Climate change impacts wheat production differently across various production zones worldwide. Some benefits of climate change may be observed in production zones at the far northern and southern latitudes, while production zones in the subtropical belt will face challenges due to rising temperatures and extended droughts (Xiong et al., 2020). It is important to note that over time, new pathogens and wheat diseases have emerged and spread, affecting yields in certain production areas around the world (Singh et al., 2008; Mottaleb et al., 2018).

---

* Corresponding author: marko.ivanisevic@pmf.unibl.org
GEOGRAPHY, GEOSCIENCE AND ASTRONOMY

Each country aims to achieve the goal of self-sufficiency in the production of certain agricultural products, especially if favorable agro-ecological conditions exist within that country. According to the FAO, the concept of food self-sufficiency is "generally viewed as the extent of production whereby a country can meet its needs from domestic production" (Thomson & Metz, 1998). The pursuit of self-sufficiency is not in alignment with the concept of free markets and trade, and many critics argue that self-sufficiency undermines achieving economic efficiency in food production (Clapp, 2017).

However, regardless of economic policy (protectionism or liberalism), most countries focus on achieving a certain level of self-sufficiency for key food products. The importance of self-sufficiency in the production of major agricultural products became particularly evident during the COVID-19 pandemic, when significant disruptions in global food supply chains were observed (Kakaei et al., 2022). Bosnia and Herzegovina, a net importer of food products, has not explicitly set goals for increasing production self-sufficiency in its strategic sectoral documents, but it has identified the deficit in foreign trade of agricultural products as a threat (Ostojic et al., 2019). Bosnia and Herzegovina imports between 300,000 and 400,000 tons of flour annually, while exports are around 40,000 tons per year (Ostojic et al., 2020). Mostly, high-quality flour is imported for the needs of the baking and food industries. Due to the inability to meet the demand for wheat and flour, the deficit must be covered through imports (Jalić et al., 2021).

The general aim of this study is to analyze the characteristics and trends of wheat production in Bosnia and Herzegovina and to assess the self-sufficiency of wheat production in order to determine the value of the production deficit in various years. The specific objectives of the study include analyzing the total production and yield of wheat in local government units in Bosnia and Herzegovina, providing insights into the geographic context of production and consumption of this crop.

STUDY AREA

Bosnia and Herzegovina is a country in Southeast Europe. It borders the Republic of Serbia, the Republic of Croatia, and Montenegro. The total area of the country is 51,129 km² and it extends between 42°33'00" and 44°16'30" north latitude and 15°44'00" and 19°37'41" east longitude. The terrain is predominantly hilly and mountainous, significantly dissected by narrow river valleys. In the north, along the Sava River, there are larger plains, while in the southern and southwestern parts of the country, the landscape is dominated by karst terrain with plateaus and karst fields. The climate is mainly temperate continental with warm summers and cold winters (Ahmetbegović et al., 2015). The southern part of

thecountry, due to the influence of the Adriatic Sea, has a modified Mediterranean climate, while areas with high altitudes have a mountain climate characterized by short, cold summers and harsh winters. Forests and wooded land dominate land use, covering more than half of Bosnia and Herzegovina's territory. Agricultural land occupies about 37% of the total area, of which only 30% is arable land (Drašković et al., 2021). According to the 2013 census, Bosnia and Herzegovina had a population of 3,531,159 (ASBiH, 2016). Bosnia and Herzegovina has a very complex state structure and is divided into two entities (Republika Srpska and the Federation of Bosnia and Herzegovina) and the Brčko District as a special unit (Fig. 1). The administrative structure of the entities is not the same. The Republika Srpska territory covers 49% of the total territory of Bosnia and Herzegovina and is composed of municipalities and cities as local government units (54 municipalities and 10 cities). On the other hand, the Federation of Bosnia and Herzegovina consists of ten cantons as the first level of administrative division, and municipalities and cities as the second level of administrative division. The total number of local government units in the Federation of Bosnia and Herzegovina is 79.
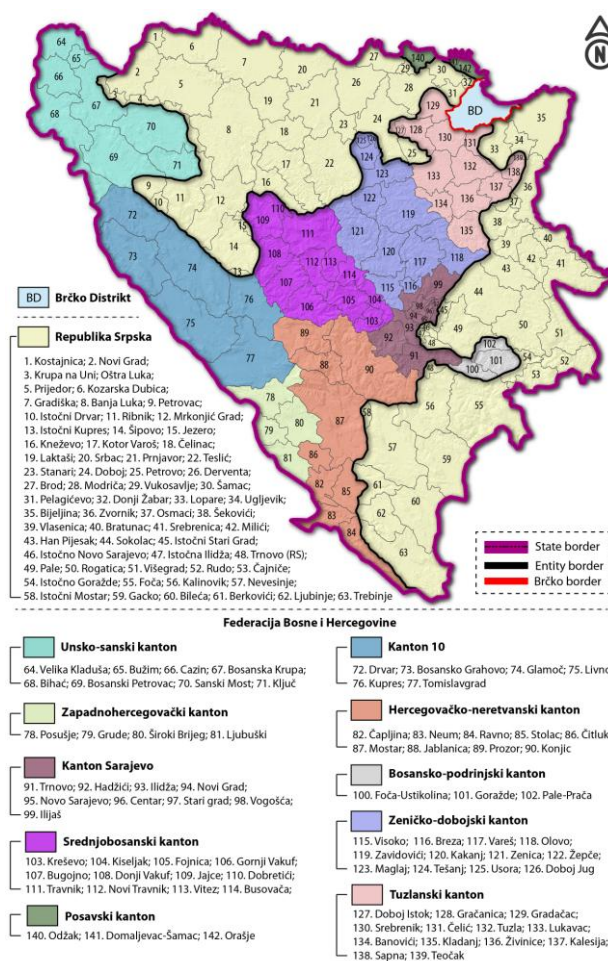

Figure 1. Administrative–territorial division of Bosnia and Herzegovina.

MATERIALS AND METHODS

The analysis of self-sufficiency in the production of an agricultural crop involves calculating the balance between production and imports on one hand, and consumption and exports on the other. Additionally, when calculating self-sufficiency, it is important to consider losses in production and storage, as well as the stock of the analyzed agricultural crop (FAO, 2017). Due to the underdevelopment and complexity of the statistical system in Bosnia and Herzegovina, and the unavailability of certain data, this study focuses solely on wheat production and consumption. Data on wheat imports and exports, which fall under the jurisdiction of the Indirect Taxation Authority of Bosnia and Herzegovina, are not available, and data on production/storage losses and stock are virtually non-existent.

The study utilized official statistical data from the Agency for Statistics of Bosnia and Herzegovina, the Republika Srpska Institute of Statistics, and the Federal Institute for Statistics of Bosnia and Herzegovina, concerning the total production and yields of wheat in local government units. The analysis covers the period from 2010 to 2019. The Republika Srpska Institute of Statistics ceased collecting and processing data on total wheat production and yields at the local level after 2019, limiting the analyzed period to 10 years. For Republika Srpska, data were sourced from Statistical Yearbooks, while for the Federation of Bosnia and Herzegovina, data were taken from thematic bulletins titled "Crop Production in the FBiH." Data on total production and yields for the Brčko District were obtained from the Agency for Statistics of Bosnia and Herzegovina. Demographic data for the entities and the Brčko District, which relate to annual estimates, were sourced from the publications "Federation of Bosnia and Herzegovina in Numbers," "Statistical Yearbook of Republika Srpska," and "Demographics in the Brčko District." Demographic data for local government units were obtained from the publication "Population, Households, and Dwellings Census in Bosnia and Herzegovina 2013" (ASBiH, 2016). Data on wheat consumption per capita, or flour equivalent, were derived as average values from the study "Analysis of Trends in Production, Foreign Trade Exchange, and Consumption of Basic Food Products" (MPVŠ, 2018).

To facilitate spatial analyses, a specialized geospatial database was developed, incorporating statistical data related to demographics, wheat production, and yields at the local government unit level. Boundaries for local government units, cantons, entities, and the national level were sourced from the Open Street Maps repository and converted to the national coordinate system. The collection, processing, and visualization of geospatial data were conducted using the open-source software package QGIS, version 3.16.3.

RESULTS AND DISCUSSION

Wheat production in Bosnia and Herzegovina during the analyzed period had an annual average of 238,500 tons. Republika Srpska contributed 64% to the total wheat production in Bosnia and Herzegovina on average. In contrast, the Federation of Bosnia and Herzegovina had a significantly lower share, averaging 30% of the total wheat production. The lowest production values were recorded in 2014, with only 170,000 tons, while the peak production during the analyzed period occurred in 2016, reaching 307,000 tons. Throughout the analyzed period, there was an observed increasing trend in wheat production in Bosnia and Herzegovina.

Wheat production in Bosnia and Herzegovina is most prominently concentrated in the northern regions of the country, specifically in Semberija, Posavina, and Lijevče Polje (Fig. 2).
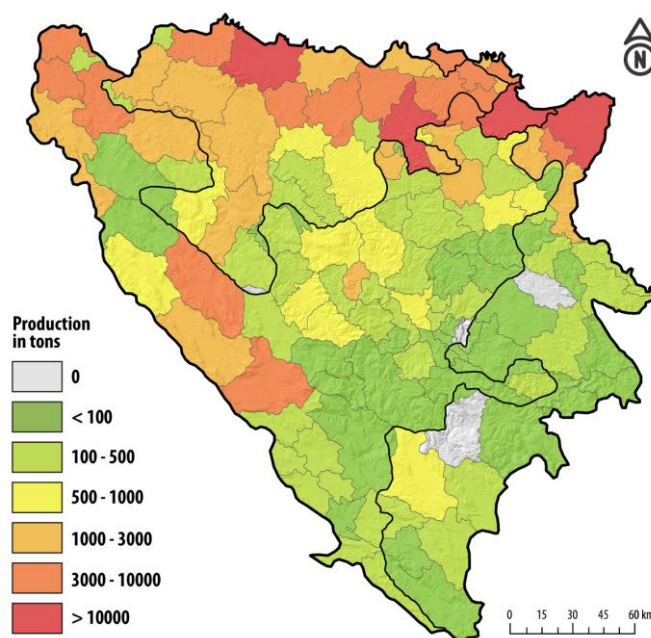

Figure 2. Average wheat production values for the period 2010–2019.

Significant wheat cultivation is also found in the middle and lower river valleys of Una, Sana, Vrbas, Bosna, and Drina, predominantly within local government units administratively belonging to Republika Srpska. In the Federation of Bosnia and Herzegovina, wheat production is most prevalent in the Posavski canton, Una-Sana canton, and Canton 10, while smaller quantities are produced in the Central Bosnia, Tuzla, and Zenica-Doboj cantons. Low levels of wheat production are observed in local government units located in the eastern part of Republika Srpska, as well as in Eastern and Western Herzegovina and the Sarajevo canton area.

According to official data from the Republika Srpska Institute of Statistics, there was no recorded wheat production in the municipalities of Kupres, Han Pijesak, and Kalinovik during the observed period. The Federal Institute for Statistics did not record wheat production in the urban municipalities of Centar, Stari Grad, and Novo Sarajevo. The local government unit with the highest average wheat production during the analyzed period was the City of Bijeljina, with an average production of 50,645 tons. Bijeljina recorded a peak production of 68,188 tons in 2017, accounting for 23.3% of the total wheat production in Bosnia and Herzegovina. The second-highest wheat-producing local government unit was Gradiška, with an average production of 13,855 tons during the observed period. The Brčko District had a slightly lower average wheat production (13,288 tons) compared to Gradiška, while the City of Doboj averaged a production of 10,622 tons. Other local government units in Bosnia and Herzegovina had annual wheat production figures below 10,000 tons during the observed period (Fig. 3).

The average annual wheat yield in Bosnia and Herzegovina was 3.66 tons per hectare. This yield is lower compared to neighboring Serbia (4.56 t/ha) and Croatia (5.6 t/ha), but higher than in neighboring Montenegro (FAOSTAT, 2022).
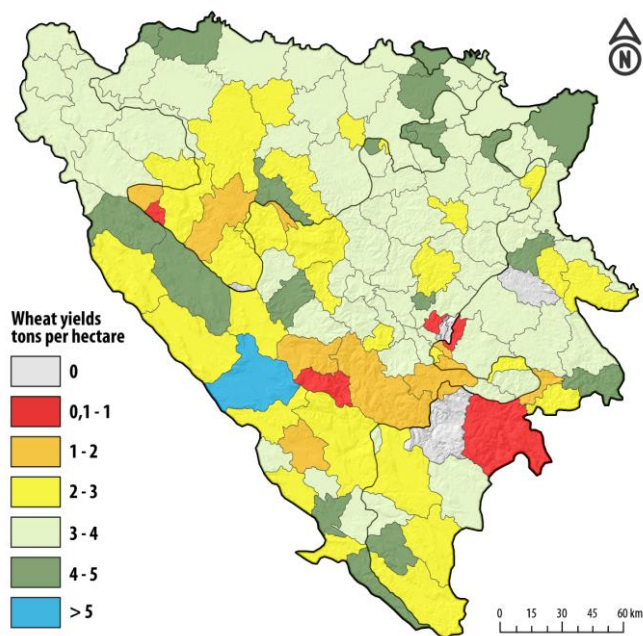

Figure 3. Average wheat yields for the period 2010–2017.

The lowest wheat yield for Bosnia and Herzegovina was recorded in 2010, at 2.7 t/ha, while the highest yield was noted in 2016, at 4.3 t/ha. During the observed period, the average wheat yield in Republika Srpska was 3.67 t/ha, whereas in the Federation of Bosnia and Herzegovina (3.63 t/ha) and the Brčko District (3.59 t/ha), the values were slightly lower. The average wheat yields per unit area showed an increasing trend

over the analyzed period. More than 50% of local government units have average annual wheat yields ranging from 3.1 to 4 tons per hectare. Slightly lower yields, ranging from 2.1 to 3 t/ha, were observed in 32 local government units. When examining the territory of Bosnia and Herzegovina, a pattern in average annual yields can be observed. The southern part of the Banja Luka region, which encompasses mountainous areas, exhibits wheat yields that are below the national average.

Areas with yields below the national average include the municipalities of Bosansko Grahovo, Livno, and Kupres, as well as most municipalities in Western and Eastern Herzegovina. In the eastern part of the country, lower average yields were observed in the municipalities of Srebrenica, Milići, and Čajniče. Across the rest of Bosnia and Herzegovina, average yields generally ranged between 3.1 and 4 tons per hectare. High average yields were noted in local government units located in Semberija and Posavina. Additionally, municipalities in Canton 10 (Drvar and Glamoč) and two municipalities in the Herzegovina-Neretva Canton (Čapljina and Ravno) also reported high yields. According to official statistics, the local government unit with the highest average yields during the observed period was Tomislavgrad, which averaged wheat yields of 6.03 t/ha.

Most local government units in Bosnia and Herzegovina have exhibited positive trends in increasing average wheat yields during the observed period. However, negative trends in yields have been identified in 15 local government units: Krupa na Uni, Petrovac, Istočni Drvar, Šipovo, Kotor Varoš, Gornji Vakuf, Busovača, Jablanica, Čapljina, Šekovići, Srebrenica, Rogatica, Pale, Trnovo (FBiH), and Trnovo (RS). The municipality of Sokolac has maintained constant yield values throughout the observed period.

Assessing the self-sufficiency of wheat production involves analyzing total wheat production and consumption. It is crucial to consider demographic dynamics, food consumption levels, and shifts in consumer preferences regarding specific food products during this analysis. Due to the insufficient number of input parameters necessary for calculating wheat consumption per capita for each year, this study has utilized values from the report "Analysis of Trends in Production, Foreign Trade, and Consumption of Basic Food Products for the Period 2014-2017," prepared by the Ministry of Agriculture, Water Management, and Forestry of Republika Srpska. According to this study, the average wheat consumption per capita was 162.9 kg, or 122.1 kg in flour equivalent. For further analysis, the value pertaining to consumption in flour equivalent was used.

The level of self-sufficiency in wheat production in Bosnia and Herzegovina during the analyzed period averaged 54.5% (Tab. 1). The highest average levels of self-sufficiency in wheat production were recorded in Brčko District (130.6%) and in Republika Srpska (109.3%).

Table 1. Estimation of wheat production self-sufficiency (in %) for the period 2010–2019.

Year	BiH	FBiH	RS	BD
2010	30,9	17,5	59,1	97,5
2011	44,8	23,8	91,3	107,6
2012	48,1	24,1	104,1	68,6
2013	61,7	26,9	125,8	88,4
2014	39,4	19,6	75,1	68,8
2015	49,6	26,6	89,4	137,7
2016	71,6	33,0	137,9	226,2
2017	68,2	28,6	139,9	177,1
2018	68,4	27,5	143,4	167,3
2019	62,1	26,5	126,8	167,4

These figures indicate that Brčko District and Republika Srpska are capable of fully meeting their wheat consumption needs through domestic production (Fig. 4). Conversely, the average self-sufficiency in wheat production in the Federation of BiH is markedly low, at only 25.4%, meaning that wheat production in the Federation of BiH can satisfy only a quarter of its population's consumption needs. Regarding the trends in self-sufficiency, it can be noted that both entities and Brčko District have shown positive trends over the analyzed period.
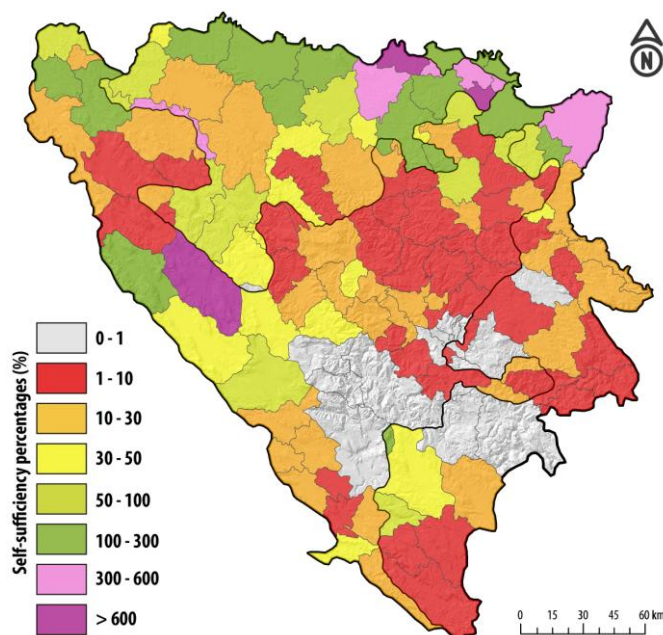

Figure 4. Assessment of wheat production self-sufficiency in local administrative units, 2010–2017.

Analyzing the average values of wheat production self-sufficiency in local administrative units, it can be concluded that 73.4% of these units have a self-sufficiency percentage below 50%. It is important to highlight that in Bosnia and Herzegovina, a total of 17 local administrative units have a self-sufficiency rate below 1%. Local administrative units that cannot meet the needs of their population with domestic production are: Han Pijesak, Pale, Trnovo (RS), Vogošća,

Ilidža, Sarajevo municipalities (Stari Grad, Novo Sarajevo, Novi Grad, and Centar), Istočno Novo Sarajevo, Foča, Kalinovik, Konjic, Mostar, Jablanica, Prozor, and Kupres (RS). These local administrative units are concentrated in the Sarajevo Canton, Herzegovina-Neretva Canton, Sarajevo-Romanija region, and the northern part of the Trebinje-Foča region. On the other hand, the analysis identified a total of 26 local administrative units where wheat production on their territory fully meets the consumption needs of the local population. Nine local administrative units even produce three times more than the needs of their local population. The municipalities with the highest levels of self-sufficiency in wheat production in Bosnia and Herzegovina are Glamoč (961%), Pelagićevo (778%), and Brod (699%).

CONCLUSION

Wheat production in Bosnia and Herzegovina between 2010 and 2019 exhibited a positive growth trend. Depending on climatic conditions, sown areas, applied agronomic measures, subsidies, and purchase prices in a given year, production varied from 145,000 to 307,000 tons during the observed period. The average wheat yield in Bosnia and Herzegovina stands at approximately 3.66 tons per hectare, which is lower compared to neighboring Serbia and Croatia. Wheat production is predominantly concentrated in the regions of Semberija, Posavina, and Lijevče polje, as well as the river valleys of Una, Sana, Vrbas, Bosnia, and Drina. Considering the entities, the Republic of Srpska accounts for about 64% of the total wheat production in Bosnia and Herzegovina.

The self-sufficiency in wheat production in Bosnia and Herzegovina is approximately 54%, indicating that domestic production covers just over half of the domestic consumption. It is important to note that a portion of the produced wheat is redirected for livestock feed due to lower prices, which implies that the effective self-sufficiency rate is somewhat lower than stated. Analysis of lower administrative units reveals that 73.4% of local administrative units in Bosnia and Herzegovina have a wheat self-sufficiency rate below 50%. This data is concerning, especially given that some local administrative units possess favorable spatial and production conditions for organizing and increasing wheat production. The wheat deficit in Bosnia and Herzegovina is covered by imports, mainly from Serbia, Croatia, and Hungary.

To enhance production, particularly wheat yields, it is essential for entity and cantonal ministries to continue their current activities aimed at supporting and improving production. Additionally, demographic trends, dietary habits, and a mild increase in wheat production suggest that the self-sufficiency rate in wheat production is expected to rise in the coming period.

REFERENCES

Agencija za statistiku BiH [ASBiH]. 2016. Popis stanovništva, domaćinstava i stanova u Bosni i Hercegovini 2013. godine. Sarajevo: Agencija za statistiku Bosne i Hercegovine.

Ahmetbegović, S., Stjepić Srkalović, Ž. & Gutić, S. 2015. Climate as a factor of population and settlements distribution in Bosnia and Herzegovina. Acta geographica Bosniae et Herzegovinae, 3, pp. 15-26.

Briggle, W. 1980. Origin and botany of wheat. In: Häfliger, E. (ed.) Wheat documenta cibageigy, Basle, pp. 6-13.

Clapp, J. 2017. Food Self-sufficiency and International Trend: A False Dichotomy. Rome: Food and Agriculture Organization of the UN (FAO). doi: 10.13140/RG.2.1.2447.2080

Dixon, J. 2007. The economics of wheat: research challenges from field to fork. In: Buck H, Nisi J, Salomon N (eds) Wheat production in stressed environments. Springer, Dordrecht, pp. 9–22. doi: 10.1007/1-4020-5497-1_2

Drašković, B., Berjan, S., Milić, V., Govedarica, B. & Radosavac, A. 2021. Structure of agricultural land losses in Bosnia and Herzegovina. Agriculture & Forestry, 67(1), pp. 91-101. doi: 10.17707/AgricultForest.67.1.08

Erenstein, O., Jaleta, M., Mottaleb, A., Sonder, K., Donovan, J. & Braun, H-J. 2022. Global trends in wheat production, consumption and trade. In: Reynolds, M., Braun, H-J. (eds). Wheat improvement – Food security in a changing climate, Springer. doi: 10.1007/978-3-030-90673-3_4

FAOSTAT. 2022. Production: Crops and livestock products. Rome: Food and Agriculture Organisation.

Food and Agriculture Organization of the United Nations. 2017. Guidelines for the compilation od food balance sheet. Rome: FAO

Jablonskyté-Raščé, D., Maikšténiené, S. & Mankevičiené, A. 2013. Evaluation of productivity and quality of common wheat (Triticum aestivum L.) and spelt (Triticum spelta L.) in relation to nutrition conditions. Zemdirbyste-Agriculture, 100(1), pp. 45-56. doi: 10.13080/z-a.2013.100.007

Jalić, N., Ostojić, A. & Vaško, Ž. 2021. Analysis and projections of wheat production i Bosnia and Herzegovina using ARIMA modelling. Albanian j. Agric. Sci., 20(3), pp. 20-26.

Kakaei, H., Nourmoradi, H., Bakhtiyari, S., Jalilian, M. & Mirzaei, A. 2022. Effect of COVID-19 on food security, hunger and food crisis. COVID-19 and the Sustainable Development Goals, 3(29). pp. 3-29. doi: 10.1016/B978-0-323-91307-2.00005-5

Kovačević, V. & Rastija, M. 2009. Osnove proizvodnje žitarica. Osijek: Sveučilište Josipa Jurija Strossmayera u Osijeku.

Leonard, H. & Martin, H. 1963. Cereal crops. New York: MacMillan Publishing.

Ministarstvo poljoprivrede, šumarstva i vodoprivrede Republike Srpske [MPVŠ]. 2018. Analiza trendova u proizvodnji, spoljnotrgovinskoj razmjeni i potrošnji osnovnih prehrambenih proizvoda za period 2014-2017. godina.

Mottaleb, K. A., Singh, P. K., Sonder, K., Kruseman, G., Tiwari, T. P., Barma, N., Paritosh, K. M., Hans-Joachim, B. & Olaf, E. 2018. Threat of wheat blast to South Asia's food security: An ex-ante analysis. PloS ONE, 13(5), e0197555. doi: 10.1371/journal.pone.0197555

Nuttonson, Y. 1955. Wheat-climatic relationships and the use of phenology in ascertaining the thermal and photothermal requirements of wheat. Washington DC: American Institute of Crop Ecology.

Oleson, B. 1996. World wheat production, utilization and trade. In: Bushuk, W., Rasper, V.F. (eds.). Wheat – Production, properties and quality. Springer Science, Dordrecht, pp. 1-11.

Ostojic, A., Vaško, Ž., Cvetković, M. & Pašalić, B. 2019. Fruit self-sufficiency assessment in Bosnia and Herzegovina. WBJAERD, 1(2), pp. 135-154. doi: 10.5937/WBJAE1902135O

Ostojic, A., Vasko, Ž. & Brković, D. 2020. Assessment of wheat self-sufficiency in Bosnia and Herzegovina. IX International Symposium on Agricultural Sciences AgroReS 2020. University of Banja Luka, Faculty of Agriculture, pp. 171-184.

Shiferaw, B., Smale, M., Braun, H., Duveiller, E., Reynolds, M. P. & Muricho, G. 2013. Crops that feed the world - Past successes and future challenges to the role played by wheat in global food security. Food Sci, 5, pp. 291–317. doi: 10.1007/s12571-013-0263-y

Singh, R. P., Hodson, D. P., Huerta-Espino, J., Jin, Y., Njau, P., Wanyera, R., Herrera-Foessel, S. A. & Ward, R. W. 2008. Will stem rust destroy the world's wheat crop? Advances in Agronomy, 98, pp. 271–309.

Thomson, A. & Metz, M. 1998. Implications of Economic Policy for Food Security: A Training Manual. Training Materials for Agricultural Planning no. 40, Rome: Food and Agriculture Organization of the UN (FAO).

Todorović, J., Lazić, B. & Komljenović, I. 2003. Ratarsko-povrtarski priručnik. Banja Luka: Grafomark.

Xiong, W., Asseng, S., Hoogenboom, G., Hernandez-Ochoa, I., Robertson, R., Sonder, K., Pequeno, D., Reynolds, M. & Gerard, B. 2020. Different uncertainty distribution between high and low latitudes in modelling warming impacts on wheat. Nat Food, 1, pp. 63–69. doi: 10.1038/s43016-019-0004-2

THE RELATIONSHIP BETWEEN GEODIVERSITY AND BIODIVERSITY – A THEORETICAL APPROACH

MARKO IVANOVIĆ[1]

[1]Faculty of Sciences and Mathematics, University of Priština in Kosovska Mitrovica, Kosovska Mitrovica, Serbia

ABSTRACT

The relationship between geodiversity and biodiversity is often considered within geoecological frameworks. Their interaction within real space forms the natural structure of landscapes. Although they are defined as two separate and equivalent systems with different structures, their relationship makes them interdependent, with geospatial distribution being the common point of contact. The term "geodiversity" is relatively recent, defined as the desire to express the opponent of the diversity of the living world – biodiversity. Thus, through a holistic concept, it is possible to observe multiple levels of interaction between geodiversity and biotic resources, revealing their interrelationship. The challenges of researching both geodiversity and biodiversity are characterized by similar shortcomings. Based on the previous researches of different authors, the work aims to define in the best possible way a biotic-abiotic relationship as an essential component in the concept of nature, the sphere of their connection and joint action. However, due to the numerous fields of their interaction, the work only partially defines them, without analyzing each field of interaction, in detail. In addition, the connection of these two concepts also requires interdisciplinary cooperation, the goal of which must be to improve the understanding of biodiversity and geodiversity, and their integration in evaluation, with the common goal of protecting and preserving nature as a whole and its individual parts. To a significant extent, these can be addressed through the application of geoinformatics tools, methods, and techniques, especially Remote Sensing (RS) and Geographic Information Systems (GIS), which offer the possibility of more adequate evaluation and interpretation of results.

Keywords: Geodiversity, Biodiversity, Connection, Interaction, Remote Sensing, GIS.

INTRODUCTION

Viewed through the lens of the holistic principle, the natural structure of the landscape can be characterized as an interaction between geodiversity and biodiversity. The general and most commonly cited opinion defining the relationship between geodiversity and biodiversity is that basically, geodiversity is often considered abiotic equivalent to biodiversity (Croft & Gordon, 2014). Geodiversity is the abiotic foundation or basis for the existing biodiversity, including humans, with abiotic elements providing the foundation for living nature by creating variations such as topographic and climatic conditions (Grey, 2013). According to Lješević (2002), the structural and quantitative-qualitative characteristics of biodiversity are largely in dependent relationships with the characteristics, i.e., the vertical structure of geodiversity, upon the basis of which biodiversity was built. The holistic approach involves viewing the natural environment as a whole rather than just its individual parts. Observing the natural environment through the lens of holism allows us to define and comprehensively understand geodiversity both within its internal structure and through its interaction with biodiversity.

Remote Sensing (RS) and Geographic Information Systems (GIS) are becoming powerful tools (Hrnjak et al.,

2014) for inputting, editing, analyzing, creating, and improving spatial data (Ivanović et al., 2023). Their multiplicity has been proven in numerous studies from various scientific fields of biological and geographical sciences. They can be a means to complete the relationship of two entities, within the natural structure of the landscape with protection and conservation as a common primary goal.

BIODIVERSITY AND GEODIVERSITY- HISTORY OF DEFINING THE TERMS

Originally, the concept "diversity" almost exclusively referred to biological diversity - biodiversity. As a term, it was first proposed in 1974 and scientifically established in 1980. It was internationally recognized only in 1992, as a term encompassing the conservation of the biosphere. At the United Nations Conference on Environment and Development in Rio de Janeiro, the Convention on Biological Diversity was defined. Represent a binding agreement on the inventory of plant and animal life, especially endangered species and those on the verge of extinction (Milentijević, 2021). On that occasion, the term "biodiversity" was defined as "the variability among living organisms from all sources, including, inter alia, terrestrial, marine, and other aquatic ecosystems and the ecological complexes of which they are part; this includes diversity within species, between species, and of ecosystems" (United Nations, 1993). At that time, great attention was given to protection on international, national, regional, and local

---

* Corresponding author: marko.ivanovic@pr.ac.rs
GEOGRAPHY, GEOSCIENCE AND ASTRONOMY

levels, as well as to increasing the biological diversity of planet Earth. In the following years, many countries created their own national plans for the protection and conservation of ecosystems and habitats of plant and animal species, their monitoring and sustainable management strategies are crucial. Biodiversity is classified at different levels- such as genetic diversity (preservation of the gene pool), species diversity (reduction or loss of species), and ecosystem diversity (maintenance and enhancement of habitats and their biological systems). However, since biodiversity does not represent just the number of species or ecosystems, but also refers to the countless interconnections between them (Grey, 2004), such views led to subsequent UN-sponsored conferences that more precisely defined biodiversity within specific types of ecosystems. Since then, more than 100 books have been published with "biodiversity" in the title, and E.O. Wilson, often known as the father of biology, has stated that this term poses some of the most fundamental problems in biological science (Grey, 2023).

As a result of the aforementioned conference about the environment in Rio de Janeiro, the term "geological and geomorphological diversity" increasingly appeared in geographic scientific literature, primarily as a "natural equivalent (twin) to the term 'biodiversity'" (Grey, 2004; Grey, 2008a; Grey, 2008b). It is difficult to determine when exactly this term started being used or who first coined it, but the year 1993 is often cited in the literature as pivotal in the use of the term "geodiversity." The publicity given to the concept of biodiversity at this conference attracted the attention of geographers to also study the diversity of geographical phenomena on our planet. Not long after, within a short period of time and independently of each other numerous geographers coined the term "geodiversity", making its (scientific) introduction become almost unavoidable (Grey, 2018).

According to Grey (2008a), the term "geodiversity" was first used in scientific publications in Germany and Australia. At the Malvern Conference (England) in 1993, Wiedenbein (1994) introduced the term, which is believed to have already been used within geological and geoecological contexts in German-speaking regions. Similar terminologies had been used much earlier within the Australian geological school. In the following years, in both European and Australian contexts, the definition of the term "geodiversity" became closely tied to its protection. Authors Serrano & Ruiz-Flaño (2007), note that the term "geodiversity" was actually conceived as early as the 1940s by Argentine geographer Federico Alberto Daus to describe "the mosaic of landscapes and cultural diversity of geographical space, and territorial complexity at different scales (locality, district, and region) related to human habitats" within the context of cultural geography. They also highlight that since the 1990s, the naturalistic concept of defining the term has prevailed. The concept of geodiversity was quickly accepted globally and emerged from the desire to shift from

the traditionally entrenched biocentric approach to environmental protection, towards a more scientifically sound holistic approach (Simić et al., 2010).

THE CONCEPT OF GEODIVERSITY

There are three main concepts related to the theory of geodiversity (Najwer & Zwolinski, 2014; Najwer et al., 2023).

Classical understandings evolved through the research work of Australian geologists and geomorphologists, which also included geoconservation (Sharples et al., 2018). In reports from commissions related to studies on the protection of areas in Tasmania and other parts of Australia, the term "geodiversity" was frequently used in publications. The term is based on previously used terminology dating back to the 1970s (such as "site", "form", "geological monument", "place", "area" and "significant geological phenomena"), which were linked to the certain features (Joyce, 2010). At that time, geologists and geomorphologists were attempting to describe the diversity of non-living nature- landform diversity or geomorphic diversity (Vasiljević, 2015) while Sharples (1993) used the term to encompass all "diversities of landforms and systems." After numerous debates and efforts to standardize terminology, several definitions of "geodiversity" emerged, with a few standing out:

- the connection between people, landscape, and culture; the diversity of geological environments, phenomena, and processes that form that landscape (relief), rocks, minerals, fossils, and soils that provided the framework for life on Earth" (Stanley, 2001);
- complex variations of rocky soil, soft sediments, landscapes, and processes that shape that landscape; the diversity of geological and geomorphological phenomena in a defined area" (Johansson, 2000).

As a result of years of continuous research on geological heritage, the Australian Heritage Commission (AHC, 2002) defines the term as "the range or diversity of geological (rocky soil), geomorphological (relief forms), and soil phenomena, structures, systems, and processes" (Gray, 2008a).

Within a second concept, geodiversity is considered the foundation for various analyses conducted on biodiversity, with the differentiation of the abiotic subsystem considered collaterally, usually as an auxiliary variable (Hjort et al., 2015; Ren et al., 2021). The third concept deviates from the classical (geological) definition of geodiversity and is characterized more broadly, including topography, elements of the hydrosphere, and human activities, among other factors (Najwer et al., 2023).

The beginning of the 21st century will mark a significant expansion in attempts to define the terminology for the study of shapes and forms, as well as the methodological evaluation of geodiversity. Authors Boothroyd & McHenry (2019) highlight that as many as 299 academic scientific articles are

related to the definition and evaluation of geodiversity. Earlier works attempting to define the terminology of geodiversity were authored exclusively by geologists who focused almost entirely on geodiversity terminology in the context of geology and geomorphology. It is noted that the incompleteness of such definitions prompted considerations of a broader perspective on this complex concept, defined as "geographical diversity of landscapes, not expressed solely through geological composition and morphological elements and processes" (Novković, 2008). The term geodiversity also refers to the "surface waters, as well as other systems created as a result of both natural (endogenous and exogenous) processes and human activities" (Kozlowski, 2004). Authors Simić et al. (2010), accept these ideas and expand the context of the term, defining geodiversity as "the diversity of the geographical environment, which is the result of geological, geographical, and anthropogenic influences".

The scientific debate over the definition of terminology has led to the publication of what is perhaps the most frequently cited definition. This, possibly the most holistic definition (Najwer et al., 2023), describes geodiversity as "the natural range (diversity) of geological (rocks, minerals, fossils), geomorphological (relief forms, topography, physical processes), soil, and hydrological phenomena. It also includes their compositions, structures, systems, and contributions to the landscape" (Gray, 2013). Around 88% of papers defining geodiversity, published between 1993 and 2019, support this definition or its similar variants (Boothroyd & McHenry, 2019).

Seeking to improve the definition promoted in M. Gray's works, many authors have tried to clarify certain parts of it in different contexts. In the publications of Ibañez et al. (1995) and Ibañez & Bockheim (2013), the term "pedodiversity" is emphasized as part of natural and cultural heritage. Based on earlier works, authors Panizza (2009) and Reynard et al. (2009), introduced the concepts of "geomorphodiversity" and "geomorphosite". The works of Ferrarin et al. (2014), Rosa et al. (2018), and Gil-Márquez et al. (2022), prefer the term "hydrodiversity" whose related to the natural and cultural heritage. In the work of Doherty et al. (2021), "topodiversity" is used to define topography. On the other hand, Grey (2023) views the term "geodiversity" as an abbreviation for "geoscientific diversity", considering that it encompasses not only geological phenomena but has a much broader meaning.

Considering all aspects of defining geodiversity, it can be concluded that although the pioneering interpretations of the term were linked to geological diversity. It also encompasses all geomorphological, pedological, and hydrological forms and phenomena, resulting from exogenous and endogenous forces, tectonic processes as well as hydrological (hydrogeological) phenomena and processes. In some scientific perspectives, this term also includes climatic processes and specificities. Regarding the Republic of Serbia, the Low on Environmental Protection of 2021 (Official Gazette of the RS, 71/2021), defines the term "geodiversity" at first as "geological diversity" and as the presence or distribution of diverse elements and forms of geological structures, geological formations and processes, geochronological units, rocks, and minerals of various compositions and origins, and diverse paleoecosystems changed in space under the influence of internal and external geodynamic factors during geological time.
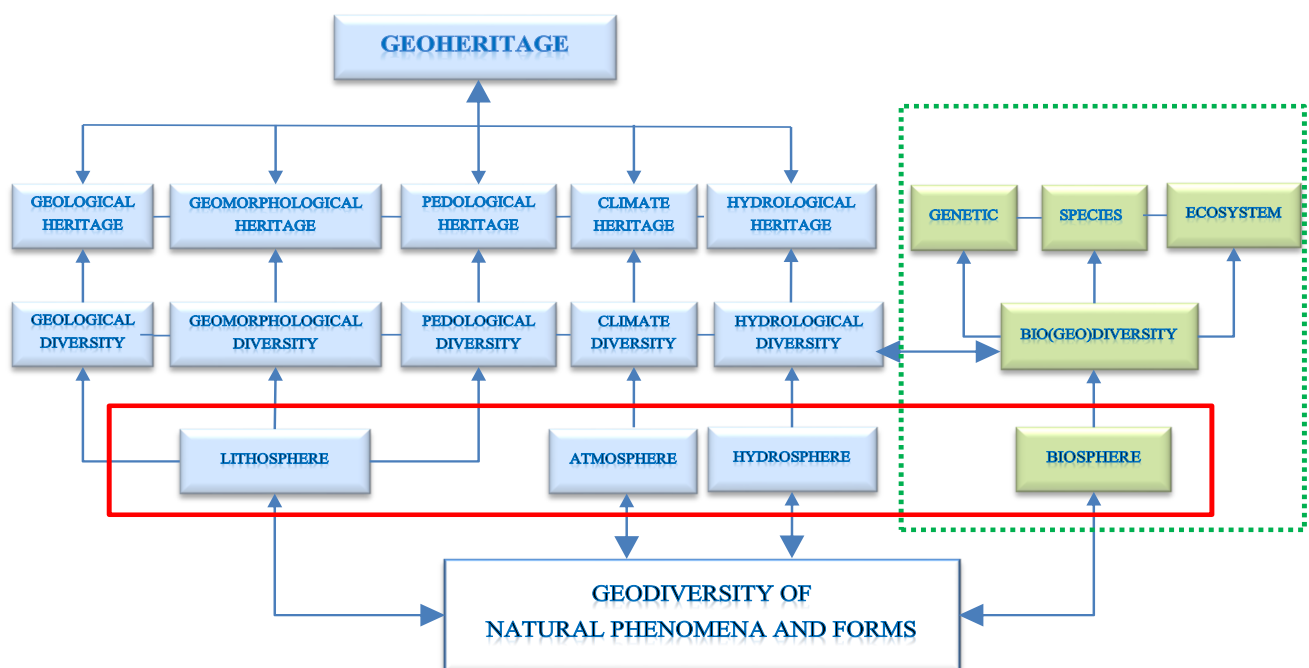

Figure 1. Schematic representation of the relationship between geodiversity and biodiversity (based on Simić et al., 2010; Miljković, 2018).

Following the holistic approach of a unified, mutually dependent system of "bio-geo-diversity," discussions about the subject of research have evolved. According to Lješević (2002), geodiversity consists of two major components: the geodiversity of natural phenomena and forms, and the geodiversity of civilization. The geodiversity of natural phenomena and forms (Figure 1) is of interest to experts in the Earth sciences. It is represented by geological diversity, geomorphological diversity, climatic diversity, hydrological diversity, soil diversity, and bio-geo-diversity.

SYSTEMIC RELATIONSHIP BETWEEN GEODIVERSITY AND BIODIVERSITY

The overall relationship between bio- and geo-diversity can be viewed through two categories (levels) of relationships. The first category focuses on the theoretical approach to interaction, defined through fields of overlap and joint action in the natural environment. Santucci (2005) considers that bio- and geo-diversity overlap and cites several areas of influence where geological resources and geodiversity impact biotic resources, which illustrates the full meaning of their mutual interconnection, with which Vasiljević (2015) also agreed:

- **Climate**- Climatic elements can influence the morphology of geological forms and the intensity of processes at a local level. Precipitation and temperature can affect certain processes (erosion, denudation, rock decomposition, etc.);
- **Hydrology**- The hydrology of geospace is largely conditioned by geological and geomorphological characteristics. Drainage areas, watersheds, aquifers, springs related to lithographic and stratigraphic contacts, and geomorphological features, such as karst topography, periglacial zones, and landslides, are examples. Biodiversity can also be influenced by water's chemical properties, salinity, and other hydrological features;
- **Soil**- Soil serves as the link between the abiotic and biotic world. Its composition and chemical properties are directly connected to the bedrock. Consequently, the distribution of many plant species depends on the mineralogical and chemical composition of the soil;
- **Biogeographical Distribution**- The geographical distribution of the ranges of flora and fauna can often be linked to geodiversity. Surface geomorphology frequently influences geographical distribution and migration routes. Mountain ranges, canyons, deserts, and water bodies are just some geological forms that can act as migration corridors but also as barriers;
- **Habitats**- The diversity of geological characteristics and processes provides an almost infinite range of habitat types for sustaining life. Changes in elevation between intermontane basins and mountain ranges typically encompass multiple life zones. Geothermal springs provide the nutrients and temperature necessary for certain bacterial forms. Cave openings, sloping landslides, and gypsum sand offer habitats for species adapted to these environments.

Altitude and the topographic characteristics of a geospace can significantly impact its biodiversity. Altitude greatly influences climatic conditions, and together with topographic features, it can significantly affect the hydrological parameters of an area and changes in soil cover. It is known that changes in altitude affect the ranges of flora and fauna, creating specific habitats.

In line with this, when discussing the overlap of two equivalent systems, it can be concluded that spatial distribution is the point of interaction where the two systems overlap. It is a fact that biodiversity and geodiversity represent individual systems, while their point of contact is defined solely through the spatial diversity and distribution of biodiversity, and only then can biodiversity be considered as part of geodiversity (Lješević, 2002). However, spatial distribution can be reflected on two levels. Horizontal spatial distribution refers to the area as a geographical surface- the territory it occupies. Under the influence of altitude, ranges can shift or change, which allows us to speak of spatial distribution in a vertical sense.

The difference in complexity is reflected on multiple levels. Often, the number of geodiversity elements in a given area is much greater than the number of plant species, with some geodiversity elements varying in composition (type) as well as in the percentage of participation of those types. Classification issues also arise, even though "international and national classifications exist" (Gray, 2023). Authors Ibáñez & Brevik (2022), are among the scientists who identify the problem of classification in geodiversity research, emphasizing that "unlike biodiversity and soil diversity, there is no universal classification in lithology and geomorphology" and that "studies dealing with geodiversity do not pay much scientific attention to the analysis and quantification of Earth's surface systems, as is the case in biodiversity studies".

The second category of relations is related to the practical approach. It implies the creation of common methods and techniques for conducting research, analysis and evaluation within the common framework of the geoecological context. The common goal of research and evaluation of both geodiversity and biodiversity is protection and conservation. Geodiversity has an important ecological value in supporting biodiversity and ecosystem functioning so the conservation of geosites and geodiversity has a fundamental role in preserving protected areas as an integral part of nature and natural heritage. Consequently, geoconservation is crucial for sustaining living species and habitats, both to maintain the abiotic setting or 'stage' and the natural processes (e.g. floods, erosion and deposition) necessary for habitat diversity and ecological functions (Croft, 2019).

Authors Zwolinski et al. (2018), explain that the evaluation process begins with classification, i.e., identifying individual entities or phenomena, followed by the selection of criteria that influence the choice of method and the selection of materials- information or digital data. So far, the methodological intentions of scholars have focused on evaluating geodiversity independently, irrespective of biodiversity (Tukiainen et al., 2023). A similar approach is taken from the aspect of biodiversity valuation, in which spatial distribution is taken into account and, to a very small extent, geodiversity as a key basis.

This also initiates the issue of measurement since, although geodiversity represents the totality of the abiotic nature of an area, measuring the overall wealth can be extremely difficult and time-consuming. As a result, measurements are often focused on studying geological, topographical, hydrological, pedological, and/or satellite imagery in smaller areas (Gray, 2023). Measurements may also pertain to geomorphological and climatic phenomena and forms that can be considered parts of geodiversity.

The assessment of geodiversity can be qualitative (descriptive methods), quantitative (valuation of geodiversity indices, metrics or statistical modeling) or qualitative–quantitative (combination of quantitative (i.e., digital) data and cause-effect (i.e., relational and explanatory) data (Zwoliński et al., 2018). However, in a review of quantitative geodiversity assessment Crisp et al. (2021), found that half of 534 publications assessed geodiversity independently, and only 12% of them strongly linked biodiversity to geodiversity. The remaining one-third of the reviewed publications discussed or reviewed biodiversity without strong empirical objectives.

The challenges of geodiversity research are more pronounced compared to those of biodiversity research. The issue lies in the much greater complexity of geodiversity, which significantly affects the challenges of assessing it.

Methods and techniques of RS, GIS, and the application of Digital Elevation Models (DEM), play a significant role in assessing geodiversity, providing opportunities for substantial revision of methodologies (Stojilković, 2022). Therefore, the use of geoinformatics tools, methods, and techniques can significantly address the challenges of researching both geodiversity and biodiversity, improving measurement, evaluation, and interpretation of results. GIS systems have the capability of storing large quantities of spatiotemporal data, enabled by advances in computing and geoinformation technologies. Automated algorithmic software processes shorten the time period, significantly enhancing the evaluation concept. The final result emphasizes the cartographic visualization of spatial distribution. This makes Geographic Information Systems (GIS) an indispensable tool in spatial visualization and analysis of results from numerous geostatistical methods in modern environmental research, even

at the macro level, thus significantly mitigating research challenges.

Quantitative assessments of geodiversity can be derived from field measurements, numerical calculations or geospatial analyses of raw data (Zwoliński et al., 2018). In geodiversity–biodiversity studies, geodiversity is commonly assessed with statistical tools (Crisp et al., 2021). Different types of RS or GIS based datasets are preferred as the source of geodiversity information (Boothroyd & McHenry, 2019). For instance, the statistical Geosite Assessment Model (GAM) and GIS-based isochronous method were used for the assessment of geosites in Toplica district (Serbia) for the purpose of geotourism development (Ivanović, et al, 2023); techniques of watershed delineation and multi-criteria decision analysis (MCDA) were used for GIS and Spatial analysis of population dynamics and water stress impact on Africa's River Systems (Valjarević, 2024); GIS-based methods and RS with geostatistical method were used for identifying river network types and changing river basins border in Serbia (Valjarević, 2024). Whereas this is an example of a resource-efficient way of quantifying geodiversity and exploring geodiversity–biodiversity relationships, identifying and choosing appropriate materials and methods (for appropriate scale and for the specific objectives of each study) require constant careful consideration (Gray 2021; Tukiainen et al., 2023).

CONCLUSION

In earlier scientific studies, the terms biodiversity and geodiversity were long regarded separately, with clear distinctions between the worlds of living and non-living nature. However, observing the natural environment through the lens of holistic philosophy reveals that these two equivalents, although distinct, actually share several fields of mutual interaction. A large number of studies linking geo- and bio-diversity emphasize the positive connection between these two basic parts of nature. Improving the understanding of their connections is the task of research in several scientific disciplines, from ecology to geographic disciplines that study the Earth, the environment, and the protection and preservation of nature. However, much remains to be explored in this relatively new field of research.

The paper provides an overview and defines mutual relations on a theoretical and practical level as well as the common characteristics of these entities of nature. It also presents new methods and techniques that provide a way and a direction to fill the gaps in geodiversity and biodiversity. In this way, the joint interaction of these entities in nature would be more adequately investigated, taking into account all factors.

Geodiversity is considered the foundation on which life, including human life, rests. It does not only encompass geological diversity but is a much more complex concept that includes broader geographical and anthropogenic components. Topography and hypsometric characteristics, climatic features

(especially local microclimates), hydrographic features, and soil composition, can significantly influence the biogeographical distribution of living organisms and the extent of their habitats. At the same time, biodiversity, through its presence in a geographic space, significantly contributes to the preservation of geodiversity characteristics- it optimizes climatic conditions (reducing soil temperature and preventing excessive soil drying), prevents denudation, ravines, and landslides, and reduces deflation, thereby ensuring the stability of geodiversity. Based on this view, these two equivalents can be viewed as part of the natural environment or geo-biosystem with similar research problems. Therefore, the principle of holism provides us with a way to conduct research in the natural environment, taking into account the cause-effect relationships of these equivalents.

However, the real challenge in the current geo-bio-diversity relationship is the multiplicity of ways of classifying, qualifying and measuring geodiversity. This type of problem is expressed to a lesser extent in the field of biodiversity. The concept of geodiversity is still in development, which is the reason for the absence of unique terminological and methodological definitions. In terminological frameworks in the literature, the interpretation of geodiversity as a holistic "geoscientific diversity" is often preferred. At the same time, in the more flexible qualifications of geodiversity, it increasingly approaches the geoecological and biological context by including climatic and biogeographical diversity, which significantly affects the methodological complexity and variability in scientific studies. A clear definition of terminology and concepts is the starting point for a better understanding of the relationship between geo- and biodiversity, which should be insisted upon, and what further initiates the importance of unifying and harmonizing the methodology. Unique approaches to measuring both diversities would be particularly useful for nature conservation and management. Also from the aspect of biodiversity, there is a noticeable absence of research on the connections of different groups of organisms with geodiversity, so more attention should be paid to research of that nature.

One of the ways of bridging methodological problems that would correct the gap between geodiversity and biodiversity is the application of geoinformatics methods and techniques, especially RS and GIS. Geoinformatics methods are interdisciplinary in nature, so their application has already been widely applied in numerous geographic and biological studies of evaluation and protection. The preservation and management of geodiversity and biodiversity urgently needs additional tools, the application of which can be of a global character, but which can also be used to investigate local changes. As geodiversity can be considered an initiator of biodiversity conservation, one of its advantages is the availability of data on geodiversity at different scales. While biodiversity data are globally sparse and concentrated, some geodiversity data can be relatively easily accessible through GIS databases or Remote Sensing techniques. Taking into account the meaning of geoinformatics methods and

techniques, they can be a means by which the shortcomings of descriptive and statistical methods are eliminated and enable a more adequate evaluation, analysis and geo-visualization of the results.

The main change towards a better understanding of the interaction and protection of geodiversity and biodiversity must be based on more effective communication and interdisciplinary cooperation of experts, identification of common goals and joint action. Therefore, joint actions are necessary because the common interest is the preservation and protection of nature.

REFERENCES

Australian Heritage Commission (AHC). 2002. Australian Natural Heritage Charter for the conservation of places of natural heritage significance. Canberra: Commonwealth of Australia, 2nd ed.

Boothroyd, A. & McHenry, M. 2019. Old processes, new movements: the inclusion of geodiversity in biological and ecological discourse. Diversity, 11(11), 216. https://doi.org/10.3390/d11110216

Crisp, J. R., Ellison, J. C. & Fischer, A. 2021. Current trends and future directions in quantitative geodiversity assessment. Progress in Physical Geography: Earth and Environment, 45, pp. 514-540. https://doi.org/10.1177/0309133320967219

Crofts, R. & Gordon, J. E. 2014. Geoheritage conservation in protected areas. Parks, 20(2), pp. 61-76. http://dx.doi.org/10.2305/IUCN.CH.2014.PARKS-20-2.RC.en

Crofts, R. 2019. Linking geoconservation with biodiversity conservation in protected areas. International Journal of Geoheritage and Parks, 7(4), pp. 211-217. https://doi.org/10.1016/j.ijgeop.2019.12.002

Doherty, K. D., Kuhlman, M. P., Durham, R. A., Ramsey, P. W. & Mummey, D. L. 2021. Fine-grained topographic diversity data improve site prioritization outcomes for bees. Ecological Indicators, 132, 108315. https://doi.org/10.1016/j.ecolind.2021.108315

Ferrarin, C., Bajo, M., Bellafiore, D., Cucco, A., De Pascalis, F., Ghezzo, M. & Umgiesser, G. 2014. Toward homogenization of Mediterranean lagoons and their loss of hydrodiversity. Geophysical Research Letters, 41(16), pp. 5935-5941. https://doi.org/10.1002/2014GL060843

Gil-Márquez, J. M., Andreo, B. & Mudarra, M. 2022. Studying hydrogeochemical processes to understand hydrodiversity and the related natural and cultural heritage.

The case of Los Hoyos area (South Spain). Catena, 216, B, 106422. https://doi.org/10.1016/j.catena.2022.106422

Gray, M. 2004. Defining Geodiversity. In: Geodiversity: Valuing and Conserving Abiotic Nature: John Wiley & Sons, Chichester, UK. 2004; pp. 1-9.

Gray, M. 2008a. Geodiversity: developing the paradigm. Proceedings of the Geologists' Association, 119, pp. 287-298. https://doi.org/10.1016/S0016-7878(08)80307-0

Gray, M. 2008b. Geodiversity: A new paradigm for valuing and conserving geoheritage: Geoscience Canada, 35, 2, pp. 51-59. https://id.erudit.org/iderudit/geocan35_2ser01

Gray, M. 2013. Geodiversity: valuing and conserving abiotic nature: John Wiley & Sons, Chichester, UK, 2nd edition.

Gray, M. 2018. Geodiversity: the backbone of geoheritage and geoconservation. In: Geoheritage, pp. 13-25. https://doi.org/10.1016/B978-0-12-809531-7.00001-0

Gray, M. 2021. Geodiversity: a significant, multi-faceted and evolving, geoscientific paradigm rather than a redundant term. Proceedings of the Geologists' Association, 132, pp. 605-619. https://doi.org/10.1016/j.pgeola.2021.09.001

Gray, M. 2023. Some observations and reflections on geodiversity, the oft-forgotten half of nature. In: Kubalíková, L., Coratza, P., Pál, M., Zwoliński, Z., Irapta, P. N. & van Wyk de Vries, B. (eds). Visages of Geodiversity and Geoheritage. Special Publications: Geological Society, London, 530, pp. 31-47. https://doi.org/10.1144/SP530-2022-100

Kozlowski, S. 2004. Geodiversity. The concept and scope of geodiversity. Polish geological review (Przeglad geologiczny), 52(8/2), pp. 833-839.

Hjort, J., Gordon, J. E., Gray, M. & Hunter, M. L. 2015. Why geodiversity matters in valuing nature's stage. Conservation Biology, 29, pp. 630-639. https://doi.org/10.1111/cobi.12510

Hrnjak, I., Lukić, T., Gavrilov, M., Marković, S., Unkašević, M. & Tošić, I. 2014. Aridity in Vojvodina, Serbia. Theor Appl Climatol. 115, pp. 323-332. https://doi.org/10.1007/s00704-013-0893-1

Ibañez, J. J., De-Albs, S., Bermúdez, F. F. & García-Álvarez, A. 1995. Pedodiversity: concepts and measures. Catena, 24(3), pp. 215-232. https://doi.org/10.1016/0341-8162(95)00028-Q

Ibáñez, J. J. & Bockheim, J. G. 2013. Pedodiversity: CRC Press.

Ibáñez, J. J. & Brevik, E. C. 2022. Geodiversity research at the crossroads: two sides of the same coin. Spanish Journal of Soil Science, 12, 10456. https://doi.org/10.3389/sjss.2022.10456

Ivanović, M., Lukić, T., Milentijević, N., Bojović, V. & Valjarević, A. 2023. Assessment of geosites as a basis for geotourism development: A case study of the Toplica District, Serbia. Open Geosciences, 15(1), 20220589. https://doi.org/10.1515/geo-2022-0589

Johansson, C. E. 2000. Geodiversitet i Nordisk Naturvard: Nordisk Ministerr°aad, Copenhagen.

Joyce, E. B. 2010. Australia's geoheritage: history of study, a new inventory of geosites and applications to geotourism and geoparks. Geoheritage, 2, pp. 39-56. https://doi.org/10.1007/s12371-010-0011-z

Lješević, M. A. 2002. Geodiversity as a condition of the environment, Collection of Papers Faculty of Geography at the University of Belgrade, 50, pp. 17-32.

Najwer, A. & Zwoliński, Z. 2014. Semantyka i metodyka oceny georóżnorodnoscí – przegląd i propozycja badawcza. Landform Analysis, 26, pp. 115-127. http://dx.doi.org/10.12657%2Flandfana.026.011

Najwer, A., Reynard, E. & Zwoliński, Z. 2023. Geodiversity assessment for geomorphosites management: Derborence and Illgraben, Swiss Alps: Geological Society, London, Special Publications, 530, 1, pp. 89-106. https://doi.org/10.1144/SP530-2022-122

Novković, I. 2008. Geoharitage of Zlatibor district: Zaštita prirode, 58(1-2), pp. 37-52.

Milentijević, N. 2021. Vrednovanje geoekoloških determinanti Bačke u funkciji održivog razvoja. Doctoral dissertation, University of Novi Sad (Serbia).

Miljković, Đ. 2018. Geomorfološko i hidrološko geonasleđe Homolja. Doctoral dissertation, University of Novi Sad (Serbia).

Official Gazette of the RS (No. 36/2009, 88/2010, 91/2010 - correct, 14/2016, 95/2018 – and other, 71/2021). https://www.paragraf.rs/propisi/zakon_o_zastiti_prirode.html Accessed: 31.11.2024.

Panizza, M. 2009. The geomorphodiversity of the Dolomites (Italy): a key of geoheritage assessment. Geoheritage, 1(1), pp. 33-42. https://doi.org/10.1007/s12371-009-0003-z

Ren, Y., Lü, Y., Hu, J. & Yin, L. 2021. Geodiversity underpins biodiversity but the relations can be complex: implications from two biodiversity proxies. Global Ecology and Conservation, 31, e01830. https://doi.org/10.1016/j.gecco.2021.e01830

Reynard, E., Coratza P. & Regolini-Bissig. 2009. Geomorphosites: Verlag Dr. Friedrich Pfeil, München.

Rosa, E., Dallaire, P. L., Nadeau, S., Cloutier, V., Veillette, J., van Bellen, S. & Larocque, M. 2018. A graphical approach for documenting peatland hydrodiversity and orienting land management strategies. Hydrological Processes, 32(7), pp. 873-890. https://doi.org/10.1002/hyp.11457

Serrano, E. & Ruiz-Flaño, P. 2007. Geodiversity: a theoretical and applied concept. Geographica Helvetica, 62(3), pp. 140-147. https://doi.org/10.5194/gh-62-140-2007

Sharples, C. 1993. A Methodology for the Identification of Significant Landforms and Geological Sites for

Geoconservation Purposes: Forestry Commission, Tasmania.

Sharples, C., McIntosh, P. & Comfort, M. 2018. Geodiversity and geoconservation in land management in Tasmania- a top-down approach. In: Reynard, E. and Brilha, J. (eds) Geoheritage: Assessment, Protection, and Management:, pp. 355-371. Elsevier. https://doi.org/10.1016/B978-0-12-809531-7.00020-4

Simić, S., Gavrilović, Lj. & Đurović, P. 2010a. Geodiversity and geoheritage: a new approach to the interpretation of the terms: Bulletin of the Serbian Geographical Society, 90(2), pp. 1-14.

Stanley, M. 2001. Welcome to the 21st century: Editorial. Geodiversity Update, 1, 1.

Stojilković, B. 2022. Towards transferable use of terrain ruggedness component in the geodiversity index. Resources, 11(2), 22. https://doi.org/10.3390/resources11020022

Tukiainen, H., Toivanen, M. & Maliniemi, T. 2023. Geodiversity and biodiversity . In: Kubalíková, L., Coratza, P., Pál, M., Zwoliński, Z., Irapta, P. N. and van Wyk de Vries, B. (eds). Visages of Geodiversity and Geoheritage. Geological Society, London, Special Publications, 530, pp. 31-47. https://doi.org/10.1144/SP530-2022-107

United Nations. 1993. Report of the United Nations Conference on Environment and Development, Rio de Janeiro, 3-14 June 1992: United Nations, New York.

Valjarević, A. 2024. Population Dynamics and Water Stress: Analyzing Impacts on Africa's River Systems Through GIS and Spatial Analysis. Available at SSRN http://dx.doi.org/10.2139/ssrn.5010532

Valjarević, A. 2024. GIS-Based Methods for Identifying River Networks Types and Changing River Basins. Water Resources Management, pp. 1-19. https://doi.org/10.1007/s11269-024-03916-7

Vasiljević, Đ. A. 2015. Geodiverzitet i geonasleđe Vojvodine u funkciji zaštite i turizma. Doctoral dissertation, University of Novi Sad (Serbia).

Wiedenbein, F.W. 1994. Origin and use of the term 'geotope' in German-speaking countries. In: O'Halloran, D., Green, C., Harley, M., Stanley, M. & Knill, J. (eds) Geological and Landscape Conservation: Geological Society, London, pp. 117-120.

Zwoliński, Z., Najwer, A., & Giardino, M. 2018. Methods for assessing geodiversity. In: Reynard, E. & Brilha, J. Geoheritage: Assessment, Protection and Management, 1st edition: Elsevier, Amsterdam, pp. 27-52. https://doi.org/10.1016/B978-0-12-809531-7.00002-2

RESTRICTED AND EXTENDED THETA OPERATIONS OF SOFT SETS: NEW RESTRICTED AND EXTENDED SOFT SET OPERATIONS

ASLIHAN SEZGİN[1*], FİTNAT NUR AYBEK[2]

[1]Faculty of Education, Amasya University, Amasya, Türkiye
[2]Graduate School of Natural and Applied Sciences, Amasya University, Amasya, Türkiye

ABSTRACT

Since its introduction by Molodtsov in 1999, soft set theory has gained widespread recognition as a method for addressing uncertainty-related issues and modeling uncertainty. It has been used to solve several theoretical and practical issues. Since its introduction, the central idea of the theory-soft set operations-has captured the attention of scholars. Numerous limited and expanded businesses have been identified, and their attributes have been scrutinized thus far. We present a detailed analysis of the fundamental algebraic properties of our proposed restricted theta and extended theta operations, which are unique restricted and extended soft set operations. We also investigate these operations' distributions over various kinds of soft set operations. We demonstrate that, when coupled with other types of soft set operations, the extended theta operation forms numerous significant algebraic structures, such as semirings in the collection of soft sets over the universe, by taking into account the algebraic properties of the extended theta operation and its distribution rules. This theoretical subject is very important from both a theoretical and practical perspective since soft sets' operations form the foundation for numerous applications, including cryptology and decision-making procedures.

Keywords: Soft sets, Soft set operations, Restricted theta operation, Extended theta operation.

INTRODUCTION

The real world is filled with a lot of uncertainty. Conventional mathematical reasoning is unable to tackle these issues. More scientific investigation that goes beyond the capability of currently accessible methodologies has been necessary to dispel these uncertainties. In this sense, Pascal and Fermat created the theory of probability in the early 17th century when they conducted an analytical study of the uncertainty problem. In the early 1800s, a large number of scientists investigated uncertainty.

Many values were discovered as a result of Heisenberg's 1920 explanation, which was the first to explain uncertainty. Early in the 1930s, Lukaisewicz developed the first three-valued logic system. A few theories that may be used to describe uncertainty include probability theory, interval mathematics, and fuzzy set theory; however, each of these theories has drawbacks of its own. Thus, the concept of "Soft Set" was first proposed by Molodtsov (1999) and has nothing to do with how the membership function evolved. While soft set theory utilizes a set-valued function instead of a real-valued one, fuzzy set theory aims to eliminate ambiguity. This idea has been successfully applied in several mathematical fields since its conception, such as Riemann integration, Perron integration analysis, game theory, probability theory, and measurement theory.

Soft set operations were first studied by Maji et al. (2003) and Pei and Miao (2005). Ali et al. introduced a number of soft set operations (2009), including restricted and extended soft set operations. In their work on soft sets, Sezgin & Atagün (2011) established and gave the characteristics of the restricted symmetric difference of soft sets. They also explored the principles of soft set operations and gave illustrations of how they relate to one another. A thorough examination of the algebraic structures of soft sets was carried out by Ali et al. (2011). A number of academics were interested in soft set operations and conducted extensive studies on the subject in (Yang, 2008; Neog & Sut, 2011; Fu, 2011; Ge & Yang, 2011; Singh & Onyeozili, 2012a; Singh & Onyeozili, 2012b; Singh & Onyeozili, 2012c; Singh & Onyeozili, 2012d; Husain et al., 2018).

In recent years, a wide variety of novel soft set operations have been implemented. The idea and characteristics of the soft binary piecewise difference operation in soft sets were initially presented and examined by Eren & Çalışıcı (2019). Sezgin et al. (2019) introduced the extended difference of soft sets, while Stojanovic (2021) characterized the extended symmetric difference along with its properties. Furthermore, a comprehensive examination of restricted and extended symmetric difference operations was carried out by Sezgin & Çağman (2024). Sezgin et al. (2023c) worked on numerous new binary set operations and defined several more, inspired by the work of Çağman (2021), who introduced two new complement

*Corresponding author: aslihan.sezgin@amasya.edu.tr

MATHEMATICS, COMPUTER SCIENCE AND MECHANICS

operations to the literature. Using this method, Aybek (2024) proposed several new restricted and extended soft set operations. Three authors, Akbulut (2024), Demirci (2024), and Sarıalioğlu (2024), focused on complementary extended soft sets operations in their attempts to alter the structure of extended operations in soft sets. Other types of soft set operations, complementary soft binary piecewise operations, were further investigated by (Sezgin & Aybek, 2023; Sezgin & Akbulut, 2023; Sezgin & Dagtoros, 2023; Sezgin & Demirci, 2023; Sezgin & Sarıalioğlu, 2024; Sezgin & Yavuz, 2023a; Sezgin et al., 2023a; Sezgin & Atagün, 2023; Sezgin & Çağman, 2024). In addition, Sezgin & Çalışıcı (2024) carried out a comprehensive analysis of the soft binary piecewise difference operation, while Sezgin & Yavuz (2023) and Yavuz (2024) investigated other soft binary piecewise operations.

Classifying algebraic structures and finding, representing, and drawing inferences from their common features are the goals of abstract algebra. The name of the abstract algebra used in this area of mathematics is due to this. Mathematicians have studied algebraic structures for millennia because they offer an abstract and universal foundation for learning and understanding mathematical topics. Many branches of mathematics depend on algebraic structures. There are several significant applications of algebraic structures, such as rings, groups, and fields, in mathematics as well as other disciplines like computer science and physics. The foundation for comprehending increasingly difficult mathematical ideas is laid by the frameworks of algebraic geometry (the study of multivariable polynomial solutions), algebraic topology, modular arithmetic, physics, number theory, and computer graphics, among other extremely significant subjects. Moreover, a foundation for comprehending and researching a broad variety of mathematical objects and their relationships is provided by mathematical structures.

Groups have applications in physics, chemistry, and cryptography and are used to study symmetries, rotations, and transformations in mathematical contexts. Studying the symmetries of fascinating geometric objects and forms requires an understanding of fundamental groups and their representations as group transformations, which are fundamental algebraic structures. Abstract algebra, coding theory, and number theory all make use of rings. Geometry and other mathematical topics require a solid understanding of field algebra. Engineering, quantum physics, and linear algebra all employ vector spaces. Algebra is used in computer science, physics, and mathematical reasoning. Both representation theory and abstract algebra make use of modules. Moreover, abstract algebra, which examines the shared structures and common features of many algebraic systems, is centered on the study of algebraic structures. By knowing these systems' features, mathematicians may create new theories, solve challenging problems, and apply ideas to a variety of

mathematical, scientific, and technical fields. Additionally, special cases of algebraic structures are frequently provided in applications, which make it easier to look at more general cases and help make sense of specific ones.

Near-rings, semirings, and semifields are a few of the most well-known binary algebraic structures, which are the generalizations of rings. For a very long time, academics have been keen to understand more about this subject. Ever since Vandiver (1935) introduced the concept of semirings, a number of researchers have studied it. Semirings are very important in mathematics and have many applications, according to Vandiver (1935). In addition to its significance in geometry, semirings have several applications in the information sciences and practical mathematics (Vandiver, 1935). Semirings are important in pure mathematics and geometry, and they are useful in many other fields as well (Ghosh, 1996; Wechsler, 1978; Golan, 1999; Hebisch & Weinert, 1998; Mordeson & Malik, 2002; Kolokoltsov & Maslov, 1997; Hopcroft & Ullman, 1979; Beasley & Pullman, 1988; Beasley & Pullman, 1992).

The categorization of algebraic structures according to the properties of the operation is one of the most important problems in algebraic mathematics. We may suggest new operations on soft sets, examine their properties, and take into account the algebraic structures they form in the collection of soft sets in order to further our grasp of this subject. Thus far, four extended soft set operations (extended intersection, union, difference, and symmetric difference for soft sets) and four limited soft set operations (restricted intersection, union, difference, and symmetric difference) have been presented.

Our goal is to make a significant contribution to the field of soft set theory by proposing a new restricted and extended soft set operation for soft set theory, which we call "restricted theta operation and extended theta operation of soft sets" and closely examining the algebraic structures associated with them and other soft set operations in the collection of soft sets. With the introduction of the so-called new operations in soft sets, an understanding of the underlying algebraic structures is crucial.

This study is organized as follows: Section 2 serves as a reminder of the basic ideas behind soft sets and other algebraic structures. In Section 3, the new soft set operations are defined. A detailed analysis is conducted on the algebraic characteristics of the theta operation and extended theta operation. Furthermore, we study how these novel soft set operations distribute over the existing soft set operations. Considering the distribution laws and the algebraic characteristics of the soft set operations, an extensive analysis of the algebraic structures formed in the set of soft sets over the universe using these operations is presented. Our demonstration reveals that the collection of soft sets throughout the universe forms several significant algebraic structures, including semirings. A comprehensive analysis expands on our knowledge of the applications and consequences of soft set theory across several

fields. In the conclusion section, we discuss the significance of the study's findings and their potential applications.

PRELIMINARIES

This section covers several algebraic structures as well as some basic ideas in soft set theory.

Definition 1. (Molodtsov, 1999) Let U be the universal set, E be the parameter set, P(U) be the power set of U, and T⊆ E. A pair (F, T) is called a soft set on U. Here, F is a function given by F : T → P(U).

Throughout this paper, the collection of all the soft sets over U (no matter what the parameter set is) is designated by $S_E(U)$ and $S_T(U)$ denotes the collection of all soft sets over U with a fixed parameter set T, where T is a subset of E.

Definition 2. (Ali et al., 2011) Let (F,T) be a soft set over U. If (x)=∅ for every x∈T, then the soft set (F,T) is called a null soft set with respect to K, denoted by $\emptyset_K$. Similarly, let (F,E) be a soft set over U. If F(x)=∅ for every x∈E, then the soft set (F,E) is called null soft set with respect to E, denoted by $\emptyset_E$ (Ali et al., 2009). A soft set with an empty parameter set is denoted as $\emptyset_\emptyset$. It is obvious that $\emptyset_\emptyset$ is the only soft set with an empty parameter set.

Definition 3. (Ali et al., 2009) Let (F,T) be a soft set over U. If F(x)=U for every x∈T, then the soft set (F,T) is called a relative whole soft set with respect to T, denoted by U_T. Similarly, let (F,E) be a soft set over U. If F(x)=U for every x∈E, then the soft set (F,E) is called an absolute soft set, and denoted by U_E.

Definition 4. (Pei & Miao; 2005) Let (F,T) and (G,Y) be soft sets over U. If T⊆Y and F(x) ⊆G(x) for every x∈T, then (F,T) is said to be a soft subset of (G,Y), denoted by (F,T)$\widetilde{\subseteq}$(G,Y). If (G,Y) is a soft subset of (F,T), then (F,T) is said to be a soft superset of (G,Y), denoted by (F,T)$\widetilde{\supseteq}$(G,Y). If (F,T)$\widetilde{\subseteq}$(G,Y) and (G,Y)$\widetilde{\subseteq}$(F,T), then (F,T) and (G,Y) are called soft equal sets.

Definition 5. (Ali et al., 2009) Let (F,T) be a soft set over U. The relative complement of (F,T), denoted by $(F,T)^r =(F^r,T)$, is defined as follows: $F^r(x)=U-F(x)$, for every x∈T.

Çağman (2021), introduced two new complements as the inclusive complement and the exclusive complement, which we denote as + and θ, respectively. For two sets X and Y, these binary operations are defined as X+Y=X'∪Y and XθY=X'∩Y'. Sezgin et al. (2023c) investigated the relationship between these two operations and also introduced three new binary operations: For two sets X and Y, these new operations are defined as X*Y=X'∪Y', XγY= X'∩Y, XλY=X∪Y' (Sezgin et al., 2023c). Let "⋈" be used to represent the set operations (i.e., here, ⋈ can be ∩, ∪,\, Δ, +,θ, *, λ,γ). Then, all types of soft set operations are defined as follows:

Definition 6. (Ali et al., 2009; Sezgin & Atagün, 2011; Ali et al., 2011; Aybek, 2024) Let (F,T) and (G,Y) be two soft sets over U. The restricted ⋈ operation of (F,T) and (G,Y) is the soft set (H, Z), denoted by (F,T) ⋈$_R$ (G,Y)= (H,Z), where Z = T ∩ Y≠ ∅ and for every x∈ Z, H(x) = F(x) ⋈G(x). Here, if Z= T ∩ Y = ∅, then (F, T) ⋈$_R$(G, Y)= $\emptyset_\emptyset$.

Definition 7. (Maji et al., 2003; Ali et al., 2009; Sezgin et al., 2019; Stojanavic, 2021; Aybek, 2024) Let (F, T) and (G, Y) be two soft sets over U. The extended ⋈ operation (F, T) and (G,Y) is the soft set (H,Z), denoted by (F, T) ⋈$_\varepsilon$(G, Y) = (H, Z), where Z= T ∪ Y, and for every x∈ Z,

$$H(x) = \begin{cases} F(x), & x \in T - Y \\ G(x), & x \in Y - T \\ F(x) \bowtie G(x), & x \in T \cap Y \end{cases}$$

Definition 8. (Demirci, 2024; Sarıalioğlu, 2024; Akbulut, 2024) Let (F,T) and (G, Y) be two soft sets over U. The complementary extended ⋈$_\varepsilon$ operation (F,T) and (G,Y) is the soft set (H,Z), denoted by (F, T) $\overset{*}{\underset{\bowtie_\varepsilon}{}}$ (G, Y) = (H, Z), where Z = T ∪ Y, and for every x∈ Z,

$$H(x) = \begin{cases} F'(x), & x \in T - Y \\ G'(x), & x \in Y - T \\ F(x) \bowtie G(x), & x \in T \cap Y \end{cases}$$

Definition 9. (Çalışıcı & Eren, 2019; Sezgin & Yavuz, 2023b; Sezgin & Çalışıcı, 2024, Yavuz, 2024) Let (F,T) and (G,Y) be two soft sets on U. The soft binary piecewise ⋈ operation of (F,T) and (G,Y) is the soft set (H,T), denoted by (F,T)$\overset{\sim}{\underset{\bowtie}{}}$(G, Y) = (H, T), where for every x∈ T,

$$H(x) = \begin{cases} F(x), & x \in T - Y \\ F(x) \bowtie G(x), & x \in T \cap Y \end{cases}$$

Definition 10. (Sezgin & Demirci, 2023; Sezgin & Aybek, 2023; Sezgin et al. 2023a, 2023b; Sezgin & Atagün, 2023; Sezgin & Yavuz, 2023a; Sezgin & Dagtoros, 2023; Sezgin & Çağman, 2024; Sezgin & Sarıalioğlu, 2024; Sezgin & Sarıalioğlu, 2024) Let (F,T) and (G,Y) be two soft sets on U. The complementary soft binary piecewise ⋈ operation of (F,T) and (G,Y) is the soft set (H,T), denoted by (F, T) $\overset{*}{\underset{\bowtie}{\sim}}$ (G, Y) = (H, T), where for every x∈ T,

$$H(x) = \begin{cases} F'(x), & x \in T - Y \\ F(x) \bowtie G(x), & x \in T \cap Y \end{cases}$$

For more about soft sets, we refer to (Mahmood et al. 2018; Jana et al., 2019; Muştuoğlu et al., 2016; Sezer et al., 2015b; Sezer, 2014; Sezgin, 2016; Atagün & Sezgin, 2018; Sezgin, 2018; Sezgin et al, 2017; Sezgin et al., 2022; Lawrence & Manoharan, 2023; Jabir et al. 2024).

Definition 11. (Clifford, 1954) Let (S, ⋆) be an algebraic structure. An element s ∈S is called idempotent if s^2=s. If s^2=s for every s∈S, then the algebraic structure (S,⋆) is said to be idempotent. An idempotent semigroup is called a band, an idempotent and commutative semigroup is called a semilattice, and an idempotent and commutative monoid is called a bounded

semilattice.

In a monoid, although the identity element is unique, a semigroup/groupoid can have one or more left identities; however, if it has more than one left identity, it does not have a right identity element, thus it does not have an identity element. Similarly, a semigroup/groupoid can have one or more right identities; however, if it has more than one right identity, it does not have a left identity element, thus it does not have an identity element (Kilp et al., 2001).

Similarly, in a group, although each element has a unique inverse, in a monoid, an element can have one or more left inverses; however, if an element has more than one left inverse, it does not have a right inverse, thus it does not have an inverse. Similarly, in a monoid, an element can have one or more right inverses; however, if an element has more than one right inverse, it does not have a left inverse, thus it does not have an inverse (Kilp et al., 2001).

Definition 12. Let S be a non-empty set, and let "+" and "⋆" be two binary operations defined on S. If the algebraic structure (S, +, ⋆) satisfies the following properties, then it is called a semiring:

  i.   (S, +) is a semigroup.
  ii. (S, ⋆) is a semigroup,
  iii. For every x, y, z ∈S, x⋆(y + z) = x⋆y + x⋆z and (x +y) ⋆z = x⋆z + y⋆z.

If for every x,y∈S, x+y=y+z, then S is called an additive commutative semiring. If for every x,y∈S, x⋆y=y⋆x, then S is called a multiplicative commutative semiring. If there exists an element 1∈S such that x⋆1=1⋆x=x for every x∈S (multiplicative identity), then S is called semiring with unity. If there exists 0∈S such that for every x∈S, 0⋆x=x⋆0=0 and 0+x=x+0=x, then 0 is called the zero of S. A semiring with commutative addition and a zero element is called a hemiring (Vandiver, 1934). We refer to Pant et al. (2024) for the possible implications of network analysis and graph applications with regard to soft sets, which are defined by the divisibility of determinants.

RESTRICTED AND EXTENDED THETA OPERATION

The new restricted theta and extended theta operations for soft sets are presented in this section. By examining the distributive laws across various types of soft sets, it also talks about their algebraic features and connections with other soft set activities. Examining these operations' algebraic structures in the $S_E(U)$ set in conjunction with other specific kinds of soft set operations yields some significant findings.

Restricted Theta Operation and Its Properties

Definition 13. Let (F, T) and (G, Z) be soft sets over U. The restricted theta of (F, T) and (G, Z), denoted by $(F, T)\theta_R(G, Z)$, is defined as $(F, T)\theta_R(G, Z) = (H, C)$, where $C=T\cap Z$, and if $C=T\cap Z\neq\emptyset$, then for every $\alpha\in C$,

$$H(\alpha)= F(\alpha)\theta G(\alpha)=F'(\alpha)\cap G'(\alpha);$$

if $C= T\cap Z=\emptyset$, then $(F,T) \theta_R (G,Z)=(H, C)= \emptyset_\emptyset$.

Since the only soft set with empty parameter set is $\emptyset_\emptyset$, if $C=T\cap Z= \emptyset$, then it is obvious that $(F,T) \theta_R (G,Z)= \emptyset_\emptyset$. Thus, in order to define the restricted theta operation of (F, T) and (G, Z), there is no condition that $T\cap Z\neq \emptyset$.

Example 1. Let $E=\{e_1,e_2,e_3,e_4\}$ be the parameter set, $T=\{e_1,e_3\}$ and $Z=\{e_2,e_3,e_4\}$ be subsets of E, $U=\{h_1,h_2, h_3,h_4, h_5\}$ be the universal set, (F,T) and (G,Z) be the soft sets over U as $(F,T)=\{(e_1,\{h_2,h_5\}),\ (e_3,\{h_1,h_2,h_5\})\}$, $(G,Z)=\{(e_2,\{h_1,h_4,h_5\}),\{(e_3,\{h_2,h_3,h_4\}),(e_4,h_3,h_5\})\}$.

Here let $(F,T)\theta_R(G,Z)=(H,T\cap Z)$, where for every $\alpha \in T \cap Z=\{e_3\}$. Thus, $H(e_3)=F'(e_3) \cap G'(e_3)=\{h_3,h_4\}\cap\{h_1, h_5\}=\{h_1, h_3, h_4, h_5\}$. Hence, $(F,T)\theta_R(G,Z)=\{(e_3, \emptyset)\}$

Theorem 1. Let (F,T), (G,Z), (H,M), (G,T), (H,T), (K,V) and (L, V) be soft sets over U. Then, we have the followings:

1) The set $S_E(U)$ is closed under θ_R.
2) $[(F,T) \theta_R(G,Z)] \theta_R(H,M) \neq (F,T) \theta_R[(G,Z) \theta_R(H,M)]$.
3) $[(F,T) \theta_R(G,T)] \theta_R(H,T)\neq(F,T) \theta_R[(G,T) \theta_R(H,T)]$.
4) $(F,T) \theta_R (G,Z)=(G,Z) \theta_R(F,T)$.
5) $(F,T) \theta_R(F,T)= (F,T)^r$.
6) $(F,T) \theta_R\emptyset_T=\emptyset_T\theta_R(F,T)=(F,T)^r$.
7) $(F,T) \theta_R \emptyset_M=\emptyset_M\theta_R (F,T)=(F, T \cap M)^r$.
8) $(F,T)\theta_R \emptyset_E=\emptyset_E \theta_R (F,T)= (F,T)^r$.
9) $(F,T)\theta_R\emptyset_\emptyset=\emptyset_\emptyset\theta_R(F,T)= \emptyset_\emptyset$.
10) $(F,T)\theta_RU_T= U_T\theta_R(F,T)= \emptyset_T$.
11) $(F,T)\theta_RU_M=U_M \theta_R(F,T)= \emptyset_{T\cap M}$.
12) $(F,T)\theta_RU_E=U_E\theta_R(F,T)= \emptyset_T$.
13) $(F,T) \theta_R (F,T)^r=(F,T)^r \theta_R(F,T)= \emptyset_T$.
14) $[(F,T) \theta_R(G,Z)]^r=(F,T) \cup_R (G,Z)$.
15) $(F,T)\theta_R(G, T)= U_T$ if and only if $(F,T) = \emptyset_T$ and $(G, T) = \emptyset_T$.
16) $\emptyset_{T\cap Z} \widetilde{\subseteq}(F,T) \theta_R(G,Z)$ and $(F,T) \theta_R(G,Z) \widetilde{\subseteq} U_T$ and $(F,T) \theta_R(G,Z) \widetilde{\subseteq} U_Z$.
17) $(F,T)\theta_R(G,Z) \widetilde{\subseteq} (F,T)^r$ and $(F,T)\theta_R(G,Z) \widetilde{\subseteq}(G,Z)^r$.
18) If $(F,T) \widetilde{\subseteq} (G, Z)$, $(F,T) \theta_R(G,Z) =(G,T)^r$.
19) If $(F,T) \widetilde{\subseteq} (G, T)$, then $(G,T) \theta_R(H,Z) \widetilde{\subseteq}(F,T) \theta_R(H,Z)$ and $(H,Z) \theta_R (G,T) \widetilde{\subseteq}(H,Z) \theta_R(G,T)$.
20) If $(G,T) \theta_R(H,Z) \widetilde{\subseteq}(F,T)\theta_R(H,Z)$, then $(F,T) \widetilde{\subseteq} (G, T)$ needs not be true. That is, the converse of Theorem 1 (19) is not ture.
21) If $(F,T) \widetilde{\subseteq} (G, T)$ and $(K,V) \widetilde{\subseteq} (L, V)$, $(G,T) \theta_R(L,V) \widetilde{\subseteq}(F,T) \theta_R (K,V)$. Similarly, $(L,V) \theta_R(G,T) \widetilde{\subseteq}(K,V) \theta_R (F,T)$.
22) $(F,T) \theta_R (G,Z) \widetilde{\subseteq}(F,T) *_R (G,Z)$ and $(G,Z) \theta_R (F,T) \widetilde{\subseteq}(G,Z) *_R (F,T)$.

Proof. 1) It is clear that θ_R is a binary operation in $S_E(U)$. That is,

$$\theta_R: S_E(U)\text{x } S_E(U)\to S_E(U)$$

$$((F,T), (G,Z)) \rightarrow (F, T)\theta_R(G, Z) = (H, T\cap Z)$$

Similarly,

$$\theta_R: S_T(U) \times S_T(U) \rightarrow S_T(U)$$
$$((F,T), (G,T)) \rightarrow (F, T)\theta_R(G, T) = (H, T\cap T) = (H,T)$$

That is, let T be a fixed subset of the set E and (F,T) and (G,T) be elements of $S_T(U)$, then so is $(F,T)\theta_R$ (G,T). Namely, $S_T(U)$ is closed under θ_R either.

2) Let $(F,T)\theta_R(G,Z)=(S,T\cap Z)$, where for every $\alpha\in T\cap Z$, $T(\alpha)=F'(\alpha)\cap G'(\alpha)$. Let $(S,T\cap Z)\theta_R(H,M)=(R,(T\cap Z)\cap M))$, where for every $\alpha\in (T\cap Z)\cap M$, $R(\alpha)=T'(\alpha)\cap H'(\alpha)$. Thus,

$$R(\alpha)=[F(\alpha)\cup G(\alpha)]\cap H'(\alpha)$$

Let $(G,Z)\theta_R(H,M)=(K,Z\cap M)$, where for every $\alpha\in Z\cap M$, $K(\alpha)=G'(\alpha)\cap H'(\alpha)$. Let $(F,T)\theta_R(K, Z\cap M)=(S,T\cap(Z\cap M))$, where for every $\alpha\in T\cap(Z\cap M)$, $S(\alpha)=F'(\alpha)\cap K'(\alpha)$. Thus,

$$S(\alpha)=F'(\alpha)\cap[G(\alpha)\cup H(\alpha)]$$

Thus, $(R,(T\cap Z)\cap M) \neq (S, T\cap(Z\cap M))$. That is, in $S_E(U)$, the operation θ_R is not associative. Here, it is obvious that if $T\cap Z=\emptyset$ or $Z\cap M=\emptyset$ or $T\cap M=\emptyset$, then since both sides of the equality is $\emptyset_\emptyset$, the operation θ_R is associative under these conditions.

3) Let $(F,T)\theta_R(G,T)=(K,T)$, where for every $\alpha\in T\cap T=T$, $K(\alpha)=F'(\alpha)\cap G'(\alpha)$. Let $(K,T)\theta_R(H,T)=(R,T)$, where for every $\alpha\in T\cap T=T$, $R(\alpha)=K'(\alpha)\cap H'(\alpha)$. Hence,

$$R(\alpha)=[F(\alpha)\cup G(\alpha)]\cap H'(\alpha)$$

Let $(G,T)\theta_R(H,T)=(L,T)$, where for every $\alpha\in T\cap T$, $L(\alpha)=G'(\alpha)\cap H'(\alpha)$. Let $(F,T)\theta_R(L,T)=(N,T)$, where for every $\alpha\in T\cap T$, $N(\alpha)=F'(\alpha)\cap L'(\alpha)$. Hence,

$$N(\alpha)=F'(\alpha)\cap[G(\alpha)\cup H(\alpha)]$$

Thus, $(R,T)\neq (N,T)$. That is, θ_R is not associative in the collection of soft sets with a fixed parameter set.

4) Let $(F,T)\theta_R(G,Z)=(H,T\cap Z)$, where for every $\alpha\in T\cap Z$, $H(\alpha)=F'(\alpha)\cap G'(\alpha)$. Let $(G,Z)\theta_R(F,T)=(S,Z\cap T)$, where for every $\alpha\in Z\cap T$, $S(\alpha)=G'(\alpha)\cap F'(\alpha)$. Thus,

$$(F,T)\theta_R(G,Z)=(G,Z)\theta_R(F,T).$$

That is, θ_R is commutative in $S_E(U)$. Here it is obvious that if $T\cap Z=\emptyset$, then since both sides is $\emptyset_\emptyset$, θ_R is commutative in $S_E(U)$ under this condition. Moreover, it is evident that $(F,T)\theta_R(G,T)=(G,T)\theta_R(F,T)$, namely, θ_R is commutative in the collection of soft sets with a fixed parameter set.

5) Let $(F,T)\theta_R(F,T)=(H,T\cap T)$. Thus, for every $\alpha\in T$, $H(\alpha)=F'(\alpha)\cap F'(\alpha)=F'(\alpha)$. Hence $(H,T)=(F,T)^r$. That is, the operation θ_R is not idempotent in $S_E(U)$.

6) Let $\emptyset_T=(S,T)$, where for every $\alpha\in T$, $S(\alpha)=\emptyset$. Let $(F,T)\theta_R(S,T)=(H,T\cap T)$, where for every $\alpha\in T$, $H(\alpha)=F'(\alpha)\cap S'(\alpha)=F'(\alpha)\cap U=F'(\alpha)$. Thus, $(H,T)=(F,T)^r$.

7) Let $\emptyset_M=(S,M)$, where for every $\alpha\in M$, $S(\alpha)=\emptyset$. Let $(S,M)\theta_R(F,T)=(H,M\cap T)$, where for every $\alpha\in T$, $H(\alpha)=S(\alpha)\cap F'(\alpha)=F'(\alpha)\cap U=F'(\alpha)$. Thus, $(H,T\cap M)=(F,T\cap M)^r$.

8) Let $\emptyset_E=(S,E)$, where for every $\alpha\in E$, $S(\alpha)=\emptyset$. $S(\alpha)=\emptyset$. Let $(F,T)\theta_R(S,E)=(H,T\cap E)$ where for every $\alpha\in T\cap E=T$, $H(\alpha)=F'(\alpha)\cap S'(\alpha)=F'(\alpha)\cap U=F'(\alpha)$. Thus, $(H,T)=(F,T)^r$.

9) Let $\emptyset_\emptyset=(S, \emptyset)$. Let $(F, T)\theta_R(S, \emptyset)=(H,T\cap\emptyset)$. Since the parameter set $\emptyset_\emptyset$ is the only soft set that is an empty set, $(H, \emptyset)=\emptyset_\emptyset$. That is, in the set $S_E(U)$, the absorbing element of the operation θ_R is the soft set $\emptyset_\emptyset$.

10) Let $U_T=(K,T)$, where for every $\alpha\in T$, $K(\alpha)=U$. Let $(F,T)\theta_R(K,T)=(H,T\cap T)$, where for every $\alpha\in T$, $H(\alpha)=F'(\alpha)\cap T'(\alpha)=F'(\alpha)\cap\emptyset=\emptyset$. Thus, $(H,T)=\emptyset_T$.

11) Let $U_M=(K,M)$, where for every $\alpha\in M$, $K(\alpha)=U$. Let $(F,T)\theta_R(K,M)=(H,T\cap M)$, where for every $\alpha\in T\cap M$, $H(\alpha)=F'(\alpha)\cap T'(\alpha)=F'(\alpha)\cap\emptyset=\emptyset$. Thus, $(H,T\cap M)=\emptyset_{T\cap M}$.

12) Let $U_E=(K,E)$, where for every $\alpha\in E$, $K(\alpha)=U$. Let $(F,T)\theta_R(K,E)=(H,T\cap E)$, where for every $\alpha\in T\cap E=T$, $H(\alpha)=F'(\alpha)\cap K'(\alpha)=F'(\alpha)\cap\emptyset=\emptyset$. Thus $(H,T)=\emptyset_T$.

13) Let $(F,T)^r=(H,T)$, where for every $\alpha\in T$, $H(\alpha)=F'(\alpha)$. Let $(F,T)\theta_R(H,T)=(L,T\cap T)$, where for every $\alpha\in T$, $L(\alpha)=F'(\alpha)\cap H'(\alpha)=F'(\alpha)\cap F(\alpha)=\emptyset$. Thus, $(L,T)=\emptyset_T$.

14) Let $(F,T)\theta_R(G,Z)=(H,T\cap Z)$, for every $\alpha\in T\cap Z$, $H(\alpha)=F'(\alpha)\cap G'(\alpha)$. Let $(H,T\cap Z)^r=(K,T\cap Z)$ where for every $\alpha\in T\cap Z$, $K(\alpha)=F(\alpha)\cup G(\alpha)$. Thus, $(K,T\cap Z)=(F,T)\cup_R (G,Z)$.

15) Let $(F, T)\theta_R(G, T)=(K,T\cap T)$, where for every $\alpha\in T$, $K(\alpha)=F'(\alpha)\cap G'(\alpha)$. Since $(K,T)=U_T$, $K(\alpha)=U$, for every $\alpha\in T$. Thus, $K(\alpha)=F'(\alpha)\cap G'(\alpha)=U$, for every $\alpha\in T\Leftrightarrow F'(\alpha)=U$ and $G'(\alpha)=U$, for every $\alpha\in T \Leftrightarrow F(\alpha)=\emptyset$ and $G(\alpha)=\emptyset$, for every $\alpha\in T\Leftrightarrow (F, T) = \emptyset_T$ and $(G,T)=\emptyset_T$, for every $\alpha\in T$.

16) Obvious.

17) Let $(F,T)\theta_R(G,Z)=(H,T\cap Z)$, where for every $\alpha\in T\cap Z$, $H(\alpha)=F'(\alpha)\cap G'(\alpha)$. Since, for every $\alpha\in T\cap Z$, $H(\alpha)=F'(\alpha)\cap G'(\alpha)\subseteq F'(\alpha)$.

Thus, $(F,T)\theta_R(G,Z)\widetilde{\subseteq}(F,T)^r$. Similarly, since $F'(\alpha)\cap G'(\alpha)\subseteq G'(\alpha)$, $(F,T)\theta_R(G,Z)\widetilde{\subseteq}(G,Z)^r$.

18) Let $(F,T)\widetilde{\subseteq}(G,Z)$. Then, $T\subseteq Z$ and for every $\alpha\in T$, $F(\alpha)\subseteq G(\alpha)$. Thus for all $\alpha\in T$, $G'(\alpha)\subseteq F'(\alpha)$.

Let $(F,T)\theta_R(G,Z)=(K,T\cap Z=T)$. Then, for every $\alpha\in T$, $K(\alpha)=F'(\alpha)\cap G'(\alpha)=G'(\alpha)$, hence $(K,T)=(F,T)\theta_R(G,Z)=(G,T)^r$. Conversely let $(F,T)\theta_R(G,Z)=(G,T)^r$. Hence, $T\cap Z=T$, and so $T\subseteq Z$. Also, for every $\alpha\in T$, $F'(\alpha)\cap G'(\alpha)=G'(\alpha)$, and so $G'(\alpha)\subseteq F'(\alpha)$. Thus, for all $\alpha\in T$, $F(\alpha)\subseteq G(\alpha)$, $(F,T)\widetilde{\subseteq}(G,Z)$.

19) Let $(F,T)\widetilde{\subseteq}(G, T)$. Thus for every $\alpha\in T$, $F(\alpha)\subseteq G(\alpha)$ and for every $\alpha\in T$, $G'(\alpha)\subseteq F'(\alpha)$. Let $(G,T)\theta_R(H,Z)=(K,T\cap Z)$. Thus for every $\alpha\in T\cap Z$, $K(\alpha)=G'(\alpha)\cap H'(\alpha)$. Let $(F,T)\theta_R(H,Z)=(L,T\cap Z)$. Hence for every $\alpha\in T\cap Z$, $L(\alpha)=F'(\alpha)\cap H'(\alpha)$. Thus, $K(\alpha)=G'(\alpha)\cap H'(\alpha)\subseteq F'(\alpha)\cap H'(\alpha)=L(\alpha)$, for every $\alpha\in T\cap Z$, hence, $(G,T)\theta_R(H,Z)\widetilde{\subseteq}(F,T)\theta_R(H,Z)$. It is clear

from the commutative property that, under the same conditions, $(H,Z)\,\theta_R(G,T)\widetilde{\cong}(H,Z)\theta_R(G,T)$ will be achieved.

20) We give a counterexample to show that the converse of Theorem 1 (19) is not true. Let $E=\{e_1,e_2,e_3,e_4,e_5\}$ be the parameter set, $T=\{e_1,e_3\}$, $K=\{e_1,e_3,e_5\}$, and $Z=\{e_1,e_3,e_5,e_6\}$ be the subsets of E, $U=\{h_1,h_2,h_3,h_4,h_5\}$ be the universal set, and (F,T), (G,T) and (H,Z) be the soft sets as follows: $(F,T)=\{(e_1,\{h_2,h_5,\}),(e_3,\{h_1,h_2,h_5,\})\}$,$(G,T)=\{(e_1,\{h_2\}),(e_3,\{h_1,h_2\})\}$,$(H,Z)=\{(e_1,U),(e_3,U),(e_5,\{h_1,h_5\})\}$.

Let $(G,T)\,\theta_R(H,Z)=(L,T\cap Z)$, where for every $\alpha\in T\cap Z=\{e_1,e_3\}$, $L(\alpha)=G'(\alpha)\cap H'(\alpha)$, $L(e_1)=G'(e_1)H'(e_1)=\emptyset$, $L(e_3)=G'(e_3)\cap H'(e_3)=\emptyset$. Thus, $(G,T)\theta_R(H,Z)=\{(e_1,\emptyset),(e_3,\emptyset)\}$. Now let $(F,T)\theta_R(H,Z)=(K,T\cap Z)$, where for every $\alpha\in T\cap Z=\{e_1,e_3\}$, $K(\alpha)=F'(\alpha)\cap H'(\alpha)$,$K(e_1)=F'(e_1)\cap H'(e_1)=\emptyset$, $K(e_3)=F'(e_3)\cap H'(e_3)=\emptyset$. Thus, $(F,T)\,\theta_R(H,Z)=\{(e_1,\emptyset),(e_3,\emptyset)\}$.

It is observed that $(G,T)\,\theta_R(H,Z)\,\widetilde{\cong}(F,T)\,\theta_R(H,Z)$; however then $(F,T)\widetilde{\cong}(G,K)$ needs not be true.

21) Let $(F,T)\widetilde{\cong}(G,T)$ and $(K,V)\widetilde{\cong}(L,V)$. Thus, for every $\alpha\in T$ and for every $\alpha\in Z$, $F(\alpha)\subseteq G(\alpha)$ and $K(\alpha)\subseteq L(\alpha)$. Hence, for every $\alpha\in T$, $G'(\alpha)\subseteq F'(\alpha)$ and for every $\alpha\in Z$, $L'(\alpha)\subseteq K'(\alpha)$. Let $(G,T)\,\theta_R\,(L,Z)=(M,T\cap Z)$. Thus, for every $\alpha\in T\cap Z$, $M(\alpha)=G'(\alpha)\cap L'(\alpha)$. Let $(F,T)\theta_R\,(K,Z)=(N,T\cap Z)$. Thus, for every $\alpha\in T\cap Z$, $N(\alpha)=F'(\alpha)\cap K'(\alpha)$. Since, for every $\alpha\in T\cap Z$, $G'(\alpha)\subseteq F'(\alpha)$ and $L'(\alpha)\subseteq K'(\alpha)$, $M(\alpha)=G'(\alpha)\cap L'(\alpha)\subseteq F'(\alpha)\cap K'(\alpha)=N(\alpha)$. Thus, $(G,T)\,\theta_R\,(L,V)\widetilde{\cong}(F,T)\,\theta_R\,(K,V)$.

22) Let $(F,T)\theta_R(G,Z)=(M,T\cap Z)$. Hence, for every $\alpha\in T\cap Z$, $M(\alpha)=F'(\alpha)\cap G'(\alpha)$. Let $(F,T)*_R(G,Z)=(N,T\cap Z)$. Thus, for every $\alpha\in T\cap Z$, $N(\alpha)=F'(\alpha)\cup G'(\alpha)$.

Since $M(\alpha)=F'(\alpha)\cap G'(\alpha)\subseteq F'(\alpha)\cup G'(\alpha)=N(\alpha)$, it implies that $(F,T)\theta_R(G,Z)\widetilde{\cong}(F,T)*_R(G,Z)$.

Theorem 2. Let (F,T), (G,Z), and (H,M) be soft sets over U. Then, restricted theta operation distributes over other soft set operations as follows:

Theorem 3. Let (F,T), (G,Z), and (H,M) be soft sets over U. Then, restricted theta operation distributes over other restricted soft set operations as follows:

i) LHS Distributions:

1)$(F,T)\theta_R[(G,Z)\cap_R(H,M)]=[(F,T)\,\theta_R(G,Z)]\cup_R\,[(F,T)\,\theta_R(H,M)]$.

Proof. Consider first the LHS. Let $(G,Z)\cap_R(H,M)=(R,Z\cap M)$, where for every $\alpha\in Z\cap M$, $R(\alpha)=G(\alpha)\cap H(\alpha)$. Let $(F,T)\,\theta_R(R,Z\cap M)=(N,T\cap(Z\cap M))$, whee for every $\alpha\in T\cap(Z\cap M)$, $N(\alpha)=F'(\alpha)\cap R'(\alpha)$. Thus, for every $\alpha\in T\cap Z\cap M$,

$$N(\alpha)=F'(\alpha)\cap[(G'(\alpha)\cup H'(\alpha)]$$

Now consider the RHS, i.e. $[(F,T)\,\theta_R(G,Z)]\cup_R\,[(F,T)\,\theta_R(H,M)]$. Let $(F,T)\,\theta_R\,(G,Z)=(V,T\cap Z)$, where for every $\alpha\in T\cap Z$, $V(\alpha)=F'(\alpha)\cap G'(\alpha)$ and let $(F,T)\theta_R\,(H,M)=(W,T\cap M)$, where for every $\alpha\in T\cap M$, $W(\alpha)=F'(\alpha)\cap H'(\alpha)$.

Let $(V,T\cap Z)\cup_R(W,T\cap M)=(S,(T\cap Z)\cap(T\cap M))$, where for every $\alpha\in T\cap Z\cap M$, $S(\alpha)=V(\alpha)\cup W(\alpha)$. Thus,

$$S(\alpha)=[F'(\alpha)\cap G'(\alpha)]\cup[F'(\alpha)\cap H'(\alpha)]$$

Hence, $(N,T\cap Z\cap M)=(S,T\cap Z\cap M)$. Here, if $T\cap Z=\emptyset$ or $T\cap M=\emptyset$ or $Z\cap M=\emptyset$, then both sides is $\emptyset_\emptyset$. Thus, the equality is satisfied in all circumstances.

2)$(F,T)\,\theta_R[(G,Z)\cup_R(H,M)]=[(F,T)\,\theta_R(G,Z)]\cap_R[(F,T)\,\theta_R\,(H,M)]$.

3)$(F,T)\,\theta_R\,[(G,Z)*_R(H,M)]=[(F,T)\,\gamma_R(G,Z)]\cap_R[(F,T)\,\gamma_R\,(H,M)]$.

4)$(F,T)\,\theta_R\,[(G,Z)\,\theta_R(H,M)]=[(F,T)\,\gamma_R(G,Z)]\cup_R[(F,T)\,\gamma_R\,(H,M)]$.

ii) RHS Distributions:

1)$[(F,T)\cup_R(G,Z)]\theta_R(H,M)=[(F,T)\,\theta_R(H,M)]\cap_R[(G,Z)\,\theta_R\,(H\,M)]$.

Proof. Consider first the LHS. Let $(F,T)\cup_R(G,Z)=(R,T\cap Z)$, where for every $\alpha\in T\cap Z$, $R(\alpha)=F(\alpha)\cup G(\alpha)$. Let $(R,T\cap Z)\,\theta_R(H,M)=(N,(T\cap Z)\cap M)$, where for every $\alpha\in(T\cap Z)\cap M$, $N(\alpha)=R'(\alpha)\cap H'(\alpha)$. Thus,

$$N(\alpha)=[F'(\alpha)\cap G'(\alpha)]\cap H'(\alpha)$$

Now consider the RHS, i.e., $[(F,T)\,\theta_R(H,M)]\cap_R[(G,Z)\,\theta_R\,(H,M)]$. Let $(F,T)\theta_R(H,M)=(S,T\cap M)$, where for every $\alpha\in T\cap M$, $T(\alpha)=F'(\alpha)\cap H'(\alpha)$ and let $(G,Z)\,\theta_R\,(H,M)=(K,Z\cap M)$, where for every $\alpha\in Z\cap M$, $K(\alpha)=G'(\alpha)\cap H'(\alpha)$. Assume that $(S,T\cap Z)\cap_R(K,Z\cap M)=(L,(T\cap Z\cap M))$, where for every $\alpha\in(T\cap Z)\cap(Z\cap M)$, $L(\alpha)=S(\alpha)\cap K(\alpha)$. Thus,

$$L(\alpha)=([F'(\alpha)\cap H'(\alpha)]\cap[G'(\alpha)\cap H'(\alpha)]$$

Hence, $(N,T\cap Z\cap M)=(L,T\cap Z\cap M)$. Here, if $T\cap Z=\emptyset$ or $T\cap M=\emptyset$ or $Z\cap M=\emptyset$, then both sides is $\emptyset_\emptyset$. Thus, the equality is satisfied in all circumstances.

2)$[(F,T)\cap_R\,(G,Z)]\theta_R(H,M)=[(F,T)\,\theta_R(H,M)]\cup_R[(G,Z)\,\theta_R(H,M)]$.

3)$[(F,T)\,\theta_R(G,Z)]\theta_R\,(H,M)=[(F,T)\backslash_R(H,M)]\cup_R\,[(G,Z)\backslash_R(H,M)]$.

4)$[(F,T)*_R(G,Z)]\theta_R(H,M)=[(F,T)\,\backslash_R\,(H,M)]\cap_R\,[(G,Z)\,\backslash_R\,(H,M)]$.

Theorem 4. Let (F,T), (G,Z), and (H,M) be soft sets over U. Then, restricted theta operation distributes over extended soft set operations as follows:

i) LHS Distributions:

1)$(F,T)\,\theta_R[(G,Z)\cap_\varepsilon(H,M)]=[(F,T)\,\theta_R(G,Z)]\cap_\varepsilon[(F,T)\,\theta_R\,(H,M)]$.

Proof. Consider first the LHS. Let $(G,Z)\cap_\varepsilon(H,M)=(R,Z\cup M)$, where for every $\alpha\in Z\cup M$;

$$R(\alpha)=\begin{cases} G(\alpha), & \alpha\in Z-M \\ H(\alpha), & \alpha\in M-Z \\ G(\alpha)\cap H(\alpha), & \alpha\in Z\cap M \end{cases}$$

Let (F,T)θ_R(R,Z∪M)=(N,(T∩(Z∪M))), where for every α∈T∩(Z∪M), N(α)=F'(α)∩R'(α). Thus,

$$N(\alpha) = \begin{cases} F'(\alpha) \cap G'(\alpha), & \alpha \in T \cap (Z-M) \\ F'(\alpha) \cap H'(\alpha) & \alpha \in T \cap (M-Z) \\ F'(\alpha) \cap [G'(\alpha) \cup H'(\alpha)], & \alpha \in T \cap (Z \cap M) \end{cases}$$

Now consider the RHS, i.e. [(F,T) θ_R(G,Z)] $\cap_\varepsilon$ [(F,T) θ_R (H,M)]. Let (F,T)θ_R(G,Z)=(K,T∩Z), where for every α∈T∩Z, K(α)=F'(α)∩G'(α) and let (F,T)θ_R(H,M)=(S,T∩M), where for every α∈T∩M, S(α)=F'(α)∩H'(α). Let (K,T∩Z) $\cap_\varepsilon$(S,T∩M)=(L,(T∩Z)∪(T∩M)), where for every α∈(T∩Z)∪(T∩M),

$$L(\alpha) = \begin{cases} K(\alpha), & \alpha \in (T \cap Z) - (T \cap M) \\ S(\alpha), & \alpha \in (T \cap Z) - (T \cap M) \\ K(\alpha) \cap S(\alpha), & \alpha \in (T \cap M) \cap (T \cap Z) \end{cases}$$

Thus,

$$L(\alpha) = \begin{cases} F'(\alpha) \cap G'(\alpha), & \alpha \in T \cap Z \cap M' \\ F'(\alpha) \cap H'(\alpha) & \alpha \in T \cap Z' \cap M \\ F'(\alpha) \cap [G'(\alpha) \cup H'(\alpha)], & \alpha \in T \cap Z \cap M \end{cases}$$

Hence, (N, T∩(Z∪M))=(L, (T∩Z)∪(T∩M)). Here, if T∩Z=∅, then N(α)=L(α)=F'(α)∩H'(α); and if T∩M=∅, then N(α)=L(α)=F'(α)∩G'(α). Thus, there is no extra condition as T∩Z≠ ∅ and/or T∩M≠ ∅ for satisfying Theorem 4 (i).

2)(F,T) θ_R[(G,Z) ∪$_\varepsilon$(H,M)]=[(F,T) θ_R(G,Z)] $\cap_\varepsilon$[(F,T) θ_R (H,M)].

ii) RHS Distributions:

1)[(F,T)∪$_\varepsilon$(G,Z)] θ_R(H,M)=[(F,T) θ_R(H,M)] $\cap_\varepsilon$ [(G,Z) θ_R (H,M)].

Proof. Consider first the LHS. Let (F,T) ∪$_\varepsilon$(G,Z)=(R,T∪Z), where for every α∈ T∪Z,

$$R(\alpha) = \begin{cases} F(\alpha), & \alpha \in T - Z \\ G(\alpha), & \alpha \in Z - T \\ F(\alpha) \cup G(\alpha), & \alpha \in T \cap Z \end{cases}$$

Assume that (R,T∪Z) θ_R(H,M)=(N,(T∪Z)∩M)), where for every α∈(T∪Z)∩M, N(α)=R'(α)∩H'(α). Thus,

$$N(\alpha) = \begin{cases} F'(\alpha) \cap H'(\alpha), & \alpha \in (T - Z) \cap M \\ G'(\alpha) \cap H'(\alpha), & \alpha \in (Z - T) \cap M \\ [F'(\alpha) \cap G'(\alpha)] \cap H'(\alpha), & \alpha \in (T \cap Z) \cap M \end{cases}$$

Now consider the RHS. Let (F,T) θ_R (H,M)=(K,T∩M), where for every α∈T∩M, K(α)=F'(α)∩H'(α) and let (G,Z) θ_R (H,M)=(S,Z∩M), where for every α∈Z∩M, S(α)= G'(α)∩H'(α). Let (K,T∩M) $\cap_\varepsilon$(S,Z∩M)=(L,(T∩M)∪(Z∩M)). Hence,

$$L(\alpha) = \begin{cases} K(\alpha), & \alpha \in (T \cap M) - (Z \cap M) \\ S(\alpha), & \alpha \in (Z \cap M) - (T \cap M) \\ K(\alpha) \cap S(\alpha), & \alpha \in (T \cap M) \cap (Z \cap M) \end{cases}$$

Thus,

$$L(\alpha) = \begin{cases} F'(\alpha) \cap H'(\alpha), & \alpha \in T \cap Z' \cap M \\ G'(\alpha) \cap H'(\alpha) & \alpha \in T' \cap Z \cap M \\ [F'(\alpha) \cap G'(\alpha)] \cap H'(\alpha), & \alpha \in T \cap Z \cap M \end{cases}$$

Therefore, (N,(T∪Z)∩M)) = (L,(T∩M)∪(Z∩M)). Here, if T∩Z=∅ and α∈T∩Z'∩M, then N(α)=L(α)=F'(α)∩H'(α) and if T∩Z=∅ and α∈T'∩Z∩M, the N(α)=L(α)=G'(α)∩H'(α). Furthermore, if Z∩M=∅, then N(α)=L(α)=F'(α)∩H'(α). Thus, there is no extra condition as T∩Z≠ ∅ and/or Z∩M≠ ∅ for satisfying Theorem 4 (ii).

2)[(F,T) $\cap_\varepsilon$(G,Z)] θ_R(H,M)=[(F,T) θ_R(G,Z)]∪$_\varepsilon$[(G,Z) θ_R (H,M)].

Theorem 5. Let (F,T), (G,Z), and (H,M) be soft sets over U. Then, restricted theta operation distributes over complementary extended soft set operations as follows:

i) LHS Distributions:

1)(F,T) θ_R[(G,Z) $*\!\!*_\varepsilon$ (H,M)]=[(F,T) γ_R(G,Z)]∩$_\varepsilon$[(F,T) γ_R (H, M)].

Proof. Consider first the LHS. Let (G,Z) $*\!\!*_\varepsilon$ (H,M)=(R,Z∪M), where for every α∈Z∪M,

$$R(\alpha) = \begin{cases} G'(\alpha), & \alpha \in Z - M \\ H(\alpha), & \alpha \in M - Z \\ G'(\alpha) \cup H'(\alpha), & \alpha \in Z \cap M \end{cases}$$

Let (F,T)θ_R(R,Z∪M)=(N,(T∩(Z∪M)), where for every α∈T∩(Z∪M), N(α)=F'(α)∩R'(α). Thus,

$$N(\alpha) = \begin{cases} F'(\alpha) \cap G(\alpha), & \alpha \in T \cap (Z-M) \\ F'(\alpha) \cap H(\alpha) & \alpha \in T \cap (M-Z) \\ F'(\alpha) \cap [G(\alpha) \cap H(\alpha)], & \alpha \in T \cap (Z \cap M) \end{cases}$$

Now consider the RHS, i.e. [(F,T) γ_R(G,Z)] ∩$_\varepsilon$[(F,T) γ_R (H,M)]. Let (F,T) γ_R (G,Z)=(K,T∩Z) where for every α∈T∩Z, K(α)=F'(α)∩G(α).

Let (F,T)γ_R(H,M)=(S,T∩M), where for every α∈T∩M, S(α)=F'(α)∩H(α). Assume that (K,T∩Z)∩$_\varepsilon$(S,T∩M)=(L,(T∩Z)∪(T∩M)), where for every α∈(T∩Z)∪(T∩M),

$$L(\alpha) = \begin{cases} K(\alpha), & \alpha \in (T \cap Z) - (T \cap M) \\ S(\alpha), & \alpha \in (T \cap Z) - (T \cap M) \\ K(\alpha) \cap S(\alpha), & \alpha \in (T \cap M) \cap (T \cap Z) \end{cases}$$

Thus,

$$L(\alpha) = \begin{cases} F'(\alpha) \cap G(\alpha), & \alpha \in T \cap Z \cap M' \\ F'(\alpha) \cap H(\alpha) & \alpha \in T \cap Z' \cap M \\ F'(\alpha) \cap [G(\alpha) \cup H(\alpha)], & \alpha \in T \cap Z \cap M \end{cases}$$

Therefore, (N,(T∩(Z∪M))=(L,(T∩Z)∪(T∩M)). Here, if T∩Z=∅, then N(α)=L(α)=F'(α)∩H(α); and if T∩M=∅, then

N(α)=L(α)=F'(α)∩G(α). Thus, there is no extra condition as T∩Z≠ ∅ and/or T∩M≠ ∅ for satisfying Theorem 5 (i).

2)(F,T) θ_R [(G,Z) $\overset{*}{\theta_\varepsilon}$ (H,M)]=[(F,T) γ_R(G,Z)] ∪$_R$[(F,T) γ_R (H,M)].

ii) RHS Distributions:

1)[(F,T) $\overset{*}{\theta_\varepsilon}$ (G,Z)]θ_R(H,M)=[(F,T) \\$_R$(H,M)]∪$_\varepsilon$[(G,Z) \\$_R$ (H,M)].

Proof. Consider first the LHS. Let (F,T) $\overset{*}{\theta_\varepsilon}$ (G,Z)=(R,T∪Z), where for every α∈T∪Z;

$$R(\alpha) = \begin{cases} F'(\alpha), & \alpha \in T - Z \\ G'(\alpha), & \alpha \in Z - T \\ F'(\alpha) \cap G'(\alpha), & \alpha \in T \cap Z \end{cases}$$

Let (R,T∪Z) θ_R(H,M)=(N,(T∪Z)∩M), where for every α∈(T∪Z)∩M, N(α)=R'(α)∩H'(α). Thus,

$$N(\alpha) = \begin{cases} F(\alpha) \cap H'(\alpha), & \alpha \in (T - Z) \cap M \\ G(\alpha) \cap H'(\alpha) & \alpha \in (Z - T) \cap M \\ [F(\alpha) \cup G(\alpha)] \cap H'(\alpha), & \alpha \in (T \cap Z) \cap M \end{cases}$$

Now consider the RHS, i.e. [(F,T) \\$_R$(H,M)] ∪$_\varepsilon$[(G,Z) \\$_R$ (H,M)]. Let (F,T)\\$_R$(H,M)=(K,T∩M), where for every α∈T∩M, K(α)=F(α)∩H'(α) and let (G,Z) \\$_R$(H,M)=(S,Z∩M), where for every α∈Z∩M, S(α)=G(α)∩H'(α).

Assume that (K,T∩M)∪$_\varepsilon$(S,Z∩M)=(L,(T∩M)∪(Z∩M)), where for every α∈(T∩M)∪(Z∩M),

$$L(\alpha) = \begin{cases} K(\alpha), & \alpha \in (T \cap M) - (Z \cap M) \\ S(\alpha), & \alpha \in (Z \cap M) - (T \cap M) \\ K(\alpha) \cup S(\alpha), & \alpha \in (T \cap M) \cap (Z \cap M) \end{cases}$$

Thus,

$$L(\alpha) = \begin{cases} F(\alpha) \cap H'(\alpha), & \alpha \in T \cap Z' \cap M \\ G(\alpha) \cap H'(\alpha) & \alpha \in T' \cap Z \cap M \\ [F(\alpha) \cup G(\alpha)] \cap H'(\alpha), & \alpha \in T \cap Z \cap M \end{cases}$$

Therefore, (N,(T∪Z)∩M)=(L,(T∩M)∪(Z∩M)). Here, if T∩Z=∅ and α∈T∩Z'∩M, then N(α)=L(α)=F(α)∩H'(α) and if T∩Z=∅ and α∈T'∩Z∩M, the N(α)=L(α)=G(α)∩H'(α). Furthermore, if Z∩M=∅, then N(α)=L(α)=F(α)∩H'(α). Thus, there is no extra condition as T∩Z≠ ∅ and/or Z∩M≠ ∅ for satisfying Theorem 5 (ii).

2)[(F,T) $\overset{*}{*_\varepsilon}$ (G,Z)] θ_R(H,M)=[(F,T)\\$_R$(G,Z)]∩$_\varepsilon$[(G,Z) \\$_R$ (H,M)].

Theorem 6. Let (F,T), (G,Z), and (H,M) be soft sets over U. Then, restricted theta operation distributes over soft binary piecewise operations as follows:
i) LHS Distributions:

1)(F,T) θ_R[(G,Z) $\overset{\sim}{\cap}$ (H,M)]=[(F,T) θ_R(G,Z)] $\overset{\sim}{\cup}$ [(F,T) θ_R (H,M)].

Proof. Consider first the LHS. Let (G,Z)$\overset{\sim}{\cap}$ (H,M)=(R,Z), where for every α∈Z;

$$R(\alpha) = \begin{cases} G(\alpha), & \alpha \in Z - M \\ G(\alpha) \cap H(\alpha), & \alpha \in Z \cap M \end{cases}$$

Let (F,T)θ_R(R,Z)=(N,T∩Z), where for every α∈T∩Z; N(α)=F'(α)∩R'(α). Thus,

$$N(\alpha) = \begin{cases} F'(\alpha) \cap G'(\alpha), & \alpha \in T \cap (Z - M) \\ F'(\alpha) \cap [G'(\alpha) \cup H'(\alpha)], & \alpha \in T \cap (Z \cap M) \end{cases}$$

Now consider the RHS. Let (F,T)θ_R(G,Z)=(K,T∩Z), where for every α∈T∩Z; K(α)=F'(α)∩G'(α).

Let (F,T) θ_R (H,M)=(S,T∩M), where for every α∈T∩M; S(α)=F'(α)∩H'(α) and assume that (K,T∩Z)$\overset{\sim}{\cup}$ (S,T∩M)=(L,T∩Z), where for every α∈T∩Z;

$$L(\alpha) = \begin{cases} K(\alpha), & \alpha \in (T \cap Z) - (T \cap M) \\ K(\alpha) \cup S(\alpha), & \alpha \in (T \cap Z) \cap (T \cap M) \end{cases}$$

Thus,

$$L(\alpha) = \begin{cases} F'(\alpha) \cap G'(\alpha), & \alpha \in (T \cap Z) - (T \cap M) \\ F'(\alpha) \cap \{G'(\alpha) \cup H'(\alpha)\}, & \alpha \in T \cap (Z \cap M) \end{cases}$$

Hence (N,T∩Z)=(L,T∩Z). Here, if T∩Z=∅, then (N,T∩Z)=(L,T∩Z)=∅$_\emptyset$; and if T∩M=∅, then N(α)=L(α)=F'(α∩)G'(α). Thus, there is no extra condition as T∩Z≠ ∅ and/or T∩M≠ ∅ for satisfying Theorem 6 (i).

2)(F,T) θ_R[(G,Z) $\overset{\sim}{\cup}$(H,M)]=[(F,T)θ_R(G,Z)] $\overset{\sim}{\cap}$ [(F,T) θ_R (H,M)].

ii) RHS Distributions:

1)[(F,T) $\overset{\sim}{\cup}$(G,Z)] θ_R(H,M)=[(F,T) θ_R(H,M)]$\overset{\sim}{\cap}$ [(G,Z) θ_R (H,M)].

Proof. Consider first the LHS. Let (F,T) $\overset{\sim}{\cup}$ (G,Z)=(R,T) , where for every α∈T;

$$R(\alpha) = \begin{cases} F(\alpha), & \alpha \in T - Z \\ F(\alpha) \cup G(\alpha), & \alpha \in T \cap Z \end{cases}$$

Let (R,T)θ_R(H,M)=(N,T∩M), where for every α∈T∩M; N(α)=R'(α)∩H'(α). Thus,

$$N(\alpha) = \begin{cases} F'(\alpha) \cap H'(\alpha), & \alpha \in (T - Z) \cap M \\ [F'(\alpha) \cap G'(\alpha)] \cap H'(\alpha), & \alpha \in (T \cap Z) \cap M \end{cases}$$

Now consider the RHS. Let (F,T)θ_R(H,M)=(K,T∩M), where for every α∈T∩M; K(α)=F'(α)∩H'(α). Assume that (G,Z) θ_R (H,M)=(S,Z∩M), where for every α∈Z∩M; S(α)=G'(α)∩H'(α) and let (K,T∩M)$\overset{\sim}{\cap}$(S,Z∩M)=(L,T∩M), where for every α∈T∩M;

$$L(\alpha) = \begin{cases} K(\alpha), & \alpha \in (T \cap M) - (Z \cap M) \\ K(\alpha) \cap S(\alpha), & \alpha \in (T \cap M) \cap (Z \cap M) \end{cases}$$

Hence,

$$L(\alpha) = \begin{cases} F'(\alpha) \cap H'(\alpha), & \alpha \in (T \cap M) - (Z \cap M) \\ [F'(\alpha) \cap G'(\alpha)] \cap H'(\alpha), & \alpha \in (T \cap Z) \cap M \end{cases}$$

Thus, $(N,T\cap M)=(L,T\cap M)$. Here, if $T\cap M=\emptyset$, then $(N,T\cap M)=(L,T\cap M)=\emptyset_\emptyset$; and if $Z\cap M=\emptyset$, then $N(\alpha)=L(\alpha)=F'(\alpha)\cap H'(\alpha)$. Thus, there is no extra condition as $T\cap M\neq \emptyset$ and/or $Z\cap M\neq \emptyset$ for satisfying Theorem 6 (ii).

2)$[(F,T) \widetilde{\cap}(G,Z)] \theta_R(H,M)=[(F,T)\theta_R(H,M)]\widetilde{\cup} [(G,Z) \theta_R (H,M)]$.

Extended Theta Operation and Its Properties

Definition 14. Let (F,T) and (G,Z) be soft sets over U. The extended theta operation of (F,T) and (G,Z) is the soft set (H,C), denoted by $(F,T) \theta_\varepsilon (G,Z)=(H,C)$, where $C=T\cup Z$ and for every $\alpha\in C$,

$$H(\alpha) = \begin{cases} F(\alpha), & \alpha \in T - Z \\ G(\alpha), & \alpha \in Z - T \\ F'(\alpha) \cap G'(\alpha), & \alpha \in T \cap Z \end{cases}$$

From the definition, it is obvious that if $T=\emptyset$, then $(F,T)\theta_\varepsilon(G,Z)=(G,Z)$; if $Z=\emptyset$, then $(F,T)\theta_\varepsilon(G,Z)=(F,T)$; if $T=Z=\emptyset$, then $(F,T)\theta_\varepsilon(G,Z)= \emptyset_\emptyset$.

Example 2. Let $E=\{e_1,e_2,e_3,e_4\}$ be the parameter set, $T=\{e_1,e_3\}$ and $Z=\{e_2,e_3,e_4\}$ be subsets of E, $U=\{h_1,h_2,h_3,h_4,h_5\}$ be the universal set, (F,T) and (G,Z) be the soft sets over U as $(F,T)=\{(e_1,\{h_2,h_5\}),(e_3,\{h_1,h_2,h_5\})\}$,$(G,Z)=\{(e_2,\{h_1,h_4,h_5\}),\{(e_3,\{h_2,h_3,h_4\}),(e_4,h_3,h_5\})\}$. Here let $(F,T) \theta_\varepsilon(G,Z)=(H,T\cup Z)$, where for every $\alpha\in T\cup Z$;

$$H(\alpha) = \begin{cases} F(\alpha), & \alpha \in T - Z \\ G(\alpha), & \alpha \in Z - T \\ F'(\alpha) \cap G'(\alpha), & \alpha \in T \cap Z \end{cases}$$

Since $T-Z=\{e_1\}$, $Z-T=\{e_2,e_4\}$, $T\cap Z=\{e_3\}$, thus, $H(e_1)=F(e_1)=\{h_2,h_5\}$,$H(e_2)=G(e_2)=\{h_1,h_4,h_5\}$,$H(e_4)=G(e_4)=\{h_3,h_5\}$, $H(e_3)=F'(e_3)\cap G'(e_3)=\{h_3,h_4\}\cap \{h_1,h_5\}=\emptyset$. Thus, $(F,T)\theta_\varepsilon(G,Z)=\{(e_1,\{h_2,h_5\}), (e_2,\{h_1,h_4,h_5\}), (e_3,\emptyset), (e_4,\{h_3,h_5\})\}$

Remark 1. In the set $S_T(U)$, where T is a fixed subset of E, restricted and extended theta operations coincide with each other. That is, $(F,T) \theta_\varepsilon(G,T)=(F,T) \theta_R(G,T)$.

Theorem 7. Let (F,T), (G,Z), (H,M), (G,T), (H,T), (K,T) and (L,T), be soft sets over U. Then, we have the followings:

1) The set $S_E(U)$ and $S_T(U)$ are closed under θ_ε.
2) If $T\cap Z\cap M=\emptyset$, then $[(F,T)\theta_\varepsilon(G,Z)] \theta_\varepsilon(H,M) = (F,T) \theta_\varepsilon [(G,Z) \theta_\varepsilon (H,M)]$.
3) $[(F,T) \theta_\varepsilon(G,T)] \theta_\varepsilon (H,T) \neq (F,T) \theta_\varepsilon[(G,T) \theta_\varepsilon(H,T)]$.
4) $(F,T) \theta_\varepsilon(G,Z)=(G,Z) \theta_\varepsilon (F,T)$.

5) $(F,T) \theta_\varepsilon(F,T)= (F,T)^r$.
6) $(F,T) \theta_\varepsilon\emptyset_T=\emptyset_T\theta_\varepsilon (F,T)= U_T$.
7) $(F,T)\theta_\varepsilon\emptyset_\emptyset=(F,T)$.
8) $\emptyset_\emptyset \theta_\varepsilon(F,T)=(F,T)$.
9) $(F, T) \theta_\varepsilon U_T = U_T\theta_\varepsilon(F, T) = \emptyset_T$.
10) $(F,T) \theta_\varepsilon(F,T)^r= (F,T)^r\theta_\varepsilon (F,T)= \emptyset_T$.
11) $[(F,T) \theta_\varepsilon(G,Z)]^r=(F,T) \overset{*}{\underset{\cup}{\sim}} (G,Z)$.
12) $(F,T) \theta_\varepsilon(G, T)= U_T$ if and only if $(F,T) = \emptyset_T$ and $(G, T) = \emptyset_T$.
13) $\emptyset_T \widetilde{\subseteq}(F,T)\theta_\varepsilon(G,Z)$, $\emptyset_Z \widetilde{\subseteq}(F,T)\theta_\varepsilon(G,Z)$. Moreover, $(F,T)\theta_\varepsilon (G,Z) \widetilde{\subseteq} U_{T\cup Z}$.
14) $(F, T)\theta_\varepsilon(G, T) \widetilde{\subseteq} (F,T)^r$ and $(F, T)\theta_\varepsilon(G, T) \widetilde{\subseteq} (G,T)^r$.
15) If $(F,T) \widetilde{\subseteq} (G, T)$, $(F,T)\theta_\varepsilon(G,T) =(G,T)^r$.
16) If $(F,T)\widetilde{\subseteq} (G, T)$, $(G,T)\theta_\varepsilon(H,T)\widetilde{\subseteq}(F,T)\theta_\varepsilon(H,T)$. The converse is not true.
17) If $(F,T) \widetilde{\subseteq} (G, T)$ and $(K,T) \widetilde{\subseteq} (L, T)$, $(G,T) \theta_\varepsilon(L,T) \widetilde{\subseteq}(F,T) \theta_\varepsilon(K,T)$.
18) $(F,T) \theta_\varepsilon (G,Z) \widetilde{\subseteq}(F,T) *_\varepsilon(G,Z)$ and $(G,Z) \theta_\varepsilon(F,T) \widetilde{\subseteq}(G,Z) *_\varepsilon (F,T)$.

Proof. 1) It is clear that θ_ε is a binary operation in $S_E(U)$. That is,

$$\theta_\varepsilon: S_E(U)\times S_E(U)\rightarrow S_E(U)$$
$$((F,T), (G,Z)) \rightarrow (F,T)\theta_\varepsilon(G,Z)=(H,T\cup Z)$$

Namely, when (F,T) and (G,Z) are soft set over U, then so $(F,T) \theta_\varepsilon (G,Z)$. Similarly, $S_T(U)$ is closed under θ_ε. That is,

$$\theta_\varepsilon: S_T(U)\times S_T(U)\rightarrow S_T(U)$$
$$((F,T), (G,T)) \rightarrow (F, T)\theta_\varepsilon(G, T)=(K,T\cup T)=(K,T)$$

Namely, θ_ε is a binary operation in $S_T(U)$.
2) First, consider the LHS. Let $(F,T)\theta_\varepsilon(G,Z)=(S,T\cup Z)$, where for every $\alpha\in T\cup Z$,

$$S(\alpha) = \begin{cases} F(\alpha), & \alpha \in T - Z \\ G(\alpha), & \alpha \in Z - T \\ F'(\alpha) \cap G'(\alpha), & \alpha \in T \cap Z \end{cases}$$

Let $(S,T\cup Z)\theta_\varepsilon(H,M)=(N,(T\cup Z)\cup M))$, where for every $\alpha\in(T\cup Z)\cup M$,

$$N(\alpha) = \begin{cases} S(\alpha), & \alpha \in (T \cup Z) - M \\ H(\alpha), & \alpha \in M - (T \cup Z) \\ S'(\alpha) \cap H'(\alpha), & \alpha \in (T \cup Z) \cap M \end{cases}$$

Thus,

$$N(\alpha)= \begin{cases} F(\alpha), & \alpha \in (T - Z) - M \\ G(\alpha) & \alpha \in (Z - T) - M \\ F'(\alpha) \cap G'(\alpha) & \alpha \in (T \cap Z) - M \\ H(\alpha), & \alpha \in M-(T\cup Z) \\ F'(\alpha) \cap H'(\alpha), & \alpha \in (T - Z) \cap M \\ G'(\alpha) \cap H'(\alpha), & \alpha \in (Z - T) \cap M \\ [F(\alpha) \cup G(\alpha)] \cap H'(\alpha) & \alpha \in (T\cap Z)\cap M \end{cases}$$

Now consider the RHS. Let $(G,Z) \theta_\varepsilon(H,M)=(R,Z\cup M)$, where for every $\alpha\in Z\cup M$;

$$R(\alpha) = \begin{cases} G(\alpha), & \alpha \in Z - M \\ H(\alpha), & \alpha \in M - Z \\ G'(\alpha) \cap H'(\alpha), & \alpha \in Z \cap M \end{cases}$$

Let $(F,T)\theta_\varepsilon(R,Z\cup M)=(L,(T\cup(Z\cup M)))$, where for every $\alpha\in T\cup Z\cup M$;

$$L(\alpha) = \begin{cases} F(\alpha), & \alpha \in T - (Z \cup M) \\ R(\alpha), & \alpha \in (Z \cup M) - T \\ F'(\alpha) \cap R'(\alpha), & \alpha \in T \cap (Z \cup M) \end{cases}$$

Hence,

$$L(\alpha)= \begin{cases} F(\alpha), & \alpha \in T - (Z \cup M) \\ G(\alpha) & \alpha \in (Z - M) - T \\ H(\alpha) & \alpha \in (M - Z) - T \\ G'(\alpha) \cap H'(\alpha) & \alpha \in (Z\cap M) - T \\ F'(\alpha) \cap G'(\alpha) & \alpha \in T \cap (Z - M) \\ F'(\alpha) \cap H'(\alpha) & \alpha \in T\cap(M - Z) \\ F'(\alpha) \cap [G(\alpha) \cup H(\alpha)] & \alpha \in T\cap(Z\cap M) \end{cases}$$

It is observed that $(N,(T\cup Z)\cup M)=(L,T\cup(Z\cup M))$, where $T\cap Z\cap M=\emptyset$. That is, in $S_E(U)$, θ_ε is associative under certain conditions.

3) The proof follows from Remark 1 and Theorem 1 (3). That is, in $S_T(U)$, where T is a fixed subset of E, θ_ε is not associative.

4) Let $(F,T) \theta_\varepsilon(G,Z)=(H,T\cup Z)$, where for every $\alpha\in T\cup Z$,

$$H(\alpha) = \begin{cases} F(\alpha), & \alpha \in T - Z \\ G(\alpha), & \alpha \in Z - T \\ F'(\alpha) \cap G'(\alpha), & \alpha \in T \cap Z \end{cases}$$

Let $(G,Z) \theta_\varepsilon(F,T)=(S,Z\cup T)$, where for every $\alpha\in Z\cup T$,

$$S(\alpha) = \begin{cases} G(\alpha), & \alpha \in Z - Z \\ F(\alpha), & \alpha \in T - Z \\ G'(\alpha) \cap F'(\alpha), & \alpha \in Z \cap T \end{cases}$$

Thus, $(F,T) \theta_\varepsilon (G,Z)=(G,Z) \theta_\varepsilon(F,T)$. Moreover, it is obvious that $(F,T) \theta_\varepsilon (G,T)=(G,T)\theta_\varepsilon(F,T)$. That is, in $S_E(U)$ and $S_T(U)$, θ_ε is commutative.

5) The proof follows from Remark 1 and Theorem 1 (5). That is, in $S_E(U)$, θ_ε is not idempotent.

6) The proof follows from Remark 1 and Theorem 1 (6).

7) Let $\emptyset_\emptyset=(S,\emptyset)$ and $(F,T) \theta_\varepsilon(S, \emptyset)=(H,T\cup\emptyset)$, where for every $\alpha\in T\cup\emptyset=T$,

$$H(\alpha) = \begin{cases} F(\alpha), & \alpha \in T - \emptyset = T \\ S(\alpha), & \alpha \in \emptyset - T = \emptyset \\ F'(\alpha) \cap S'(\alpha), & \alpha \in T \cap \emptyset = \emptyset \end{cases}$$

Thus, $H(\alpha)=F(\alpha)$, for every $\alpha\in T$, implying that $(H,T)=(F,T)$.

8) Let $\emptyset_\emptyset=(S,\emptyset)$ and $(F,T) \theta_\varepsilon(S, \emptyset)=(H,T\cup\emptyset)$, where for every $\alpha\in T\cup\emptyset=T$,

$$H(\alpha) = \begin{cases} S(\alpha), & \alpha \in \emptyset - T = \emptyset \\ F(\alpha), & \alpha \in T - \emptyset = T \\ S'(\alpha) \cap F'(\alpha), & \alpha \in \emptyset \cap T = \emptyset \end{cases}$$

Thus, for every $\alpha\in T$, $H(\alpha)=F(\alpha)$, $(H,T)=(F,T)$.

By Theorem 7 (7) and (8), we can conclude that in $S_E(U)$, the identity element of θ_ε is the soft set $\emptyset_\emptyset$. In classical set theory, it is well-known that $A\cup B=\emptyset\Leftrightarrow A=\emptyset$ and $B=\emptyset$. Thus, it is evident that in $S_E(U)$, we cannot find $(G, K) \in S_E(U)$ such that $(F, T) \theta_\varepsilon(G, K)= (G,K) \theta_\varepsilon(F, T) = \emptyset_\emptyset$; as this situation requires that $T\cup K=\emptyset$ and thus, $T=\emptyset$ and $K=\emptyset$. Since in $S_E(U)$, the only soft set with an empty parameter set is $\emptyset_\emptyset$, it follows that only the identity element $\emptyset_\emptyset$ has an inverse and its inverse it its own as usual. Thus, in $S_E(U)$, any other element except $\emptyset_\emptyset$ does not have an inverse for the operation θ_ε.

Corollary 1. Let (F,T), (G,Z), and (H,M) be the elements of $S_E(U)$. By Theorem 7 (1), (2), (4), (7) and (8), $(S_E(U), \theta_\varepsilon)$ is a commutative monoid whose identity is $\emptyset_\emptyset$ where $T\cap Z\cap M=\emptyset$. Since $(S_A(U), \theta_\varepsilon)$ is not associative, where A is a fixed subset of E, this algebraic structure can not be a semigroup.

9) The proof follows from Remark 1 and Theorem 1 (10).

10) The proof follows from Remark 1 and Theorem 1 (13).

11) Let $(F,T) \theta_\varepsilon(G,Z) =(H,T\cup Z)$, where for every $\alpha\in T\cup Z$;

$$H(\alpha) = \begin{cases} F(\alpha), & \alpha \in T - Z \\ G(\alpha), & \alpha \in Z - T \\ F'(\alpha) \cap G'(\alpha), & \alpha \in T \cap Z \end{cases}$$

Let $(H,T\cup Z)^r =(K,T\cup Z)$, for every $\alpha\in T\cup Z$;

$$K(\alpha) = \begin{cases} F'(\alpha), & \alpha \in T - Z \\ G'(\alpha), & \alpha \in Z - T \\ F(\alpha) \cup G(\alpha), & \alpha \in T \cap Z \end{cases}$$

Thus, $(K,T\cup Z)= (F,T) \overset{*}{\underset{\cup}{\sim}} (G,Z)$.

12) The proof follows from Remark 1 and Theorem 1 (15).

13) The proof is obvious.

14) The proof follows from Remark 1 and Theorem 1 (17).

15) The proof follows from Remark 1 and Theorem 1 (18).

16) The proof follows from Remark 1 and Theorem 1 (19) and (20).

17) The proof follows from Remark 1 and Theorem 1 (21).

18) Let $(F,T)\theta_\varepsilon(G,Z)=(H,T\cup Z)$, where for every $\alpha\in T\cup Z$,

$$H(\alpha) = \begin{cases} F(\alpha), & \alpha \in T - Z \\ G(\alpha), & \alpha \in Z - T \\ F'(\alpha) \cap G'(\alpha), & \alpha \in T \cap Z \end{cases}$$

Let $(F,T) *_\varepsilon (G,Z)=(K,T\cup Z)$, where for every $\alpha\in T\cup Z$,

$$K(\alpha) = \begin{cases} F(\alpha), & \alpha \in T - Z \\ G(\alpha), & \alpha \in Z - T \\ F'(\alpha) \cup G'(\alpha), & \alpha \in T \cap Z \end{cases}$$

for every $\alpha \in T-Z$; $H(\alpha)=F(\alpha) \subseteq F(\alpha)=K(\alpha)$, for every $\alpha \in Z-T$; $H(\alpha)=G(\alpha) \subseteq G(\alpha)=K(\alpha)$, for every $\alpha \in T \cap Z$; $H(\alpha)=F'(\alpha) \cap G'(\alpha) \subseteq F'(\alpha) \cup G'(\alpha) = H(\alpha)$, $(F,A)\theta_\varepsilon(G,B) \widetilde{\cong} (F,A) *_\varepsilon (G,B)$ is obtained.

Theorem 8. Let (F,T), (G,Z), and (H,M) be soft sets over U. Then, extended theta operation distributes over other soft set operations as follows:

Theorem 9. Let (F,T), (G,Z), and (H,M) be soft sets over U. Then, extended theta operation distributes over extended soft set operations as follows:

i) LHS Distributions

The following equations are satisfied if $T \cap (Z \Delta M) = TZ \cap M = \emptyset$.

1) $(F,T) \theta_\varepsilon[(G,Z) \cup_\varepsilon(H,M)] = [(F,T) \theta_\varepsilon(G,Z)] \cup_\varepsilon[(F,T) \theta_\varepsilon (H,M)]$.

Proof. Consider first the LHS. Let $(G,Z) \cup_\varepsilon(H,M)=(R,Z\cup M)$, where for every $\alpha \in Z\cup M$,

$$R(\alpha) = \begin{cases} G(\alpha), & \alpha \in Z - M \\ H(\alpha), & \alpha \in M - Z \\ G(\alpha) \cup H(\alpha), & \alpha \in Z \cap M \end{cases}$$

Let $(F,T) \theta_\varepsilon(R,Z\cup M)=(N,(T\cup(Z\cup M)))$, where for every $\alpha \in T\cup(Z\cup M)$;

$$N(\alpha) = \begin{cases} F(\alpha) & \alpha \in T - (Z \cup M) \\ R(\alpha) & \alpha \in (Z \cup M) - T \\ F'(\alpha) \cap R'(\alpha) & \alpha \in T \cap (Z \cup M) \end{cases}$$

Thus,

$$N(\alpha)= \begin{cases} F(\alpha), & \alpha \in T - (Z \cup M) \\ G(\alpha), & \alpha\in(Z - M) - T \\ H(\alpha), & \alpha \in (M - Z) - T \\ G(\alpha) \cup H(\alpha), & \alpha\in(T \cap Z) - T \\ F'(\alpha) \cap G'(\alpha), & \alpha \in T \cap (Z - M) \\ F'(\alpha) \cap H'(\alpha), & \alpha \in T \cap (M - Z) \\ F'(\alpha) \cap [G'(\alpha) \cap H'(\alpha)], & \alpha\in(T \cap Z)\cap M \end{cases}$$

Now consider the RHS, i.e.$[(F,T) \theta_\varepsilon(G,Z)] \cup_\varepsilon[(F,T) \theta_\varepsilon (H,M)]$. $(F,T)\theta_\varepsilon(G,Z)=(K,T\cup Z)$, where for every $\alpha \in T\cup Z$;

$$K(\alpha) = \begin{cases} F(\alpha), & \alpha \in T - Z \\ G(\alpha), & \alpha \in Z - T \\ F'(\alpha) \cap G'(\alpha), & \alpha \in T \cap Z \end{cases}$$

Let $(F,T) \theta_\varepsilon (H,M)=(S,T\cup M)$, where for every $\alpha \in T\cup M$;

$$S(\alpha) = \begin{cases} F(\alpha), & \alpha \in T - M \\ H(\alpha), & \alpha \in M - T \\ F'(\alpha) \cap H'(\alpha), & \alpha \in T \cap M \end{cases}$$

Assume that $(K,T\cup Z) \cup_\varepsilon (S,T\cup M)=(L,(T\cup Z)\cup(T\cup M))$, where for every $\alpha \in (T\cup Z) \cup (T\cup M)$ Thus,

$$L(\alpha) = \begin{cases} K(\alpha), & \alpha \in (T \cup Z) - (T \cup M) \\ S(\alpha), & \alpha \in (T \cup M) - (T \cup Z) \\ K(\alpha) \cup S(\alpha), & \alpha \in (T \cup M) - (T \cup Z) \end{cases}$$

Thus,

$$L(\alpha) = \begin{cases} F(\alpha), & \alpha \in (T - Z) - (T\cup M) \\ G(\alpha), & \alpha \in (Z - T)\text{-}(T\cup M) \\ F'(\alpha) \cap G'(\alpha), & \alpha \in (T \cap Z) - (T\cup M) \\ F(\alpha), & \alpha \in (T - M) - (T\cup Z) \\ H(\alpha), & \alpha \in (M - T) - (T\cup Z)=\emptyset \\ F'(\alpha) \cap H'(\alpha), & \alpha \in (T \cap M) - (T\cup Z) \\ F(\alpha) \cup F(\alpha), & \alpha \in (T - Z) \cap (T - M) \\ F(\alpha) \cup H(\alpha), & \alpha \in (T - Z) \cap (M - T)=\emptyset \\ F(\alpha) \cup [F'(\alpha) \cap H'(\alpha)], & \alpha \in (T - Z) \cap (T \cap M)=\emptyset \\ G(\alpha) \cup F(\alpha), & \alpha \in (Z - T) \cap (T - M)=\emptyset \\ G(\alpha) \cup H(\alpha), & \alpha \in (Z - T) \cap (M - T) \\ G(\alpha) \cup [F'(\alpha) \cap H'(\alpha)], & \alpha \in (Z - T) \cap (T \cap M) \\ [F'(\alpha) \cap G'(\alpha)] \cup F(\alpha), & \alpha \in (T \cap Z) \cap (T - M)=\emptyset \\ [F'(\alpha) \cap G'(\alpha)] \cup H(\alpha), & \alpha \in (T \cap Z) \cap (M - T) \\ [F'(\alpha) \cap G'(\alpha)] \cup [F'(\alpha) \cap H'(\alpha)], & \alpha \in T \cap Z \cap M \end{cases}$$

Hence,

$$L(\alpha)= \begin{cases} G(\alpha), & \alpha \in T' \cap Z \cap M \\ H(\alpha), & \alpha \in T' \cap Z' \cap M \\ F(\alpha), & \alpha \in T \cap Z' \cap M' \\ F(\alpha) \cup H'(\alpha), & \alpha \in T \cap Z' \cap M \\ G(\alpha) \cup H(\alpha), & \alpha \in T' \cap Z \cap M \\ G'(\alpha) \cup H(\alpha), & \alpha \in T \cap Z \cap M' \\ F'(\alpha) \cap [G'(\alpha) \cup H'(\alpha)], & \alpha \in T \cap Z\cap M \end{cases}$$

Therefore, N=L under the condition $T\cap Z'\cap M=T\cap Z\cap M'=T\cap Z\cap M=\emptyset$. It is obvious that the condition $T\cap Z'\cap M=T\cap Z\cap M'=\emptyset$ is equivalent to the condition $T\cap (Z\Delta M)=\emptyset$.

2) $(F,T) \theta_\varepsilon[(G,Z) \cap_\varepsilon(H,M)]=[(F,T) \theta_\varepsilon(G,Z)]\cup_\varepsilon[(F,T) \theta_\varepsilon (H,M)]$

ii) RHS Distributions

The following equations are satisfied if $(T\Delta Z)\cap M=T\cap Z\cap M=\emptyset$.

1) $[(F,T) \cap_\varepsilon(G,Z)] \theta_\varepsilon(H,M)=[(F,T) \theta_\varepsilon(H,M)]\cap_\varepsilon[(G,Z) \theta_\varepsilon (H,M)]$.

Proof. Consider first the LHS. Let $(F,T)\cap_\varepsilon(G,Z)=(R,T\cup Z$, where for every $\alpha \in T\cup Z$;

$$R(\alpha) = \begin{cases} F(\alpha), & \alpha \in T - Z \\ G(\alpha), & \alpha \in Z - T \\ F(\alpha) \cap G(\alpha), & \alpha \in T \cap Z \end{cases}$$

Let $(R,T\cup Z)\theta_\varepsilon(H,M)=(N,(T\cup Z)\cup M)$. Thus, for every $\alpha \in (T\cup Z)\cup M$;

$$N(\alpha) = \begin{cases} R(\alpha), & \alpha \in (T \cup Z) - M \\ H(\alpha), & \alpha \in M - (T \cup Z) \\ R'(\alpha) \cap H'(\alpha), & \alpha \in (T \cup Z) \cap M \end{cases}$$

Hence,

$$N(\alpha)=\begin{cases} F(\alpha), & \alpha \in (T-Z)-M \\ G(\alpha), & \alpha \in (Z-T)-M \\ H(\alpha), & \alpha \in M-(T \cup Z) \\ F(\alpha) \cap G(\alpha), & \alpha \in (T \cap Z)-M \\ F'(\alpha) \cap H'(\alpha), & \alpha \in (T-Z) \cap M \\ G'(\alpha) \cap H'(\alpha), & \alpha \in (Z-T) \cap M \\ [F'(\alpha) \cup G'(\alpha)] \cap H'(\alpha), & \alpha \in T\cap(Z\cap M) \end{cases}$$

Now consider the RHS. Let $(F,T)\theta_\varepsilon(H,M)=(S,T\cup M)$, where for every $\alpha\in T\cup M$;

$$S(\alpha) = \begin{cases} F(\alpha), & \alpha \in T-M \\ H(\alpha), & \alpha \in M-T \\ F'(\alpha) \cap H'(\alpha), & \alpha \in T \cap M \end{cases}$$

Let $(G,Z) \theta_\varepsilon (H,M)=(K,Z\cup M)$, where for every $\alpha\in Z\cup M$

$$K(\alpha) = \begin{cases} G(\alpha), & \alpha \in Z-M \\ H(\alpha), & \alpha \in M-Z \\ G'(\alpha) \cup H'(\alpha), & \alpha \in Z \cap M \end{cases}$$

Assume that $(S,T\cup Z)\cap_\varepsilon(K,Z\cup M)=(W,(T\cup Z)\cap(Z\cup M))$, where for every $\alpha\in(T\cup Z)\cup(Z\cup M)$;

$$L(\alpha) = \begin{cases} K(\alpha), & \alpha \in (T \cup Z)-(T \cup M) \\ S(\alpha), & \alpha \in (T \cup M)-(T \cup Z) \\ K(\alpha) \cap S(\alpha), & \alpha \in (T \cup M)-(T \cup Z) \end{cases}$$

Thus,

$$L(\alpha)=\begin{cases} F(\alpha), & \alpha\in(T-M)-(Z\cup M) \\ H(\alpha), & \alpha\in(M-T)-(Z\cup M) \\ F'(\alpha) \cap H'(\alpha), & \alpha\in(T\cap M)-(Z\cup M) \\ G(\alpha), & \alpha\in(Z-M)-(T\cup M) \\ H(\alpha), & \alpha\in(M-Z)-T\cup M)=\emptyset \\ G'(\alpha) \cap H'(\alpha), & \alpha\in(Z\cap M)-(T\cup M) \\ F(\alpha) \cap G(\alpha), & \alpha\in(T-M)\cap(Z-M) \\ F(\alpha) \cap H(\alpha), & \alpha\in(T-M)\cap(M-Z)=\emptyset \\ F(\alpha) \cap [G'(\alpha) \cap H'(\alpha)], & \alpha\in(T-M)\cap(Z\cap M)=\emptyset \\ H(\alpha) \cap G(\alpha), & \alpha\in(M-T)\cap(Z-M)=\emptyset \\ H(\alpha) \cap H(\alpha), & \alpha\in(M-T)\cap(M-Z) \\ H(\alpha) \cap [G'(\alpha) \cap H'(\alpha)] & \alpha\in(M-T)\cap(Z\cap M) \\ H(\alpha) \cap [G'(\alpha) \cap H'(\alpha)], & \alpha\in(T\cap M)\cap(Z-M)=\emptyset \\ [F'(\alpha) \cap H'(\alpha)] \cap H(\alpha), & \alpha\in(T\cap M)\cap(M-Z) \\ [F'(\alpha) \cap H'(\alpha)] \cap [G'(\alpha) \cap H'(\alpha)], & \alpha\in T\cap Z\cap M \end{cases}$$

Hence,

$$L(\alpha)=\begin{cases} F(\alpha), & \alpha \in T \cap Z' \cap M' \\ G(\alpha), & \alpha \in T' \cap Z \cap M' \\ H(\alpha), & \alpha \in T' \cap Z' \cap M \\ F(\alpha) \cap G(\alpha), & \alpha \in T \cap Z \cap M' \\ \emptyset, & \alpha \in T' \cap Z \cap M \\ \emptyset, & \alpha \in T \cap Z' \cap M \\ [F'(\alpha) \cap G'(\alpha) \cap H'(\alpha), & \alpha \in T \cap Z \cap M \end{cases}$$

Therefore, $N=L$ under the condition $T'\cap Z\cap M=T\cap Z'\cap M=T\cap Z\cap M'=\emptyset$. It is obvious that the

condition $T'\cap Z\cap M=T\cap Z'\cap M=\emptyset$ is equivalent to the condition $(T\Delta Z)\cap M=\emptyset$.

2)$[(F,T) \cup_\varepsilon(G,Z)] \theta_\varepsilon(H,M)=[(F,T) \theta_\varepsilon(H,M)]\cap_\varepsilon[(G,Z) \theta_\varepsilon (H,M)]$.

Corollary 2. $(S_E(U),\cup_\varepsilon,\theta_\varepsilon)$ is an additive idempotent commutative semiring without zero, but with unity under certain conditions.

Proof. Ali et al. (2011) showed that $(S_E(U),\cup_\varepsilon)$ is a commutative, idempotent monoid with identity $\emptyset_\emptyset$, that is, a bounded semilattice (hence a semigroup). $(S_E(U), \theta_\varepsilon)$ is a commutative monoid (hence a semigroup) whose identity is $\emptyset_\emptyset$ under the condition $T\cap Z\cap M=\emptyset$, where (F,T), (G,Z) and (H,M) are soft sets over U. Moreover, by Theorem 9 (i) (1), θ_ε distributes over $\cup_\varepsilon$ from LHS under $T\cap (Z\Delta M)=T\cap Z \cap M=\emptyset$, and, θ_ε distributes over $\cup_\varepsilon$ form RHS under the condition $(T\Delta Z)\cap M=T\cap Z\cap M=\emptyset$. Consequently, under the conditions $T\cap Z\cap M=(T\Delta Z)\cap M=T\cap(Z\Delta M)=\emptyset$, $(S_E(U), \cup_\varepsilon ,\theta_\varepsilon)$ is an additive idempotent commutative semiring without zero, but with unity under certain conditions.

Corollary 3. $(S_E(U),\cap_\varepsilon,\theta_\varepsilon)$ is an additive idempotent commutative semiring without zero, but with unity under certain conditions.

Proof. Ali et al. (2011) showed that $(S_E(U),\cap_\varepsilon)$ is a commutative, idempotent monoid with identity $\emptyset_\emptyset$, that is, a bounded semilattice (hence a semigroup). $(S_E(U), \theta_\varepsilon)$ is a commutative monoid (hence a semigroup) whose identity is $\emptyset_\emptyset$ under the condition $T\cap Z\cap M=\emptyset$, where (F,T), (G,Z) and (H,M) are soft sets over U. Moreover, θ_ε distributes over $\cap_\varepsilon$ from LHS under $T\cap (Z\Delta M)=T\cap Z \cap M=\emptyset$, and θ_ε distributes over $\cap_\varepsilon$ from RHS under the condition $(T\Delta Z)\cap M=T\cap Z\cap M=\emptyset$. Consequently, under the condition $T\cap Z\cap M=(T\Delta Z)\cap M=T\cap(Z\Delta M)=\emptyset$. $(S_E(U),\cap_\varepsilon,\theta_\varepsilon)$ is an additive idempotent commutative semiring without zero, but with unity under certain conditions.

Theorem 10. Let (F,T), (G,Z), and (H,M) be soft sets over U. Then, extended theta operation distributes over soft binary piecewise operations as follows:

i) LHS Distributions

The following equations are satisfied if $T\cap Z\cap M=T\cap(Z\Delta M)=\emptyset$.

1)$(F,T) \theta_\varepsilon[(G,Z) \widetilde{\cap} (H,M)]= [(F,T)\theta_\varepsilon(G,Z)] \widetilde{\cap} [(F,T) \theta_\varepsilon (H,M)]$.

Proof. First, consider the LHS. Let $(G,Z) \widetilde{\cap} (H,M)=(R,Z)$, where for every $\alpha\in Z$;

$$R(\alpha) = \begin{cases} G(\alpha), & \alpha \in Z-M \\ G(\alpha) \cap H(\alpha), & \alpha \in Z \cap M \end{cases}$$

$(F,T) \theta_\varepsilon(R,Z)=(N,T\cup Z)$, where for every $\alpha\in T\cup Z$;

$$N(\alpha) = \begin{cases} F(\alpha), & \alpha \in T-Z \\ R(\alpha), & \alpha \in Z-T \\ F'(\alpha) \cap R'(\alpha), & \alpha \in T \cap Z \end{cases}$$

Thus,

$$N(\alpha)=\begin{cases} F(\alpha), & \alpha \in T - Z \\ G(\alpha), & \alpha \in (Z - M) - T \\ G(\alpha) \cap H(\alpha), & \alpha \in (Z \cap M) \\ F'(\alpha) \cap G'(\alpha), & \alpha \in T \cap (Z\text{-}M) \\ F'(\alpha) \cap [G'(\alpha) \cup H'(\alpha)], & \alpha \in T \cap (Z \cap M) \end{cases}$$

Now consider the RHS, i.e. $[(F,T)\theta_\varepsilon(G,Z)]$ $\tilde{\cap}[(F,T) \theta_\varepsilon (H,M)]$. Let $(F,T) \theta_\varepsilon(G,Z)=(K,T\cup Z)$, where for every $\alpha \in T \cup Z$;

$$K(\alpha) = \begin{cases} F(\alpha), & \alpha \in T - Z \\ G(\alpha), & \alpha \in Z - T \\ F'(\alpha) \cap R'(\alpha), & \alpha \in T \cap Z \end{cases}$$

Let $(F,T) \theta_\varepsilon(H,M)=(S,T\cup M)$, where for every $\alpha \in T \cup M$;

$$S(\alpha) = \begin{cases} F(\alpha), & \alpha \in T - M \\ H(\alpha), & \alpha \in M - T \\ F'(\alpha) \cap H'(\alpha), & \alpha \in T \cap M \end{cases}$$

Let $(K,T\cup Z) \tilde{\cap} (S,T\cup M)=(L,(T\cup Z)\cup(T\cup M))$, where for every $\alpha \in (T\cup Z)\cup(T\cup M)$;

$$L(\alpha) = \begin{cases} K(\alpha), & \alpha \in (T \cup Z) - (T \cup M) \\ K(\alpha) \cap S(\alpha), & \alpha \in (T \cup Z) \cap (T \cup M) \end{cases}$$

Thus,

$$L(\alpha)=\begin{cases} F(\alpha), & \alpha \in (T - Z) - (T\cup M)=\emptyset \\ G(\alpha), & \alpha \in (Z - T) - (T \cup M) \\ F'(\alpha) \cap G'(\alpha), & \alpha \in (T \cap Z) - (T\cup M)=\emptyset \\ F(\alpha) \cap F(\alpha), & \alpha \in (T - Z) \cap (T - M) \\ F(\alpha) \cap H(\alpha), & \alpha \in (T - Z) \cap (M - T)=\emptyset \\ F(\alpha) \cap [F'(\alpha) \cap H'(\alpha)], & \alpha \in (T - Z) \cap (T \cap M) \\ G(\alpha) \cap F(\alpha), & \alpha \in (Z - T) \cap (T - M)=\emptyset \\ G(\alpha) \cap H(\alpha), & \alpha \in (Z - T) \cap (M - T) \\ G(\alpha) \cap [F'(\alpha) \cap H'(\alpha)], & \alpha \in (Z - T) \cap (T \cap M)=\emptyset \\ [F'(\alpha) \cap G'(\alpha)] \cap F(\alpha), & \alpha \in (T \cap Z) \cap (T - M) \\ [F'(\alpha) \cap G'(\alpha)] \cap H(\alpha), & \alpha \in (T \cap Z) \cap (M - T)=\emptyset \\ [F'(\alpha) \cap G'(\alpha)] \cap [F'(\alpha) \cap H'(\alpha)], & \alpha \in T \cap Z \cap M \end{cases}$$

Thus,

$$L(\alpha)=\begin{cases} G(\alpha), & \alpha \in T \cap Z \cap M' \\ F(\alpha), & \alpha \in T \cap Z' \cap M' \\ \emptyset, & \alpha \in T' \cap Z' \cap M \\ G(\alpha) \cap H(\alpha), & \alpha \in T' \cap Z \cap M \\ \emptyset, & \alpha \in T \cap Z \cap M' \\ F'(\alpha) \cap [G'(\alpha) \cap H'(\alpha], & \alpha \in T \cap Z \cap M \end{cases}$$

When considering T-Z in the function N, since T-Z=T∩Z', if an element is in the complement of Z, it is either in M-Z, or (M∪Z)'. Thus, if $\alpha \in$ T-Z, then either $\alpha\in$ T∩M∩Z' or $\alpha\in$ T∩M'∩Z'. Therefore, N=L under the condition T∩Z∩M=T∩Z'∩M=T∩Z∩M'=∅. It is obvious that the condition T'∩Z∩M=T∩Z'∩M=∅ is equivalent to the condition (TΔZ)∩M=∅.

2)$(F,T) \theta_\varepsilon [(G,Z) \tilde{\cup} H,M)]= [(F,T)\theta_\varepsilon(G,Z)] \tilde{\cup} [(F,M) \theta_\varepsilon (G,Z)]$.

ii) RHS Distributions

The following equations are satisfied if (TΔZ)∩M=T∩Z∩M =∅.

1)$[(F,T)\tilde{\cup} (G,Z)] \theta_\varepsilon (H,M)=[(F,T)\theta_\varepsilon(H,M)] \tilde{\cup} [(G,Z) \theta_\varepsilon(H,M)]$.

Proof. First, consider the LHS of the equality. Let $(F,T) \tilde{\cup}(G,Z)=(R,T)$, where for every $\alpha\in T$;

$$R(\alpha) = \begin{cases} F(\alpha), & \alpha \in T - Z \\ F(\alpha) \cup G(\alpha), & \alpha \in T \cap Z \end{cases}$$

Let $(R,T) \theta_\varepsilon (H,M) =(N,T\cup M)$, where for every $\alpha\in T\cup M$;

$$N(\alpha) = \begin{cases} R(\alpha), & \alpha \in T - M \\ H(\alpha), & \alpha \in M - T \\ R'(\alpha) \cap H'(\alpha), & \alpha \in T \cap M \end{cases}$$

Thus,

$$N(\alpha)=\begin{cases} F(\alpha), & \alpha \in (T - Z) - M \\ F(\alpha) \cup G(\alpha), & \alpha \in (T \cap Z) - M \\ H(\alpha), & \alpha \in M - T \\ F'(\alpha) \cap H'(\alpha), & \alpha \in (T - Z) \cap M \\ [F'(\alpha) \cap G'(\alpha)] \cap H'(\alpha), & \alpha \in T \cap (Z \cap M) \end{cases}$$

Now consider the RHS. Let $(F,T) \theta_\varepsilon(H,M)=(K,T\cup M)$, where for every $\alpha\in T\cup M$;

$$K(\alpha) = \begin{cases} F(\alpha), & \alpha \in T - M \\ H(\alpha), & \alpha \in M - T \\ F'(\alpha) \cap H'(\alpha), & \alpha \in T \cap M \end{cases}$$

Let $(G,Z) \theta_\varepsilon (H,M)=(S,T\cup M)$, where for every $\alpha\in Z\cup M$;

$$S(\alpha) = \begin{cases} G(\alpha), & \alpha \in Z - M \\ H(\alpha), & \alpha \in M - Z \\ G'(\alpha) \cap H'(\alpha), & \alpha \in Z \cap M \end{cases}$$

Let $(K,T\cup M) \tilde{\cup} (S,Z\cup M)=(L,(T\cup M)\cup(Z\cup M))$, where for every $\alpha\in(T\cup M)\cup(Z\cup M)$;

$$L(\alpha) = \begin{cases} K(\alpha), & \alpha \in (T \cup M) - (Z \cup M) \\ K(\alpha) \cup S(\alpha), & \alpha \in (T \cup M) \cap (Z \cup M) \end{cases}$$

$$L(\alpha)=\begin{cases} F(\alpha), & \alpha \in (T - M) - (Z\cup M) \\ H(\alpha), & \alpha \in (M - T) - (Z \cup M)=\emptyset \\ F'(\alpha) \cap H'(\alpha), & \alpha \in (T \cap Z) - (Z\cup M)=\emptyset \\ F(\alpha) \cup G(\alpha), & \alpha \in (T - M) \cap (Z - M) \\ F(\alpha) \cup H(\alpha), & \alpha \in (T - M) \cap (M - Z)=\emptyset \\ F(\alpha) \cup [G'(\alpha) \cap H'(\alpha)], & \alpha \in (T - M) \cap (Z \cap M)=\emptyset \\ H(\alpha) \cup G(\alpha), & \alpha \in (M - T) \cap (Z\text{-}M)=\emptyset \\ H(\alpha) \cup H(\alpha), & \alpha \in (M - T) \cap (M - Z) \\ H(\alpha) \cup [G'(\alpha) \cap H'(\alpha)], & \alpha \in (M - T) \cap (Z \cap M) \\ [F'(\alpha) \cap H'(\alpha)] \cup G(\alpha), & \alpha \in (T \cap M) \cap (Z\text{-}M)=\emptyset \\ [F'(\alpha) \cap H'(\alpha)] \cup H(\alpha), & \alpha \in (T \cap Z) \cap (M\text{-}Z)=\emptyset \\ [F'(\alpha) \cap H'(\alpha)] \cup [G'(\alpha) \cap H'(\alpha)], & \alpha \in T \cap Z \cap M \end{cases}$$

Hence,

$$L(\alpha)= \begin{cases} F(\alpha), & \alpha \in T \cap Z' \cap M' \\ F(\alpha) \cup G(\alpha), & \alpha \in T \cap Z \cap M' \\ H(\alpha), & \alpha \in T' \cap Z' \cap M \\ H(\alpha) \cup G'(\alpha), & \alpha \in T' \cap Z \cap M \\ F'(\alpha) \cup H(\alpha), & \alpha \in T \cap Z' \cap M \\ [F'(\alpha) \cup G'(\alpha)] \cap H'(\alpha), & \alpha \in T \cap Z \cap M \end{cases}$$

When considering M-T in the function N, since M-T=M∩T', if an element is in the complement of T, then it is either in Z-T or (Z∪T)'. Thus if α∈M-T, then α∈ M∩Z∩T' or α∈M∩Z'∩T'. Thus, N=L under T'∩Z∩M= T∩Z'∩M = T∩Z∩M =∅.

2) $[(F,T) \widetilde{\cap} (G,Z)] \theta_\varepsilon (H,M) = [(F,T)\theta_\varepsilon(H,M)] \widetilde{\cap} [(G,Z) \theta_\varepsilon (H,M)]$.

Corollary 4. $(S_E(U), \widetilde{\cup}, \theta_\varepsilon)$ is an additive idempotent multiplicative commutative semiring without zero, but with unity under certain conditions.

Proof. Yavuz (2024) showed that $(S_E(U), \widetilde{\cup})$ is an idempotent, non-commutative semigroup (that is a band) under the condition T∩Z'∩M =∅, where (F,T), (G,Z) and (H,M) are soft sets. $(S_E(U), \theta_\varepsilon)$ is a commutative monoid (hence a semigroup) whose identity is $\emptyset_\emptyset$ under the condition T∩Z∩M=∅, where (F,T), (G,Z) and (H,M) are soft sets over U. Moreover, θ_ε distributes over $\widetilde{\cup}$ from LHS under T∩Z∩M=T∩(Z∆M)=∅, and θ_ε distributes over $\widetilde{\cup}$ from RHS under the condition (T∆Z)∩M=T∩Z∩M =∅. Consequently, under the conditions T∩Z∩M=T∩(Z∆M)=(T∆Z)∩M=T∩Z'∩M=∅, $(S_E(U), \widetilde{\cup}, \theta_\varepsilon)$ is an additive idempotent multiplicative commutative semiring without zero, but with unity under certain conditions.

Corollary 5. $(S_E(U), \widetilde{\cap}, \theta_\varepsilon)$ is an additive idempotent multiplicative commutative semiring without zero, but with unity under certain conditions.

Proof. Yavuz (2024) showed that $(S_E(U), \widetilde{\cap})$ is an idempotent, commutative semigroup (that is a band) under the condition T∩Z'∩M =∅, where (F,T), (G,Z) and (H,M) are soft sets. $(S_E(U), \theta_\varepsilon)$ is a commutative monoid (hence a semigroup) whose identity is $\emptyset_\emptyset$ under the condition T∩Z∩M=∅, where (F,T), (G,Z) and (H,M) are soft sets over U. Moreover, θ_ε distributes over $\widetilde{\cap}$ from LHS under T∩Z∩M=T∩(Z∆M)=∅ and θ_ε distributes over $\widetilde{\cap}$ from RHS under the condition (T∆Z)∩M=T∩Z∩M=∅. Consequently, under the conditions T∩Z∩M=T∩(Z∆M)=(T∆Z)∩M=T∩Z'∩M=∅, $(S_E(U), \widetilde{\cap}, \theta_\varepsilon)$ is an additive idempotent multiplicative commutative semiring without zero, but with unity under certain conditions.

CONCLUSION

Parametric techniques like soft sets and soft operations are very useful when dealing with uncertainty. Introducing new soft operations and figuring out their algebraic properties and uses opens up new ways to solve problems with parametric data. This work introduces a novel restricted and extended soft set operation in this manner. By putting out the idea of "restricted and extended theta operations of soft sets" and by carefully examining the algebraic structures associated with these and other specific kinds of soft set operations, we hope to make a meaningful contribution to the field of soft set theory. Specifically, an extensive analysis is conducted on the algebraic characteristics of these new soft set operations. Taking into account the algebraic properties of these soft set operations and distribution laws, a thorough study of the algebraic structures formed by these operations in the collection of soft sets over the universe is presented. We demonstrate that, under some assumptions, $(S_E(U), \theta_\varepsilon)$ is a commutative monoid with identity $\emptyset_\emptyset$. Furthermore, we demonstrate how several significant algebraic structures, including semirings, are formed in the collection of soft sets over the universe combined with extended theta operations and other kinds of soft set operations: $(S_E(U), \cup_\varepsilon, \theta_\varepsilon)$, $(S_E(U), \cap_\varepsilon, \theta_\varepsilon)$ are all additive idempotent commutative semirings without zero but with unity under certain conditions. $(S_E(U), \widetilde{\cap}, \theta_\varepsilon)$, $(S_E(U), \widetilde{\cup}, \theta_\varepsilon)$ are all additive idempotent multiplicative commutative semirings without zero but with unity under certain conditions.

By examining novel soft set operations and the algebraic structures of soft sets, we can fully comprehend their application. This can advance soft set theory and the classic algebraic literature in addition to offering new examples of algebraic structures. Future research might look at other varieties of new restricted and extended soft set operations, as well as the matching distributions and characteristics, to add to this body of knowledge.

ACKNOWLEDGMENTS

REFERENCES

Akbulut, E. 2024. New Type of Extended Operations of Soft Sets: Complementary Extended Lambda and Difference Operation. (Master Thesis), Amasya University the Graduate School of Natural and Applied Sciences, Amasya.

Ali, M. I., Feng, F., Liu, X., Min, W.K. & Shabir, M. 2009. On some new operations in soft set theory, Computers Mathematics with Applications, 57(9), pp. 1547-1553.

Ali, M. I., Shabir, M. & Naz M. 2011. Algebraic structures of soft sets associated with new operations, Computers and Mathematics with Applications, 61(9), pp. 2647-2654.

Aybek, F. 2024. New restricted and extended soft set operations. (Master Thesis), Amasya University The Graduate School of Natural and Applied Sciences, Amasya.

Birkhoff, G. 1967. Lattice theory, American Mathematical Society, Providence, Rhode.

Çağman, N. 2021. Conditional complements of sets and their application to group theory, Journal of New Results in Science, 10(3), pp. 67-74.

Çağman, N., Çıtak, F. & Aktaş, H. 2012. Soft int-group and its applications to group theory, Neural Computing and Applications, 2, pp. 151-158.

Clifford, A. H. 1954. Bands of semigroups, Proceedings of the American Mathematical Society, 5(3), pp. 499-504.

Eren, Ö.F. & Çalışıcı, H. 2019. On some operations of soft sets, The Fourth International Conference on Computational Mathematics and Engineering Sciences (CMES 2019), Antalya, Türkiye.

Ge, X. & Yang, S. 2011. Investigations on some operations of soft sets, World Academy of Science, Engineering and Technology, 75, pp. 1113-1116.

Hoorn, W. G. V. & Rootselaar, V. B. 1967. Fundamental notions in the theory of seminearrings, Compositio Mathematica, 18(1-2), pp. 65-78.

Husain, S. & Shivani K. M. 2018. A study of propertıes of soft set and its applications, International Research Journal of Engineering and Technology, 5(1), pp. 363-372.

Jabir, N. J., Abdulhasan, A. M. R. & Hassan, A. F. 2024. Algebraic properties of operations on n-ary relation soft set, Applied Geomatics, 16(1), pp. 41-45.

Jana, C., Pal, M., Karaaslan, F. & Sezgin, A. 2019. (α, β)-soft intersectional rings and ideals with their applications, New Mathematics and Natural Computation, 15(2), pp. 333-350.

Kilp, M., Knauer, U. & Mikhalev, A. V. 2001. Monoids, acts and categories (Second edition). Berlin: De Gruyter Expositions in Mathematics, (29).

Lawrence S. & Manoharan R. 2023. New approach to De Morgan's laws for soft sets via soft ideals, Applied Nanoscience, 13, pp. 2585-2592.

Liu, X. Y., Feng F. & Jun, Y. B. 2012. A note on generalized soft equal relations, Computers and Mathematics with Applications, 64(4), pp. 572-578.

Mahmood, T., Rehman, Z. U. & Sezgin, A. 2018. Lattice ordered soft near rings, Korean Journal of Mathematics, 26(3), pp. 503-517.

Maji, P. K, Biswas, R. & Roy, A. R. 2003. Soft set theory, Computers and Mathematics with Applications, 45(1), pp. 55-562.

Molodtsov, D. 1999. Soft set theory-first results, Computers and Mathematics with Applications, 37(4-5), pp. 19-31.

Muştuoğlu, E., Sezgin, A. & Türk, Z. K. 2016. Some characterizations on soft uni-groups and normal soft uni-groups, International Journal of Computer Applications, 155(10), pp. 1-8.

Neog,T. J. & Sut D. K. 2011. A new approach to the theory of soft set, International Journal of Computer Applications, 32(2), pp. 1-6.

Sezgin, A. 2016. A new approach to semigroup theory I: Soft union semigroups, ideals and bi-ideals, Algebra Letters, 2016(3), pp. 1-46.

Pant, S., Dagtoros, K., Kholil, M. I. & Vivas A. 2024. Matrices: Peculiar determinant property, Optimum Science Journal, 1, pp. 1-7.

Pei, D. & Miao, D. 2005. From soft sets to information systems, IEEE International Conference on Granular Computing, 2, pp. 617-621.

Sezer, A. S. 2014. Certain Characterizations of LA-semigroups by soft sets, Journal of Intelligent and Fuzzy Systems, 27(2), pp. 1035-1046.

Sezer, A. S., Çağman, N. & Atagün, A. O. 2015. Uni-soft substructures of groups, Annals of Fuzzy Mathematics and Informatics, 9(2), pp. 235-246.

Sezgin, A. 2018. A new view on AG-groupoid theory via soft sets for uncertainty modeling, Filomat, 32(8), 2995-3030.

Sezgin, A., Ahmad S., Mehmood A. 2019. A new operation on soft sets: Extended difference of soft sets, Journal of New Theory, 27, pp. 33-42.

Sezgin, A. & Aybek, F.N. 2023. A new soft set operation: Complementary soft binary piecewise gamma operation, Matrix Science Mathematic (1), pp. 27-45.

Sezgin, A., Aybek, F. N. & tagün A. O. 2023a. A new soft set operation: Complementary soft binary piecewise intersection operation, Black Sea Journal of Engineering and Science, 6(4), pp. 330-346.

Sezgin, A., Aybek, F. N. & Güngör, N. B. 2023b. A new soft set operation: Complementary soft binary piecewise union operation, Acta Informatica Malaysia, (7)1, pp. 38-53.

Sezgin, A., Atagün, A. O., Çağman, N. & Demir H. 2022. On near-rings with soft union ideals and applications, New Mathematics and Natural Computation, 18(2), pp. 495-511.

Sezgin, A. & Atagün, A. O. 2011. On operations of soft sets. Computers and Mathematics with Applications, 61(5), pp. 1457-1467.

Sezgin, A. & Atagün, A.O. 2023. A new soft set operation: Complementary soft binary piecewise plus operation, Matrix Science Mathematic, 7(2), pp. 125-142.

Sezgin, A. & Çağman, N. 2024. A new soft set operation: Complementary soft binary piecewise difference operation, Osmaniye Korkut Ata University Journal of the Institute of Science and Technology, 7(1), pp. 58-94.

Sezgin, A., Çağman, N. & Atagün, A. O. 2017. A completely new view to soft intersection rings via soft uni-int product, Applied Soft Computing, 54, pp. 366-392.

Sezgin, A., Çağman, N., Atagün, A. O. & Aybek, F. 2023c. Complemental binary operations of sets and their pplication to group theory. Matrix Science Mathematic, 7(2), pp. 114-121.

Sezgin, A & Çalışıcı, H. 2024. A comprehensive study on soft binary piecewise difference operation, Eskişehir Teknik Üniversitesi Bilim ve Teknoloji Dergisi B - Teorik Bilimler, 12(1), pp. 32-54.

Sezgin, A. & Dagtoros, K. 2023. Complementary soft binary piecewise symmetric difference operation: A novel soft set operation, Scientific Journal of Mehmet Akif Ersoy University, 6(2), pp. 31-45.

Sezgin, A. & Demirci, A.M. 2023. A new soft set operation: complementary soft binary piecewise star operation, Ikonion Journal of Mathematics, 5(2), pp. 24-52.

Sezgin, A. & Sarıalioğlu M. 2024. A new soft set operation complementary soft binary piecewise theta operation, Journal of Kadirli Faculty of Applied Sciences, 4(1), pp. 1-33.

Sezgin, A. & Yavuz, E. 2023a. A new soft set operation: complementary soft binary piecewise lambda operation, Sinop University Journal of Natural Sciences, 8(2), pp. 101-133.

Sezgin, A. & Yavuz, E. 2023b. A new soft set operation: Soft binary piecewise symmetric difference operation, Necmettin Erbakan University Journal of Science and Engineering, 5(2), pp. 189-208.

Singh, D. & Onyeozili, I. A. 2012a. Notes on soft matrices operations, ARPN Journal of Science and Technology, 2(9), pp. 861-869.

Singh, D. & Onyeozili, I. A. 2012b. On some new properties on soft set operations, International Journal of Computer Applications, 59(4), pp. 39-44.

Singh, D. & Onyeozili, I. A. 2012c. Some conceptual misunderstanding of the fundamentals of soft set theory, ARPN Journal of Systems and Software, 2(9), pp. 251-254.

Singh, D. & Onyeozili, I. A. 2012d. Some Results on Distributive and Absorption Properties on Soft Operations. IOSR Journal of Mathematics, 4(2), pp. 18-30.

Stojanovic, N. S. 2021. A new operation on soft sets: Extended symmetric difference of soft sets, Military Technical Courier, 69(4), pp. 779-791.

Vandiver, H. S. 1934. Note on a simple type of algebra in which the cancellation law of addition does not hold, Bulletin of the American Mathematical Society, 40(12), pp. 914-920.

Yang, C. F. 2008. "A note on: "Soft set theory" [Computers and Mathematics with Applications, 45(4-5) (2003) 555–562]," Computers and Mathematics with Applications, 56(7), pp. 1899-1900.

Yavuz E., 2024. Soft binary piecewise operations and their properties, (Master Thesis), Amasya University the Graduate School of Natural and Applied Sciences, Amasya.

APPLICATION OF COMPRESSIVE SENSING TECHNIQUES FOR ADVANCED IMAGE PROCESSING AND DIGITAL IMAGE TRANSMISSION

NENAD STEFANOVIĆ[1], BOBAN SAZDIĆ-JOTIĆ[2], VLADIMIR ORLIĆ[3], VLADIMIR MLADENOVIĆ[4], STEFAN ĆIRKOVIĆ[4]

[1]Center for Applied Mathematics and Electronics, Belgrade, Serbia
[2]Military Technical Institute, Belgrade, Serbia
[3]Vlatacom Institute, Belgrade, Serbia
[4]Faculty of Technical Sciences in Čačak, University of Kragujevac, Čačak, Serbia

ABSTRACT

The field of compressive sensing (CS) has emerged as a transformative approach in the acquisition and processing of high-dimensional data. This paper presents a comprehensive study on the application of compressive sensing techniques to advanced image processing and digital image transmission. By leveraging the inherent sparsity in natural images, CS allows for significant reductions in the amount of data required for accurate reconstruction, thereby overcoming the limitations imposed by the traditional Shannon-Nyquist sampling theorem. We explore the theoretical foundations of CS, including the principles of sparsity and incoherence, and provide a detailed overview of the Orthogonal Matching Pursuit (OMP) algorithm, a prominent greedy algorithm used for sparse signal recovery. Experimental results demonstrate the efficacy of CS in improving image reconstruction quality, as evidenced by enhancements in peak signal-to-noise ratio (PSNR) and structural similarity index (SSIM). Additionally, we discuss the practical implementation of CS in single-pixel cameras and its potential impact on future imaging technologies. The findings suggest that CS offers a robust framework for efficient image acquisition and processing, making it a valuable tool for various applications in multimedia, medical imaging, and remote sensing.

Keywords: Sensing, Reconstruction, Transmission, Sparsity, Algorithms.

INTRODUCTION

One of the most prevalent trends in contemporary technologies is the collection (acquisition), transmission, analysis, and processing of large amounts of data. Mass data processing is a common issue when it comes to multimedia data, medical and biomedical data, radar signals, and similar, and traditional sensor devices face strict requirements when performing acquisition according to the already standard Shannon-Nyquist criterion (sampling theorem), which states that the sampling rate of a signal must be at least twice the highest frequency present in the signal spectrum.

In the last decade, decade and a half, new methods and techniques known collectively as compressive sensing have been intensively developed, which surpass the boundaries of the existing sampling theory by applying the concept of data compression during the sampling/observing process itself. This reduces the amount of collected-measured data and thereby significantly reduces the engagement of available resources (time, energy, device complexity, etc.) on the end, i.e., the sensor side of the system.

This paper, in addition to describing the concept of compressive sensing, examines the application of a specific algorithm from the group of "greedy algorithms" for fast image reconstruction. The paper is divided into three main parts: theoretical framework with an intuitive approach, adaptation of the algorithm for advanced image processing, and presentation of the results achieved by applying such an algorithm on concrete examples and obtained performances from the perspective of peak signal-to-noise ratio (PSNR) and structural similarity index (SSIM).

THEORETICAL PART

Compressive sensing (cs)

Definition and Basic Concept

The concept of compressive sensing has received different names over a relatively short period, depending on its application (compressive sampling, sub-sampling, sparse sensing, sub-space sampling, etc.), and a relatively small number of papers have been published in Serbian where the general terminology in this field has not been adopted. Taking into account all these applications and perspectives on the unique principle, the terms used in this paper are those the author considered appropriate translations for the given

---

*Corresponding author: stefan.cirkovic@ftn.kg.ac.rs

context. Thus, the term observation (of images) can in this case be considered synonymous with the term reading (of spectra) or sampling (of signals), while essentially retaining the same observational course.

The initial setup of the concept known as compressive sensing, presented in (Donoho, 2006), states that a signal can be reconstructed from only a small set of randomly measured values - samples, if the signal can be represented in a sparse (compressed) form in some transform domain. Sparsity, as a property of the signal, means that the signal can be represented in a certain (transform) domain with a small number of non-zero samples, implying fewer numerical computations, memory, and consumption for signal reconstruction. The second condition, of a technical nature, is the incoherence between the measurement (sampling) and the transformation (sparsifying) operator matrices.

The principle, initially adopted from image and signal compression techniques, can be compared with classical sampling theory and represented with a block diagram (Stankovic et al., 2016) in (Fig. 1):
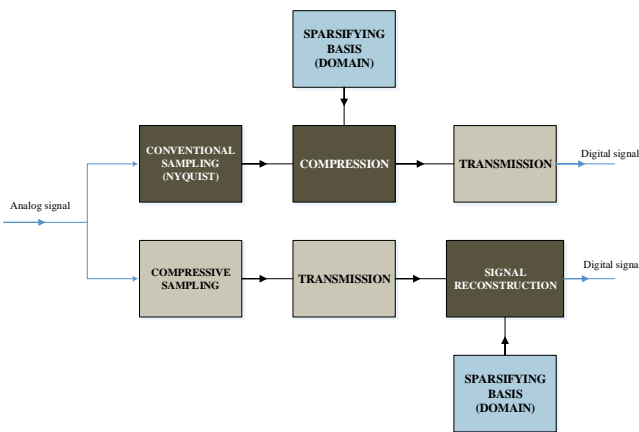

Figure 1. Comparative overview of classical and compressive sensing.

Parts of both systems are illustratively represented by blocks of different colors, with lighter shades representing blocks that are less burdened in terms of engaged resources. It is noticeable that in the case of compressive sensing, given the smaller amount of information collected, the focus of engaged resources shifts from the end points of the system (sensors, acquisition cards, high-resolution cameras, magnetic resonance scanners, geo-scanners, etc.) to the platform where signal reconstruction is performed.

The mathematical foundation that has led to a true "explosion" of publications and papers in the past decade lies in the premise that the process of data acquisition can be represented by a system of linear equations Eq. (1), (Foucart & Rauhut, 2013):

$$y = Ax \tag{1}$$

where from $y \in C^M$ the labeled vector of measured data (M - dimensional column), with $x \in C^N$ (N-dimensional column) vector of input data from the set of real numbers, and the matrix $A \in C^{M \times N}$ the operator of the linear measurement process, where $M<N$. The input signal is practically sampled at a smaller number of samples than the length of the input signal, resulting in an underdetermined system of linear equations (a greater number of unknowns – N than the number of equations – M). Assuming that the signal possesses the property of sparsity in the domain Ψ (which could be the domain of Fourier, DCT, Haar wavelet transform, etc.) and if the operator A has the corresponding properties, then it is possible to reconstruct the signal x from the vector y. For a more concise presentation of the theory, which can be found in numerous literature sources, we summarize the procedure step by step:

Sparsity of the signal: Let x represent an $N \times 1$ column vector of the input analog signal discretized in time, as previously mentioned. For a given orthonormal basis matrix $\psi \in R^{N \times N}$, whose columns represent the basis elementary vectors $\{\psi_i\}_{i=1}^N$ x can be represented as a linear combination of basis vectors Eq. (2):

$$x = \sum_{i=1}^{N} \alpha_i \psi_i \tag{2}$$

or more compactly, $x = \Psi\alpha$, where α represents an $N \times 1$ column vector of coefficients. These coefficients, in fact, represent the inner product of the vector x and the elementary basis vectors ψ_i, $\alpha_i < x$, $\psi_i > \psi_i^T x$, where (^{T}) signifies the transpose operation. If the basis-domain Ψ mapping the input vector x to a vector with a small number, let's say K, of non-zero coefficients, then it can be written as

$$x = \sum_{i=1}^{K} \alpha_{n_i} \psi_{n_i} \tag{3}$$

the sparse version of the input vector, where ni are the indices of coefficients and basis vectors (referred to in literature as dictionary atoms Ψ) corresponding to K non-zero coefficients. Then α, a dimension $N \times 1$, column vector with only K non-zero coefficients, denoted as $\|\alpha\|_0 = K$, where $\|\bullet\|_p$ denotes the lp-norm, or

$$\|x\|_p = \left(\sum_i \left| x_i^{\ p} \right| \right)^{\frac{1}{p}} \tag{4}$$

Calculating the norm of a specific vector or matrix represents different ways of measuring their length or magnitude (Patel et al., 2013). In the case where $p \rightarrow 0$, the practically obtained l0-norm, namely the previously mentioned

number of non-zero coefficients of the vector, is obtained. Real signals cannot practically be considered sparse in any domain, but the vast majority possess compressive, compressible properties – meaning the property of being compressible or compressive signals. Compressibility implies that if the amplitudes of signal coefficients are arranged in a decreasing order $\alpha_{(1)} \geq \alpha_{(2)} \geq ... \geq \alpha_{(N)}$, results in their exponential decay

$$|\alpha|_n \leq C.n^{-s} \tag{5}$$

where $|\alpha|_{(n)}$ is the nth largest coefficient value, $s \geq 1$, C constant. In that case, the error signal, or the difference between the signal obtained by a linear combination of basis vectors and the input signal, would also exponentially decay with the increase in the number of used coefficients

$$\|x_L - x\|_2 \leq CK^{-s\left(s-\frac{1}{2}\right)} \tag{6}$$

In other words, a small number of basic elementary vectors from Ψ can enable a precise approximation of x. Such approximation is known as nonlinear approximation.

Incoherence: The coefficients α_i from Eq. (2) are not directly measured in compressive sampling. Instead, the measurement of M ($M \ll N$) projections of vector x is performed using a collection of vectors $\{\psi_i\}_{i=1}^M$, arranged as rows of an arbitrary permutation matrix Φ, dimension $M \times N$, resulting in a measured column vector y, dimension $M \times 1$, whose elements are $y_j = \langle x, \phi_j \rangle$. The measurement process can now be written as

$$y = \Phi x = \Phi \Psi \alpha = A\alpha \tag{7}$$

where A represents the measurement or observation matrix mentioned in Eq. (1). Reconstruction refers to the recovery of the sparse version of the input vector x, the vector α from which, by the inverse transformation Ψ^{-1}, an approximation of the input vector is obtained. An illustrative representation of the reconstruction, or obtaining the measured vector, is shown in (Fig. 2). In this case, the matrix Ψ is pictorially represented as a transformational matrix operator coefficients of the discrete cosine transformation *(DCT)*, commonly used for image processing and compression.
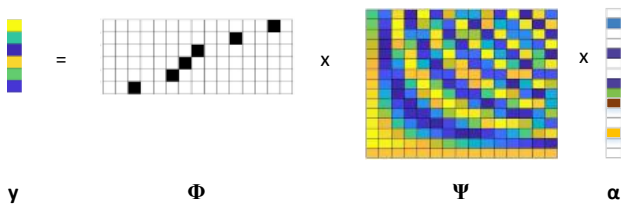

Figure 2. Illustrated representation of obtaining the measurement vector from compressively sampled signal.

For the algorithm to be successful, it is necessary for A to possess two fundamental properties:

The property of restricted isometry: known in the literature as *RIP (Restricted Isometry Property)*. For a matrix A to be said to possess the property of restricted isometry of order K, with constants $\delta_k \in (0,1)$, it must satisfy

$$(1-\delta_K)\|v\|_2^2 \leq \|Av\|_2^2 \leq (1+\delta_K)\|v\|_2^2 \tag{8}$$

for any vector v whose $\|v\|_0 \leq K$. An equivalent description would be that all subsets of K columns (vectors) taken from A are nearly orthogonal, implying that K-sparse vectors cannot lie in the null space of the matrix A. When *RIP* holds, A approximately preserves the Euclidean length (l_2-norm) of K-sparse vectors, i.e.,

$$(1-\delta_{2K})\|v_1 - v_2\|_2^2 \leq \|Av_1 - Av_2\|_2^2 \leq (1+\delta_{2K})\|v_1 - v_2\|_2^2 \tag{9}$$

applies to all K-sparse vectors v_1 and v_2. The related condition known as incoherence requires that the rows of Ψ cannot sparsely represent the columns of Ψ and vice versa.

Matrix incoherence: As a measure of mutual independence of constituent vectors for matrices Φ and Ψ is defined as

$$\mu(\Phi, \Psi) = \sqrt{N} \max \left| \langle \phi_i, \psi_j \rangle \right|, \quad 1 \leq i, j \leq N \tag{10}$$

The number μ represents the measure of similarity between two vectors of the matrix $A = \Phi\Psi$ and ranges between 1 and $\sqrt{N}$. The matrix A is said to be incoherent if μ is a very small number. Incoherence holds for various pairs of matrices, such as delta impulses and the Fourier basis, and with high probability between any matrix and a random matrix with Gaussian or Bernoulli distribution.

Reconstruction

As mentioned, algorithms for reconstructing compressively acquired signals involve finding a sparse approximation of the original input signal from compressive measurements, in an appropriate basis, framework, or dictionary. Research and development of various algorithms are motivated by reducing the number of measurements, noise resilience, speed, complexity, reliability, and credibility, etc. Algorithms are generally classified into six approaches for reconstruction, as shown in (Fig. 3), (Rani & Sushma, 2018).

The convex optimization approach involves finding the solution to formulation Eq. (1) using linear programming techniques. Some of the popular ones include the simplex algorithm, interior-point algorithm, Bregman algorithm, gradient projection for sparse representation (*GPSR*), fixed-point continuation, and others. These represent a global optimization approach.
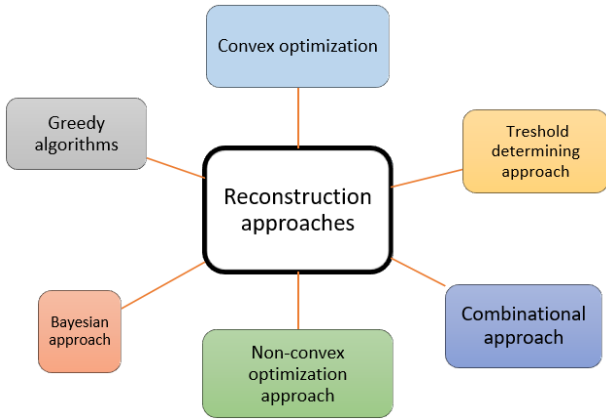
Figure 3. Approaches to compressive sensing reconstruction.

The approach using greedy algorithms, unlike convex ones, is an iterative step-by-step approach. During each iteration, the solution is updated by selecting only the columns of the reconstruction matrix that are highly correlated with the measurements. The selected columns are called atoms. Once selected, atoms are not used in subsequent algorithm steps, greatly reducing its computational complexity. The solution is obtained by iteratively choosing the best (closest to the original vector) solution in a "greedy" manner ("only the best is taken"), hence the name. These fall into the category of fast algorithms, but require some prior knowledge of the signal's sparsity measure. These algorithms can be further classified into two categories: serial and parallel.

The thresholding approach involves algorithms that work with K atoms from the reconstruction matrix, while also employing a certain thresholding sensitivity definition that sets all values below the threshold to zero, thereby reducing the impact of noise. The rest of the algorithm is very similar to the previously mentioned group. Some examples include Iterative Hard Thresholding, Iterative Soft Thresholding, Approximate Message Passing, etc.

Combinatorial approaches are primarily developed for finding sparse approximations during group testing, aiming to minimize the number of tests required to be conducted. They work on computing the minimum or mean values of measurements identified as constituent samples.

Non-convex optimization approach fundamentally differs from convex ones in the type of norm used to solve the minimization problem, specifically referring to norms located between l_0 and l_1. Examples of algorithms using this approach include solving focal undetermined system solutions and iteratively re-weighted least squares.

Bayesian approach is used for non-deterministic (stochastic) signals belonging to some probability distribution. Sparse Bayesian learning and others are known.

Orthogonal Matching Pursuit - OMP

Within the group of serial greedy algorithms, orthogonal matching pursuit (OMP) is included. Each iteration of these algorithms selects only one atom and calculates the corresponding non-zero element of the solution vector. The basic steps of these algorithms are depicted in the (Fig. 4), and the difference lies only in the solution update step:

Initialization: The residual vector r, dimension $M \times 1$, together with the measurement vector y, are initialized to initial values. The solution, sparse vector α, dimension $N \times 1$, and the index set Λ, dimension $M \times 1$, are dimensioned as zero vectors, and the initial dictionary matrix D, which will be established during iterations, is initialized as a zero matrix. The cycle counter i is set to the value 1.

Atom search: In this step, the column of the reconstruction matrix A that has the maximum correlation with the residual vector r is found. The position of this atom is updated in the index set Λ.

Update of the sparse solution vector: Depending on the selected atoms, the solution set α_i is updated and the approximation of the measurement y_i is found. The way the solution is updated is the step that distinguishes algorithms of this classification. In the OMP algorithm, this is the well-known least squares method.

Update of the residual: The new residual is calculated by subtracting the obtained approximation y_i (product of $D_i\alpha_i$) from the measurement vector y. These steps are repeated up to the desired sparsity level (K times) or until a desired residual value (less than some level $\varepsilon \geq 0$) is reached.
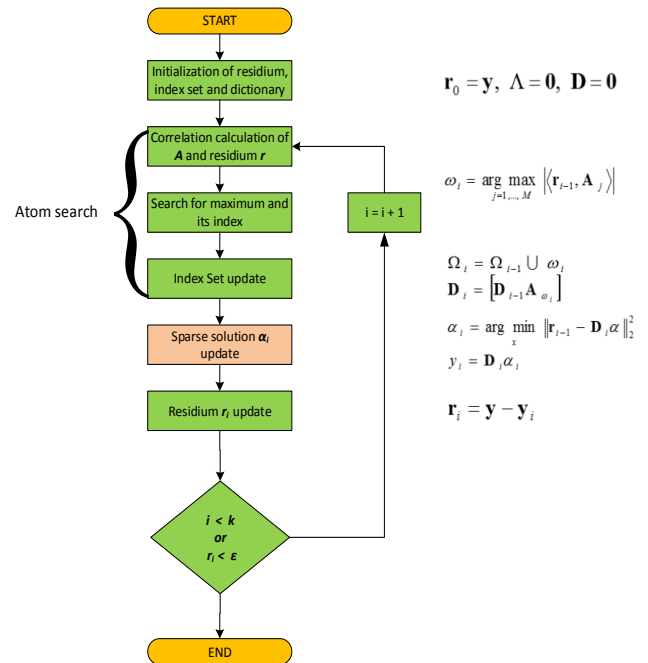

Figure 4. Algorithm for orthogonal matching pursuit.

For a clearer understanding of the principle of the orthogonal matching pursuit process, let's consider an example. The assumption is that for a given system

$$y = A \, \alpha$$

the measurement vector is known $y = \begin{bmatrix} 1.65 \\ -0.25 \end{bmatrix}$ and the matrix

$A = \begin{bmatrix} -0.707 & 0.8 & 0 \\ 0.707 & 0.6 & -1 \end{bmatrix}$ and it is necessary to find α, which

must be of dimension 3×1, and at the initialization phase, it is

set as a zero-column vector $\alpha = \begin{bmatrix} 0 \\ 0 \\ 0 \end{bmatrix}$ whose coefficients are

gradually updated during the steps.

We start from the premise that we consider the compressive matrix as a collection of basic column vectors or atoms:

$A = \begin{bmatrix} -0.707 & 0.8 & 0 \\ 0.707 & 0.6 & -1 \end{bmatrix} = \begin{bmatrix} b_1 & b_2 & b_3 \end{bmatrix}$, where

$b_1 = \begin{bmatrix} -0.707 \\ 0.707 \end{bmatrix}, b_2 = \begin{bmatrix} 0.8 \\ 0.6 \end{bmatrix}, b_3 = \begin{bmatrix} 0 \\ -1 \end{bmatrix}.$

If we denote that $\alpha = \begin{bmatrix} \alpha_1 \\ \alpha_2 \\ \alpha_3 \end{bmatrix}$ then A is

$\alpha = \begin{bmatrix} b_1 & b_2 & b_3 \end{bmatrix} \begin{bmatrix} \alpha_1 \\ \alpha_2 \\ \alpha_3 \end{bmatrix} = b_1\alpha_1 + b_2\alpha_2 + b_3\alpha_3 = y$

From this expression, it can be seen that the contribution of each atom from A depends on the values of the coefficient of the (un)sparse vector α. Thus, at the initial moment, it is necessary to find the atom that contributes the most to y. This process, for now, requires as many iterations as there are atoms.

1 step: The contribution of each atom is calculated by measuring the magnitude of its projection onto the measurement vector, i.e., by inner product.

$\left| \langle b_1, y \rangle \right| = \left\| \begin{bmatrix} -0.707 \\ 0.707 \end{bmatrix} \cdot \begin{bmatrix} 1.65 \\ -0.25 \end{bmatrix} \right\| =$

$\left| -0.70 \cdot (-0.25) + 0.707 \cdot 1.65 \right| = 1.34$

$\left| \langle b_2, y \rangle \right| = \left\| \begin{bmatrix} 0.8 \\ 0.6 \end{bmatrix} \cdot \begin{bmatrix} 1.65 \\ -0.25 \end{bmatrix} \right\| = 1.17$ and

$\left| \langle b_3, y \rangle \right| = \left\| \begin{bmatrix} 0 \\ -1 \end{bmatrix} \cdot \begin{bmatrix} 1.65 \\ -0.25 \end{bmatrix} \right\| = 0.25$

It can be seen that the largest contribution is from atom b_1, and therefore this vector is taken for updating the selected basis, whose coefficient is $\alpha = \begin{bmatrix} \alpha_1 \end{bmatrix} = -1.34$ (the coefficient of the most influential base vector in obtaining the final solution).

The contribution of each vector, of course, can be calculated in one step as $A^T y = \begin{bmatrix} -1.34 \\ 1.17 \\ 0.25 \end{bmatrix}$. The residual vector

is calculated as

$r = y - \alpha_1 b_1 = \begin{bmatrix} 1.65 \\ -0.25 \end{bmatrix} - (-1.34) \begin{bmatrix} -0.707 \\ 0.707 \end{bmatrix} = \begin{bmatrix} 0.7 \\ 0.7 \end{bmatrix}.$

When the first vector is selected, the reconstruction matrix is updated and filled in a way that it adopts this vector as its new basis $D(1) = b_1 = \begin{bmatrix} -0.707 \\ 0.707 \end{bmatrix}.$

2 step: Now, the calculation of contributions continues by searching for maximum correlations for the remaining atoms from matrix A (b_2 and b_3), but in relation to the residue vector r. In one step, we calculate contributions with

$\begin{bmatrix} b_2 & b_3 \end{bmatrix}^T \cdot r = \begin{bmatrix} 0.8 & 0.6 \\ 0 & -1 \end{bmatrix} \begin{bmatrix} 0.7 \\ 0.7 \end{bmatrix} = \begin{bmatrix} -0.98 \\ -0.7 \end{bmatrix}.$

From this, it is concluded that the vector b_2 has the largest contribution in absolute value, based on which we choose this vector to add to the new base. In this second iteration, the new matrix is $D(2) = \begin{bmatrix} b_1 & b_2 \end{bmatrix}$ and how close we are to the solution is calculated through least squares (Strang, 2016) $\min \| D(2) \cdot \alpha(2) - y \|_2$.

It is known that this problem in linear algebra can be solved with:

$$\alpha = D^+ y,$$

where D^+ denotes the pseudo-inverse matrix of matrix D, for which $D^+ = (D^T D)^{-1} D^T$. Now is $D^+(2) = \begin{bmatrix} -0.6062 & 0.8082 \\ 0.7143 & 0.7143 \end{bmatrix}$

(in MATLAB, the command is pinv), so at this moment (iteration) $\alpha = D^+ y = \begin{bmatrix} -0.6062 & 0.8082 \\ 0.7143 & 0.7143 \end{bmatrix} \cdot \begin{bmatrix} 1.65 \\ -0.25 \end{bmatrix} = \begin{bmatrix} -1.2 \\ 1 \end{bmatrix}.$

The new residual will be

$r = y - D(2)\alpha = y - \begin{bmatrix} b_1 & b_2 \end{bmatrix}$

$\alpha = \begin{bmatrix} 1.65 \\ -0.25 \end{bmatrix} - \begin{bmatrix} -0.707 & 0.8 \\ 0.707 & 0.6 \end{bmatrix} \begin{bmatrix} -1.2 \\ 1 \end{bmatrix} = \begin{bmatrix} 0 \\ 0 \end{bmatrix}$

Considering that we have reached orthogonal overlap (the residual between the measurement vector and the approximation is a zero vector), and knowing that the dimension of the vector is 3×1, we add as the last

element 0, so $\alpha = \begin{bmatrix} -1.2 \\ 1 \\ 0 \end{bmatrix}.$

When dealing with larger matrices, the process is iteratively repeated.

EXPERIMENTAL

Image processing using compressive sensing technique

Acquisition

One of the first devices that practically demonstrated the application of compressive sensing technique is the Rice single-pixel camera (SPC), (Patel et al., 2013). This camera essentially measures the inner product between an N-pixel sampled incident light beam from the scene and a set of N-pixel test functions, as shown in (Fig. 5).
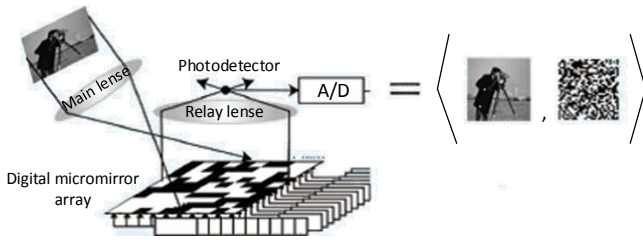

Figure 5. The operating principle of the Rice single-pixel camera, (Uzeler et al., 2013).

Such architecture utilizes only one photodetector to capture the scene. A digital micromirror device *(DMD)* array is used for the function of a pseudo-random binary sequence. The light beam is projected onto this array, and the beam intensity is measured with a photodetector. The orientations of the mirrors in the array can be rapidly changed, allowing for a series of different pseudo-random projections to be measured in a relatively short time. Reconstruction is then performed using some of the mentioned algorithms.

One of the main limitations of this architecture is that it requires the camera to focus on the object of interest until a sufficient number of measurements are collected, which can be restrictive for certain applications. Some of the other main architectures for compressive image sensing can be found in (Baraniuk et al., 2017).

Results of Reconstruction

For the quality of the reconstruction, the choice of the right transform domain in which the sparse image is observed is essential, i.e., the choice of the sensing matrix, as indicated by expressions Eq. (8) and Eq. (10). The Fourier domain is often used for the selection of the basis, especially for signals sparse in the frequency domain, followed by the Discrete Cosine Transform domain, Wavelet Transform domain (of various classes), etc. For the presentation of results in this work, two domains were comparatively used: Fourier *(F)* and Discrete Cosine *(DCT)*. Considering that one of the motivations for the work was the use of low-power cameras for terrain surveillance, an initial landscape image of dimensions 256×256 was used, followed by faces in the second part (known test image "Lena"), and a drawing image (parrot) of similar dimensions, as shown in (Fig. 6).

The platform used for simulation is based on an i7 processor with two cores at 2.8 GHz and 8 GB of RAM. The compressive sampling simulation is implemented by selecting the ratio of the measurement vector length to the sample size

(M/N), i.e., how many pixel samples are taken for reconstruction. Initially, the Fourier matrix operator (identity, normalized) was chosen as the transformation operator. Variants with 60, 50, 40 percent of sampled pixels are shown in (Fig. 7) along with their corresponding reconstructions.

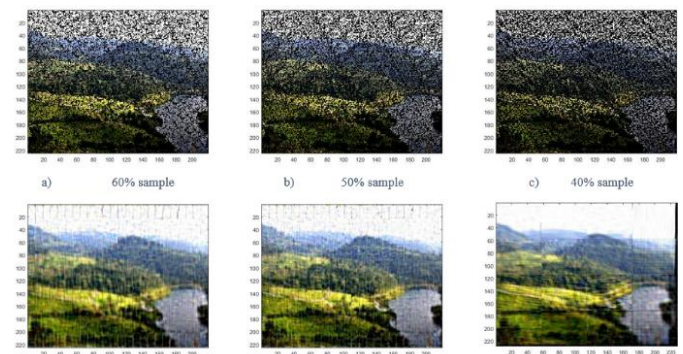**Figure 5.** Original images used in the study: a) Lake b) Lena c) Parrot.

Figure 6. Reconstruction results by sparsifying in the Fourier domain with various M/N ratios.

For the sampled segment, column vectors of the two-dimensional image matrix were taken as samples, except in case (v) where, for clarity, the sampled vector was taken as a square block segment. In these cases, a relatively long reconstruction time was observed (several tens of minutes and over an hour for larger samples), primarily due to the large operator matrix and associated computational operations.

A better characterization of image sparsity was sought in the domain of discrete cosine transformation, considering that spectral analysis of one segment revealed the presence of a larger number of frequency components, as shown in (Fig. 8).
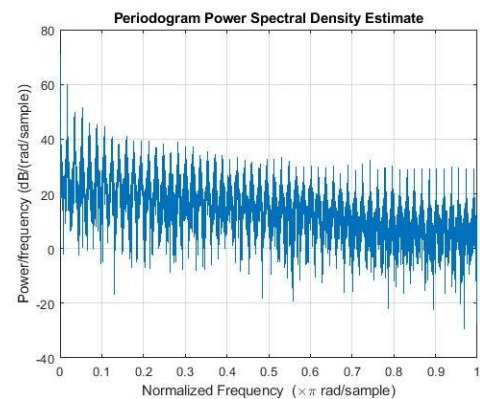

Figure 7. The spectral power density of one segment of the original image.

Even with just the replacement of the transformation matrix, a certain improvement was observed, as shown in (Fig.9).
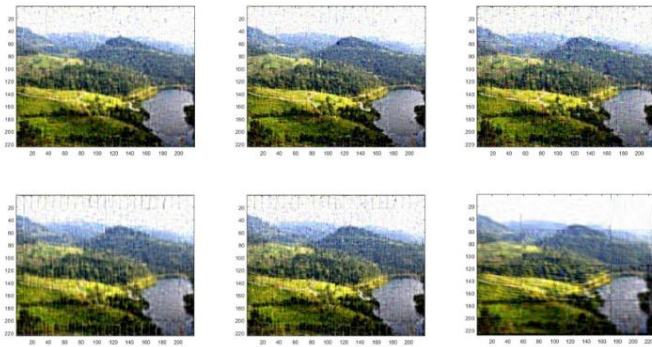

Figure 8. A comparative display of reconstruction with 60%, 50%, and 40% of points, in different sparse domains: top row DCT, bottom row FFT.

The reconstruction times, however, remained significant in terms of the required speed. For further improvements, it was necessary to enhance the reconstruction time, which initiated further exploration of possible solutions. One approach was to reduce the dimensions of the transformation matrix.

Algorithm Improvements

The proposed solutions to the problem, in terms of reducing the dimension of the transformation matrix, were investigated in (Gan, 2007) and (Sermwuthisarn & Parichat, 2009). In both cases, acquisition was considered block by block (dimension $n \times n$ pixels), but they differ in the approach to reconstruction. While in the first case, a Wiener filter, projection onto a convex set, and hard thresholding were used as reconstruction algorithms, in the second case, the approach of searching for orthogonal matches was used, called block-based OMP (Block-based Orthogonal Matching Pursuit). In this work, the latter method was used, only applied to color images and with some differences in parameterization.

When using block segments of the image, sized $n \times n$ pixels, the dimensions of the measurement matrix are expanded to $n_2 \times n_2$. For blocks of 64×64, the matrix is of size 4096×4096, for 16×16 blocks the matrix size is 256×256, while for 8×8 blocks the matrix size is 64×64.

Comparative reconstruction results by segmentation, with achieved reconstruction times, are shown in (Table 1), while the obtained appearances are shown in (Fig. 10).

Segmentation is implemented without overlapping between segments, but for further analysis, it can also be considered with overlap. Regarding the presented data in (Sermwuthisarn & Parichat, 2009), better times have been achieved, especially considering that in this work, the reconstruction of RGB color images compared to the monochromatic (grayscale) image used in the reference

(dimensions are roughly similar), considering the triple pass through the algorithm (for each of the R, G, and B two-dimensional matrices individually). The table provides an approximate block size because to ensure proper segmentation, images are extended by a sufficient number of pixels divisible by the square root of the total number of segments.
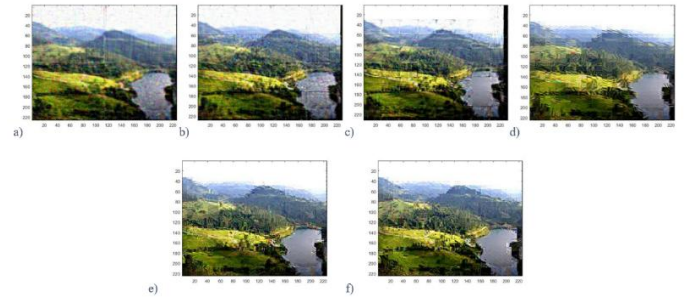

Figure 9. Reconstructions with 30% samples obtained by segmenting into segments: a) 4 b) 16 c) 64 d) 256 e) improvements of 256 segments, 3 times larger K f) improvements of 256 segments, 6 times larger K.

Table 1. Reconstruction time for different segment sizes and sparsity levels.

Point image	Block Size ($n \times n$)	M/N Ratio	Segments	Sparsity (K)	Reconstruction Time
a)	128×128	30	4	M/6	Several hours
b)	64×64	30	16	M/6	51.95 s
c)	32×32	30	64	M/6	10.58 s
d)	8×8	30	256	M/6	1.79 s

A better assessment of reconstruction quality is considered when it comes to face recognition. An example taken is the test image "Lena," which is often used in the references provided. Segmentation was performed on 256 blocks with different sparsity levels, (Fig. 11).
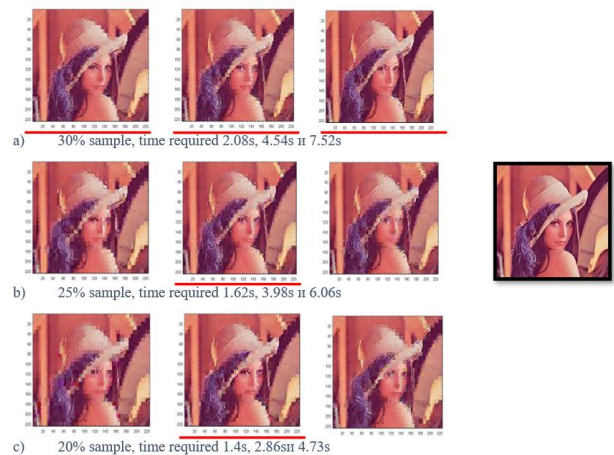

Figure 10. Image face reconstruction: in the first column with sparsity degree M/6, in the second M/2, in the third column M, the original image is framed on the right.

By observing, one can directly assess the recognizability of the face compared to the original (for example, the author has personally highlighted some of the reconstruction results with a red line). In step (Orthogonal Matching Pursuit – OMP) of the residue update, it has already been stated that the algorithm terminates after K iterations (sparsity level, thus directly affecting the reconstruction speed), or until the residual vector magnitude is reduced to some minimum match ($\varepsilon \geq 0$). The value of this minimum can be viewed as a number indicating the level of approximation and solution match, and for $\varepsilon=0$, the match is perfect.

In (Fig. 12), we notice that the level of matching actually determines the level of detail in the image, but also that details are not decisive, and sometimes a lower level of detail may be more useful for drawing conclusions about the necessary information from the image (whether it's a certain person or not, which person or characteristic it is). The reconstruction speed, logically, doubled in the case of $\varepsilon=550$ compared to the case with $\varepsilon=0$. When $\varepsilon=0$, we also notice small errors in the reconstruction (blue square at the far right and two yellow squares at the top and bottom). Errors appear in areas of the same color shades and when a complete level of matching is defined. The algorithm corrects itself by taking values greater thanzero.
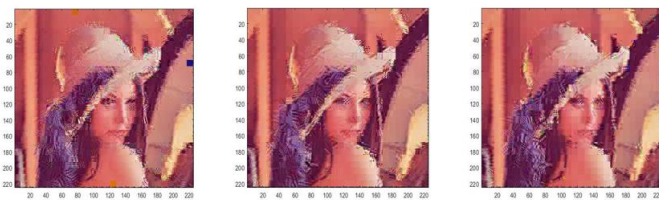

Figure 11. Reconstruction for different levels of matching, sequentially $\varepsilon = 0$ for 4.53s, $\varepsilon = 250$ for 2.45s, and $\varepsilon = 550$ for 2.19s.

The question of assessing the quality of reconstruction in the current analysis is based on subjective evaluation. The Peak-Signal-to-Noise-Ratio (PSNR) is one of the commonly used parameters for objectively measuring the quality of reconstruction in image codec (encoder/decoder) for image compression. PSNR is actually an approximation of the eye's perception of reconstruction quality. PSNR is most easily defined through the Mean Squared Error (MSE): for a given monochromatic image i and its noise-degraded approximation K, it is

$$SKG = \frac{1}{mn}\sum_{i=0}^{m-1}\sum_{j=0}^{n-1}\left[I(i,j)-K(i,j)\right]^2 , PSNR \text{ (dB) is}$$

$$PSNR = 10\log_{10}\left(\frac{MAX_I^2}{SKG}\right) = 20\log_{10}\left(\frac{MAX_I}{\sqrt{SKG}}\right) =$$

$$20\log_{10}(MAX_I)-10\log_{10}(SKG)$$

where MAX_I is the maximum possible pixel value in the image. In our case, images with 8-bit pixel values were used, so the maximum value is 255. For color images with three RGB values per pixel, as used in the study, the same definition of the PSNR parameter is taken, except that MSE is calculated as the sum of sums for each color divided by the size of the image (dimensions $m \times n$) and multiplied by 3. A closer criterion to human eye perception is when this value is calculated on the luminance channel (Y channel of the YC_bC_r image format), as shown in (Fig. 13). The acceptable value of this parameter for lossy compression, according to the source (Thomos, et al., 2006), is from 20 to 25 dB.
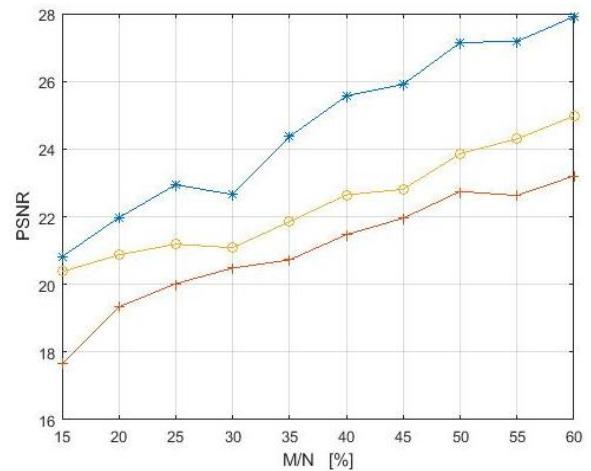

Figure 12. Peak Signal-to-Noise Ratio (PSNR) values for different types of images.

Another method considered here for quality assessment is measuring the Structural Similarity Index (SSIM) (Wang et al., 2004). This parameter describes the measure of similarity between two images, i.e., the perception of the resulting image change in its structure, and falls into the group of parameters for which complete referencing of the obtained reconstruction result with the original is necessary. Without delving into the details of the mathematical model, this parameter was used here as a complementary parameter to the traditional approach of measuring the peak signal-to-noise ratio. The concept of structural information in the image is related to the idea that pixels have strong mutual dependence when spatially close, and this dependency carries important information about the structure of objects in the visual scene (Thomos, et al., 2006). The value of the index ranges from -1 to 1 and is a decimal value, where 1 represents an identical set of data (perfect similarity), while 0 represents no structural similarity at all. The obtained index values for all three types of images used are shown in (Fig. 14).

In (Fig. 14), the change of Structural Similarity Index (SSIM) with the percentage of samples (M/N) is shown for three images: Lena, Parrot, and Nature. SSIM is a measure that describes how similar two images are in terms of their

structure, where a value of 1 indicates perfect similarity and a value of 0 means no structural similarity.

The X-axis represents the percentage of samples used for image reconstruction, ranging from 15% to 60%. The Y-axis shows the SSIM value, ranging from 0.4 to 0.85. Three lines on the graph represent three different images: Lena (marked with asterisks), Parrot (marked with plus signs), and Nature (marked with circles).

For the Lena image, SSIM starts around 0.55 at 15% of samples and gradually increases to approximately 0.85 at 60% of samples. This indicates that the reconstruction of the Lena image is very good, with a high level of similarity to the original. The Parrot image shows lower initial SSIM values, starting around 0.42 at 15% of samples and reaching about 0.7 at 60% of samples, indicating moderate similarity to the original image. The Nature image has an initial SSIM of around 0.46 at 15% of samples, gradually increasing to about 0.75 at 60% of samples, showing good similarity to the original but not as high as the Lena image.

Figure 14 shows that all SSIM indices increase with higher percentages of samples, indicating improved image reconstruction quality with increased sample usage. The Lena image exhibits the highest reconstruction quality, while the Parrot image is the most challenging to reconstruct. The Nature image falls somewhere in between in terms of reconstruction quality. These results demonstrate the effectiveness of the reconstruction algorithm used, as even at higher compression levels, the reconstructed images maintain acceptable levels of structural similarity to the originals.
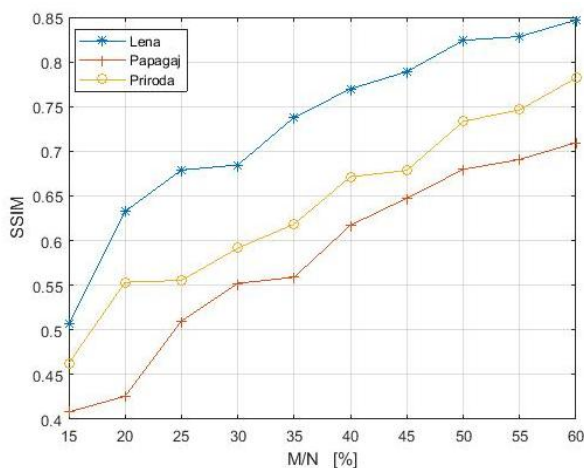

Figure 13. Values of the Structural Similarity Index for different types of images.

Based on the images, we can observe how the Peak Signal-to-Noise Ratio (PSNR) and Structural Similarity Index (SSIM) increase with the growth of sample percentage (M/N). From the presented results, it can be concluded that even under significant compression, the chosen algorithm maintains reconstructed approximations above the commonly acceptable threshold of 20dB PSNR. Additionally, the obtained SSIM values consistently align with previous findings (higher SSIM indicating a higher signal-to-noise ratio in the image). These parameters are utilized, for instance, in pattern recognition in images, faces, objects, etc.

CONCLUSION

The concept of compressive image sensing is presented in the paper, along with the basic conditions for its application, current approaches to reconstructing such signals, mathematical formulation with an intuitive example of orthogonal matching pursuit algorithm, and the method of image acquisition with compressive sampling. Furthermore, results obtained based on the applied algorithm are presented using three structurally different images: faces, natural landscapes, and drawings.

It can be concluded that acceptable results are achieved for a compression level of around 25-30% of samples (over 20 dB PSNR), and better structural similarity is obtained for faces compared to images of natural landscapes and drawings, which is important from the perspective of automated recognition. Input vectors have shown better sparsity properties in the Discrete Cosine Transform (DCT) domain compared to the Fourier domain (FFT). Some references claim that the compression level can be lowered to 4-10% using atoms from the Wavelet Transform dictionary, with a cautious note that the orthogonality of the matrix in this domain is not unequivocally determined and must be carefully considered during its design.

The method of forming the input vector also showed its impact on the algorithm's performance, primarily in terms of reconstruction time for the desired quality. Thus, the reconstruction results in this work are very comparable to the results in (Sermwuthisarn & Parichat, 2009). A wide range of possibilities remains open for the application of more advanced variants of this method, as well as improvements to the algorithm itself in some other sense. One of the possible improvements is presented in (Safavi, 2016). The relevance of the topic today is demonstrated by recent algorithm enhancements achieved (Zhao et al., 2019).

By employing compressive sensing/selecting methods, it is possible to form a signal at the end sensor points using simpler, cheaper, and low-power devices, which will enable satisfactory image reconstruction at the destination in the transmission system. This avoids the use of expensive hardware with high power consumption and provides an advantage over classical image compression methods. A small amount of data acquired at the end points lessens the burden on the transmission network and the connection of a large number of sensors to it.

REFERENCES

Baraniuk, R. G., Goldstein, T., Sankaranarayanan, A. C., Studer, C., Veeraraghavan, A. & Wakin, M. B. 2017. Compressive Video Sensing: Algorithms, architectures, and applications, IEEE Signal Processing Magazine, 34(1), pp. 52-66, Jan. 2017, doi: 10.1109/MSP.2016.2602099.

Donoho, D. L. 2006. Compressed Sensing. IEEE Transactions on information theory, 52(4), pp.1289-1306.

Gan, L. 2007. Block Compressed Sensing of Natural Images. In: Proceedings of the 2007 15th International Conference on Digital Signal Processing, Cardiff, UK, 1-4 July 2007.

Rani, M. & Sushma R. 2018. A Systematic Review of Compressive Sensing: Concepts, Implementations and Applications. IEEE Access, 6.

Patel, V.M., Vishal M. & Rajesh C. 2013. Sparse Representations and Compressive Sensing for Imaging and Vision. New York: Springer.

Foucart, S. & Rauhut, H., 2013. A Mathematical Introduction to Compressive Sensing. New York: Springer.

Sermwuthisarn, P., Auethavekiat, S., & Patanavijit. V. 2009. A fast image recovery using compressive sensing technique with block based orthogonal matching pursuit. In 2009 International Symposium on Intelligent Signal Processing and Communication Systems (ISPACS). IEEE. https://doi.org/10.1109/ispacs.2009.5383863

Stankovic, S., Orovic, I. & Sejdic, E. 2016. Multimedia Signals and Systems: Basic and Advanced Algorithms for Signal Processing. London: Springer.

Strang, G. 2016. Introduction to Linear Algebra, 5th ed. Wellesley: Wellesley - Cambridge Press.

Seyed, H. S., & Farah T-A. 2016. Sparsity-aware adaptive block-based compressive sensing. IET Signal Processing. pp. 36-42, https://doi.org/10.1049/iet-spr.2016.0176.

Thomos, N., Boulgouris, N. V., & Strintzis, M. G. 2006. Optimized transmission of JPEG2000 streams over wireless channels. IEEE Transactions on Image Processing, 15(1), 54-67. doi: 10.1109/TIP.2005.860338.

Uzeler, H., Cakir, S., & Ayta,, T. 2013. Image generation for single detector infrared seekers via compressive sensing. Proceedings of SPIE - The International Society for Optical Engineering, 8896. doi: 10.1117/12.2030104.

Wang, Z., Bovik, A. C., Sheikh, H. R., & Simoncelli, E. P. 2004. Image quality assessment: from error visibility to structural similarity, IEEE Transactions on Image Processing, 13(4), pp. 600-612, doi: 10.1109/TIP.2003.819861.

Zhao, L., Hu, Y., & Liu, Y. 2019. Stochastic Gradient Matching Pursuit Algorithm Based on Sparse Estimation. Electronics, 8(2), p165, doi: 10.3390/electronics8020165.

RADON IN WATER FROM PRIVATE WELLS AND ITS CONTRIBUTION TO INTERNAL EXPOSURE OF POPULATION IN RURAL AREAS AT TOPLICA REGION, SOUTHERN SERBIA

BILJANA VUČKOVIĆ[1*], IVANA PENJIŠEVIĆ[1], NATAŠA TODOROVIĆ[2], JOVANA NIKOLOV[2], DRAGAN RADOVANOVIĆ[1], ALEKSANDAR VALJAREVIĆ[3]

[1]Faculty of Sciences and Mathematics, University of Priština in Kosovska Mitrovica, Kosovska Mitrovica, Serbia
[2]Department of Physics, Faculty of Science, University of Novi Sad, Novi Sad, Serbia,
[3]Faculty of Geography, University of Belgrade, Belgrade, Serbia

ABSTRACT

The results presented in this paper are part of the investigating of radon the concentrations from natural sources in the Toplica region. The results refer only to the radon concentrations in water from private captured wells at 12 locations. Radon concentration in water was measured by alpha spectrometry using the RAD 7 – RAD H2O system. The range of radon concentration is from (2.8±1.2) to (76.0±4.0) kBq/m^3, and the contribution of radon released from water to the air in the premises was in range (0.8±0.3) to (22.8±1.2) Bq/m^3. The annual effective doses of inhaled and ingested radon were determined, the mean values were (114.8±14.8) and (3.2±0.3) μSv/y.

Keywords: Radon in water, Private wells, Annual effective radiation doses.

INTRODUCTION

Groundwater is the largest freshwater resource and it is very important to investigate radon in groundwater to protect the population from health hazards caused by radon and its progeny (UNSCEAR 2000). Radon is a radioactive gas product of the uranium sequence and a direct progeny of radium. It is characterized by a half-life of 3.82 days, four short-lived progeny and is an important source of alpha particle emission (Ravikumar et al., 2014; Di Carlo et al., 2019). In the literature, radon from water is recognized as secondary sources of indoor radiation (WHO 2004; Anjos et al., 2010; Rožmarić et al., 2012; Kendall & Smith 2002; Isinkaie et al., 2021). Radon is soluble in water, leaves it very quickly under pressure or at elevated temperature and accumulates in the air in a closed space and thus can cause damage to organs, tissues and cause changes in the DNA chain (Fakhri et al., 2016). Radon in water can lead to body irradiation in two ways: by ingesting radon-rich water and by inhaling radon that is released from it into the interior of the room when the water is used for bathing, cooking, washing, etc. (UNSCEAR 2000). Radon moves from the water into the closed space through the process of diffusion, so it can be said that the concentration of radon in the closed space increases simultaneously with the high content of radon in the water.

Although the radiation dose from radon ingestion from drinking water is lower than the radiation dose from inhalation, excessive radon intake from drinking water can not only cause lung cancer, but can also increase the risk of stomach and colon cancer (Bonotto 2004; WHO 2004; Anjos et al., 2010; ICRP 2010; Vogeltanz-Holm & Schvartz, 2018).

Population in Toplica region is supplied with drinking water from natural sources of underground water in the selected localities. The aim of these studies was to determine the radon concentration in water from private captured wells, to calculate the contribution of radon from water to the total radon in the air in a closed space, and to assess to what extent is the population exposed to radiation through ingestion and inhalation of radon.

STUDY AREA

Toplica region is a medium-developed industrial center and an important fruit growing and agricultural area of Serbia. Toplica region situated in the South Serbia with geographical coordinates 42°52′ – 43°24′N of latitude and 20°56′ – 21°50′E of longitude (Fig.1). The area of Toplica region is 2180 km^2. According to the last census in 2022, the total number of inhabitants is 77.900 (SORS, 2023), making it the smallest region by population in Serbia.

This geographical area is defined by the basins of the Toplica and Kosanica rivers. This sub-region is bordered in the east with the South Morava river, in the west with the Mountain Kopaonik. The south border occupied territory with the Mountains Majdan and Radan. The border in the north of the Toplica region are Mountain Veliki and Mali Jastrebac (Pavlović, 2019). The administrative regionalization of Toplica followed four municipalities: Prokuplje, Kuršumlija, Žitorađa and Blace.
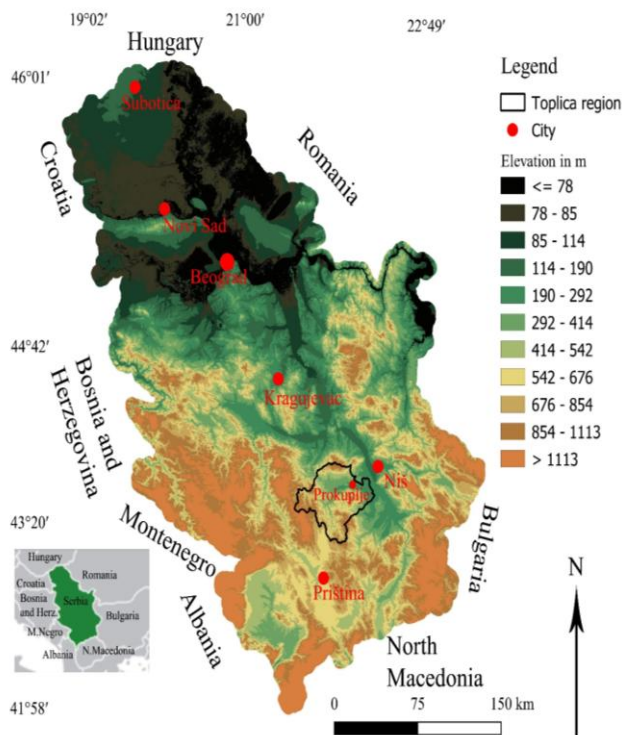
PHYSICS

Figure 1. The geographical position of Toplica region in the Republic of Serbia.

MATERIAL AND METHODS

The paper presents the results of radon concentration of radon in water that the population uses both for drinking and for other purposes from 12 selected localities in the Toplica region. In this research seven samples were taken in Kuršumlija, one in Blace, one in Žitorađa and three in Prokuplje (Fig.2).
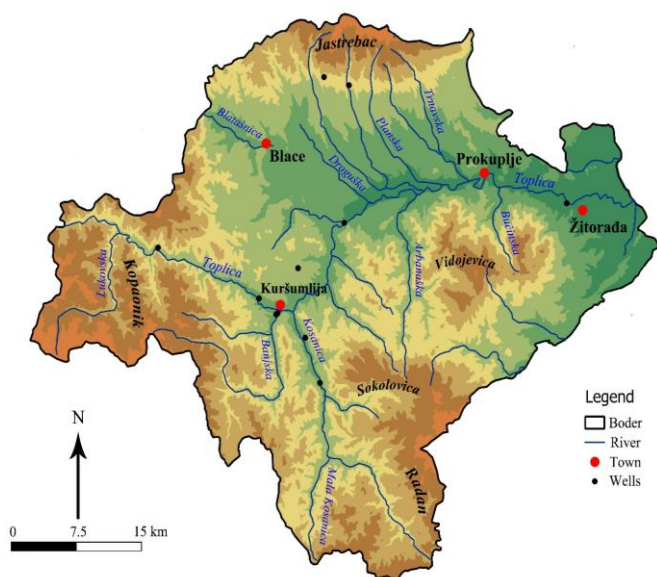

Figure 2. The position of private wells in the Toplica region.

GIS and remote sensing methodology

In this research the GIS methodology were used to analyze better spatial distribution of wells. The wells distributions are approved by handled Garmin GPS 72H with an accuracy of 3 m. All data were used and analyzed with this device and after that mapped. The geodetic projection was WGS 84 4326 and this projection is reprojected to be at national scale and national coordinate system. The national projection is UTM zone 7. This projection is good because is in the correlation with old topographic maps (Valjarević et al., 2018). GIS methods, such as the method of interpolation and graduated method are provided to present the final geographical position (latitude and longitude) of analyzed wells (Fig. 2). These methods also showed very clearly the position of wells.

Geological structure of studying area

In the geological past the Toplica region was a region with very strong volcanic activity (Geological Atlas of Serbia 2002). The Rhodopes are considered as the oldest mountains of the Balkan Peninsula and Serbia; they are built of the archaic and Paleozoic crystalline schist (Stevanović et al., 2018). Even today in this region there are many paleovulcanic forms. The main types of crystalline schists are andesite, fine-grained gneisses, amphibolites, magmatites, leptinoliths, mica schists, quartzite, marble, amphibole schist, pegmatite and mica rocks. Due to volcanic activity the most dominant rocks are andesite. Green shale and metamorphosed gabbro found on the mountain Jastrebac belong to the Cambrian rocks, while low metamorphosed rocks from Devon period have been discovered in tectonic contacts of crystalline shale, serpentinisedperidotite and Senonian sediments (Geological Atlas of Serbia 2002; Valjarević et al., 2014). From the Mesozoic era, the oldest rocks are related to Middle Triassic and widespread northwest of Kuršumlija. The rocks formed during the Late Jurassic are positioned in the west of the region in the form of mass or elongated, but discontinuous zones having the direction of the NNW–SSE are presented by basic and ultra-basicmetamorphites and diabase-chert formation (Geological Atlas of Serbia 2002). This geological structure supported occurrences of thermo-mineral springs and underground wells with high concentration of radon. Observing the geomorphological structure of the terrain, the examined terrain contains various rock masses subjected to physical and chemical changes in the surface parts. It allows water to accumulate in the systems of cracks and fissures, the degree of which is variable and depends on the external conditions. A detailed description of geological structure of chosen private wells is given in Table 1. which based on the detailed geological map of Toplica region.

Population is supplied with drinking water from natural sources, due to unreliable supply from the public water supply

system. The sources from which the population is supplied with drinking water are captivated natural wells in the immediate vicinity of the houses, so that the spring water is carried inside the houses through a closed system of pipes. There is a fountain in every yard at the point where the spring is. Family houses built in the midterm of 20th century, with concrete floors, without basement rooms and approximately similar layout of rooms were selected. Rooms where inhabitants spent the most of the time are the living rooms, the kitchen is most often an integral part of them, and they are of the same or very similar dimensions.

Table 1. The geological structure of chosen private wells.

No	Geological background
1	Proluvium
2	Coarse-grained sandstones and microconglomerates
3	Pleistocene river terrace of the Banjska river
4	Jurassic diabase and spilite
5	Pleistocene river terrace of the Banjska river
6	Senonian siltstones, marlstones and thinly-layered limestones
7	Volcanic breccias and tuffs
8	Red series. siltstones and sandstones
9	Proluvial deluvial sediments
10	Marbles
11	Alluvium
12	Proluvium

Sempling procedure and detection of radon

Before sampling, the water temperature was measured with a digital thermometer (Testo Se & KGaA, Germany). After that, the water was sampled in original glass bottles with a volume of 250 ml up to the very top. When filling the vials, water flowed from the tap in a small stream, in order to avoid the formation of bubbles in the sample. The closure was performed under a jet of water, which prevented the forming of a free air space under the closure, in which radon could accumulate due to exhalation from the water. Since the concentration could not be measured during the sampling itself, it was necessary to deliver the samples as soon as possible to the Laboratory for testing the radioactivity of samples and doses of ionizing and non-ionizing radiation at the Faculty of Science, University of Novi Sad, where the radon concentration in water samples was measured by the RAD7 RAD H2O system (Durrige Co.). Part of the entire measuring system is an air pump that continuously exhales radon within 5 minutes through the closed loop aeration process of the water sample. In this process, almost 94% of radon was extracted from the sample. After that, the pump is automatically stopped, and then the system is idle for 5 minutes, in order to restore the balance between water, air and radon products in the detector. The lower detection limit of the device is 0.37 Bq/l. So, as the true value of radon concentration in water samples, its corrected value is used according to the formula (Todorovic et al., 2012):

$$C_{Rn} = C_o \bullet \delta. \tag{1}$$

where: $\delta = e^{\lambda t}$, where for radon decay $\lambda = 0.00756$ h^{-1}, C_o defines value of radon concentration in water sampling measured in laboratory and t defines the time elapsed from sampling to laboratory analysis. The time elapsed from sampling to analysis was 4 days.

As the population uses water in the household, the contribution of radon from the water to the closed space in the room was calculated, according to the pattern (Zelewski et al., 2001):

$$C_{aRn} = C_{wRn} \times W \times \frac{e}{(V \times \lambda_c)}. \tag{2}$$

where: C_{aRn} is the contribution of radon from water to the total radon in the air, C_{wRn} is the activity concentration of radon in water, W is the average intake of water (0.01 m^3/h per person), e is the coefficient of exhalation of radon from water into air (0.5), V is the volume of the room (30 m^3), and λ_c is the coefficient of the change of air in the room (0.7 h^{-1}) (UNSCEAR; 1993; Xinwei, 2006).

The carcinogenic effects of radon, in the long term, is reflected in the determination of the total effective dose of internal irradiation with radon dissolved in water, which consists of two components: the first is defined by the effective dose of radon inhalation, while the second is defined by the effective dose of radon ingestion. According to the 2000 UNSCEAR Report, these quantities can be determined as follows:

-The annual effective doses for inhalation waterborne radon were calculated by using the parameter established in the UNSCEAR 2000 as (Somlai et al., 2007; El-Araby et al., 2019; Deeba et al., 2021):

$$E_{inh}\left(\frac{\mu Sv}{y}\right) = C_{wRn} \times C_{aw} \times DCF \times F \times t. \tag{3}$$

where: E_{inh} is the effective dose for inhalation, C_{WRn} is the radon concentration in water (Bq/l or kBq/m^3), C_{aW} is the radon in air to the radon in water ratio (10^{-4}), F is the equilibrium factor between radon and its progenies (0.4), t is the average indoor occupancy time per individual (7000 h/y) and DCF is the dose conversion factor for radon exposure (9 nSv (Bq h m^{-3})$^{-1}$).

According to data presented in UNSCEAR (2000), the transfer factor C_{aw} has an order magnitude of 10^{-4}. As part of these investigations, the exact value of the ratio of radon concentration in water and its contribution in air was

determined, so the calculated value presented in Table 1. is used in equation 2.

-The annual effective doses for ingestion radon were calculated using the following formula (UNSCEAR, 2000):

$$E_{ing}\left(\frac{\mu Sv}{y}\right) = C_{wRn} \times C_w \times EDC. \qquad (4)$$

where: E_{ing} is the effective dose for ingestion, C_{wRn} is the radon concentration in water (Bq/l or kBq/m^3), C_w is the the weighted estimate of water consumption (60 l/y) and EDC is the effective dose coefficient for ingestion (3.5 nSv/Bq), respectively.

RESULTS OF RESEARCH

The summarized results of the research in this work are presented in 2. In addition to temperature and radon concentration in samples from 12 selected localities, the contribution of radon from water to the total radon in the air in closed rooms is also presents in Table 2. In the last column, there is C_{aw} - the calculated value of the transfer factor within these studies and which is used in equation 2 for determination the annual effective dose from radon inhalation.

Table 2. Summarized results of research.

No	T (°C)	C_{wRn} (kBq/m^3)	C_{aRn} (Bq/m^3)	$C_{aw} = C_{aRn}/C_{wRn}$ (10^{-4})
1	8	8.7±1.4	2.6±0.4	2.9
2	12	6.6±1.6	2.0±0.5	3.0
3	12	13.8±3.6	4.1±1.1	2.9
4	14	19.1±1.4	5.7±0.4	2.9
5	13	21.5±2.5	6.5±0.7	3.0
6	14	11.8±2.9	3.5±0.9	2.9
7	12	6.6±1.2	2.0±0.3	3.0
8	12	6.8±1.4	2.1±0.4	3.0
9	13	2.8±1.2	0.8±0.3	2.8
10	11	6.4±1.7	1.9±0.5	2.9
11	22	76.0 ±4.0	22.8±1.2	3.0
12	13	4.3±0.8	1.3±0.2	3.0
Min	8	2.8±1.2	0.8±0.3	2.8
AV	13	15.3±2.0	4.5±0.6	2.9
Max	22	76.0±4.0	22.8±1.2	3.0

In order to correctly determine the contribution of radon from water to the total radon in the air in a closed room, instead of Bq/l, the radon concentration in water is expressed in kBq/m^3, whereby a radon concentration in water of 1mBq/l corresponds to a radon concentration of 1Bq/ m^3 in air.

According to the temperature range from 8°C to 22°C, these underground waters can be classified as cold waters. Intervals of measured values of radon concentration in water ranged from 2.8±1.2 kBq/m^3 to 76.0±4.0 kBq/m^3, with an average value of 15.3±2.0 kBq/m^3. Radon concentration values

in the sampled waters are relatively low. All values are below the recommended WHO (2004) value. This could be expected if one takes into account the geological structure of the place where the springs are located (Table 2). According to the presented data, it can be said that the waters from these areas are radiologically correct and can be used for drinking, since their values are far below the recommended value of 100 kBq/m^3 (WHO, 2004). In seven samples radon concentration in the water was below 11 kBq/m3 on seven sites, which is the upper limit of the radon concentration in drinking water (Fig 3) according to the recommendation of the US-EPA (1999).
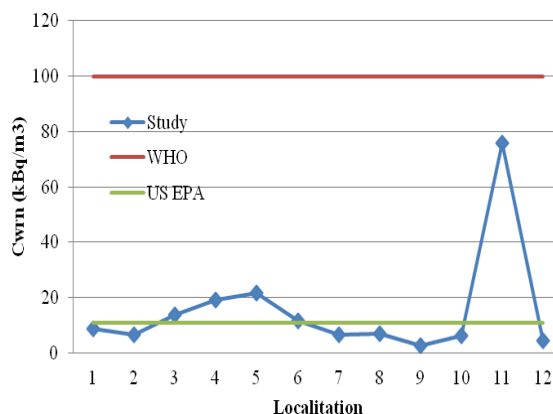

Figure 3. Range of radon concentration in water related to recommended values.

Considering the geological structure of the places where the sources of the sampled water are located, the presented results are expected (Table 1). The terrain itself does not contain minerals and rocks containing radionuclides, primarily uranium and radium, so radon concentrations are low. There was only location 11 with a detected higher radon concentration (76.0±4.0 kBq/m^3), but the geology of the place itself does not point to that. This pronounced concentration may be a consequence of the movement of groundwater over rocks rich in radon. Groundwater dissolves rocks and carries dissolved radon with it on its further way. This could be the reason why there is a higher concentration of radon at location 11. Concentration of radon in water measured in this research are comparable with the data of other researchers (Khandaker et al., 2020; Mehnati et al., 2022; Kumar et al., 2022; Vučković et al., 2022).

As radon is a radionuclide that easily leaves water, water with an elevated radon level can cause radon diffusion into the interior of the room and lead to an increase in the total radon level. This leads to the conclusion that the population from these localities is exposed both ingestion and inhalation of radon from water. The interval of certain values of radon concentration that is released from the water, and thus increases the total concentration of radon in closed rooms, is

from 0.8±0.3 Bq/m^3 do 22.8±1.2 Bq/m^3, with mean value of 4.5±0.6 Bq/m^3.

The value interval of the transfer factor C_{aw} is from 2.8x10^{-4} to 3x10^{-4} and corresponds to the recommended range of transfer factor values from 10^{-5} to 3x10^{-4} (paragraph 93 in UNSCEAR 2000).

When consuming radon-rich water, the first cells to be exposed to alpha particle irradiation emitted during the decay of radon and its short-lived progeny are gastric tissue cells (WHO, 2004). During inhalation of radon and its decay products, lung tissue is exposed to direct radiation. Based on this, the total annual exposure of the population to radon from water can be determined through: the annual effective dose of inhalation (E_{inh}) and the annual effective dose of radon ingestion (E_{ing}). Table 3. shows the values of the annual effective doses of inhalation and ingestion of radon present in water.

Table 3. Estimation of radiation doses of population to radon from water on the selected sites.

No	E_{inhal} (μSv/y)	E_{ingest} (μSv/y)	Doses to organs (μSv/y	
			lungs	stomach
1	63.6±12.4	1.8±0.3	7.6	0.2
2	49.9±12.1	1.4±0.4	5.9	0.1
3	100.8±26.3	2.9±0.8	12	0.3
4	139.5±10.2	4.0±0.3	16.7	0.5
5	162.5±18.9	4.5±0.5	19.5	0.5
6	86.2±21.2	2.5±0.6	10.3	0.3
7	49.9±9.1	1.4±0.2	5.9	0.2
8	51.4±10.6	1.4±0.3	6.2	0.2
9	19.8±8.5	0.6±0.2	2.4	0.07
10	46.7±12.4	1.3±0.4	5.6	0.1
11	574.5±30.2	16.0±0.8	68.9	1.9
12	32.5±6.0	0.9±0.2	3.9	0.1
Min	19.8±8.5	0.6±0.2	2.4	0.07
AV	114.8±14.8	3.2±0.3	13.8	0.4
Max	574.5±30.2	16.0±0.8	68.9	1.9

The interval in which the annual effective inhalation dose ranges is from 19.8±8.5 μSv/y to 574.5±30.2 μSv/y. The mean value of the annual effective dose of radon inhalation is 114.8±14.8 μSv/y, and it corresponds to the recommended value of 100 μSv/y (WHO, 2004). The extreme value of 574.5±30.2 μSv/y measured in sample 11 is a consequence of the increased presence of radon in the water. In all other locations (1, 2, 6, 7, 8, 9, 10 and 12) the annual effective inhalation dose is below the recommended value, while the inhalation dose values in locations 3, 4 and 5 apears to be close to the recommended value of 100 μSv/y. Range of annual effective doses of ingestion is from 0.6±0.2 μSv/y to 16.0±0.8 μSv/y, while a mean value is 3.2±0.3 μSv/y. Mean value of the total annual effective dose of exposure is 118.0±15.3 μSv/y. In

the special case, that no other organ is exposed the dose contribution from this source to the lungs and stomach is calculated by multiplying the inhalation and ingestion dose with tissue weighting factor (w_t) of 0.12 for lungs and stomach, respectively (UNSCEAR 2000). Two last colons in Table 3. represent the radiation dose contribution of radon in drinking water to lung and stomach. Mean values of these doses are 13.8 μSv/y and 0.4 μSv/y, respectively. Based on all the presented values of the selected parameters, it can be concluded that the selected localities can use for consumption and for other domestic usage from the point of view of radiation protection.

CONCLUSION

Research presented in this paper includes 12 carefully selected localities where the population is supplied with drinking water from natural captured sources. The research included only those households that are very similar in terms of their habits and the spatial organization of the houses they live in. Interval of radon concentration present in water is from 2.8±1.2 kBq/m^3 to 76.0±4.0 kBq/m^3, with a mean value of 15.3±2.0 kBq/m^3. As the measured values are below the recommended level of 100 kBq/m^3 (WHO, 2004), the waters from these localities are safe for wider household use. Contribution of radon from water to radon in the air in closed rooms is llow, but it should be taken into account because natural springs are the only way to supply drinking water in this area. Mean value of the calculated transfer factor is 2.9x10^{-4} and corresponds to the generally accepted parameter from the literature (UNSCEAR 2000). According to the average value of the annual effective dose of inhalation and ingestion radon from water, it can also be said that waters in these areas are safe for use both for drinking and for other numerous household needs.

REFERENCES

Anjos, R. M., Umisedo, N., da Silva, A. A. R., Estellita, L., Rizzotto, M., Yoshimura, E. M., Velasco, H. & Santos, A. M. A. 2010. Occupational exposure to radon and natural gamma radiation in the La Carolina, a former gold mine in San Luis Province, Argentina. J. Environ. Radioactiv. 101(2), pp. 153-158, https://doi.org/10.1016/j.jenvrad.2009.09.010

Bonotto, D. M. 2004. Doses from 222Rn, 226Ra, and 228Ra in groundwater from Guarani aquifer, South America. J. Environ. Radioactiv. 76(3), pp. 319-335, https://doi.org/10.1016/j.jenvrad.2003.11.010

PHYSICS

Deeba, F., Rahman, S. H. & Kabir, M. Z. 2021. Assessment of annual effective dose due to inhalation and ingestion of radon from groundwater at the southeast coastal area, Bangladesh. Radiation Protect. Dosimetry 194(2-3), pp. 169-177, https://doi.org/10.1093/rpd/ncab096

Di Carlo, C., Lepore, L., Venoso, G., Ampollini, M., Carpentieri, C., Tannino, A., Ragno, E., Magliano, A., D´Amario, C., Remetti, R. & Bochicchio, F. 2019. Radon concentration in selfbottled mineral spring waters as a possible public health issue, Sci Rep, 9, 14252, https://doi.org/10.1038/s41598-019-50472-x

El-Araby, H., E., Soliman, H. A. & Abo-Elmagd, M. 2019. Measurement of radon levels in water and the associated health hazards in Jazan, Saudi Arabia. Journal of Radiation Research and Applied Sciences, 12(1), pp. 31-36, https://doi.org/10.1080/16878507.2019.1594134

Fakhri, Y., Mahvi, A. H., Langarizadeh, G., Zandsalimi, Y., Amirhajeloo, L. R., Kargosha, M., Moradi, M., Moradi, B. & Mirzaei, M. 2016. Effective dose of radon 222 bottled water in different age groups humans: Bandar Abbas City, Iran. Glob. J. Health Sci. 8(2), pp. 64-71, https://doi.org/10.5539/gjhs.v8n2p64

Geological Atlas of Serbia 2002. Ministry of Environment and Spatial Planning Republic of Serbia.

ICRP (2010). Lung Cancer Risk from Radon and Progeny and Statement on Radon. ICRP Publication 115, Ann. ICRP 40(1).

Isinkaye, M. O., Matthew-Ojelabi, F., Adegun, C. O., Fasanmi, P. O., Adeleye, F. A. & Olowomofe, O. G. 2021. Annual effective dose from 222Rn in groundwater of a Nigeria University campus area. Appl Water Sci.11., https://doi.org/10.1007/s13201-021-01417-1.

Kendall, G. M. & Smith, T. J. 2002. Doses to organs and tissues from radon and its decay products. J. Radiol. Prot. 22(4), pp. 389-406, DOI: 10.1088/0952-4746/22/4/304

Khandaker, M. U., Baballe, A., Tata, S. & Adamu, M. A. 2020. Determination of radon concentration in groundwater of Gadau, Bauchi State, Nigeria and estimation of efective dose. Radiat Phys Chem. 178, 108934. https://doi.org/10.1016/j.radphyschem.2020.108934

Kumar, M., Kumar, P., Agrawal, A. & Sahoo, B. K. 2022. Radon concentration measurement and effective dose assessment in drinking groundwater for the adult population in the surrounding area of a thermal power plant. J Water Health 20(3), pp. 551-559, https://doi.org/10.2166/wh.2022.265

Mehnati, P., Doostmohammadi, V., & Jomehzadeh, A. 2022. Determination of Rn- 222 concentration and annual effective dose of inhalation in the vicinity of hot springs in Kerman province, southeastern Iran. International Journal of Radiation Research, DOI:10.52547/ijrr.20.1.32

Pavlović, A. M. 2019. Geographical regions of Serbia II - Mountain-basin-valley macroregion. Faculty of Geography, University of Belgrade. Belgrade

RAD7 RAD H2O, Radon in Water Accessory, DURRIDGE Co., USA

Ravikumar, P. & Somashekar, R. K. 2014. Determination of the radiation dose due to radon ingestion and inhalation.

Int. J. Environ. Sci. Technol., 11(2), pp. 493-508, DOI: 10.1007/s13762-013-0252-x

Rožmarić M, Rogić M, Benedik L, Strok M. 2012. Natural radionuclides in bottled drinking waters produced in Croatia and their contribution to radiation dose. Sci Total Environ., 437, pp. 53-60. https://doi.org/10.1016/j.scitotenv.2012.07.018

Somlai, K., Tokonami, S., Ishikawa, T., Vancsura, P., Gaspar, M., Jobbagy, V., Somlai, J. & Kovacs, T. 2007. Rn-222 concentrations of water in the Balaton highland and in the southern part of Hungary, and assessment of the resulting dose. Radiat. Measur. 42(3), pp. 491-495, https://doi.org/10.1016/j.radmeas.2006.11.005

SORS 2023. Population Census. Statistical Office of Republic of Serbia. Belgrade.

Stevanović, V., Gulan, Lj., Milenković, B., Valjarević, A., Zeremski, T. & Penjišević, I. 2018. Enviromental risk assessment from radioactivity and heavy metals in soil of Toplica region, South Serbia. Environmental Geochemistry and Health, 40, pp. 2101-2118, https://doi.org/10.1007/s10653-018-0085-0

Todorović, N., Nikolov, J., Forkapić, S., Bikit, I., Mrdja, D., Krmar, M. & Vesković, M.2012a. Public exposure to radon in drinking water in Serbia. Appl. Radiat. Isot., 70(3), pp. 543-549, https://doi.org/10.1016/j.apradiso.2011.11.045

UNSCEAR (1993). United Nations Scientific Committee on the Effects of Atomic Radiation. Sources and effects of ionizing radiation, united nations scientific committee on the effects of atomic radiation ,Annex A report: report to the general assembly, with scientific annexes.

UNSCEAR (2000). United Nations Scientific Committee on the effects of Atomic Radiation Report to general assembly with scientific annexes. Appendix B: 97-105, New York. https://www.unscear.org/docs/publications/2000/UNSCEAR_2000_Annex-B.pdf

USEPA (1999). US Environmental Protection Agency Radon in drinking water health risk reduction and cost analysis. EPA Federal Register 64 (USEPA, Office of Radiation Programs), Washington, DC. https://archive.epa.gov/water/archive/web/html/hrrcafr.html

Valjarević, A., Srećković-Batoćanin, D., Valjarević, D. & Matović, V. 2018. A GIS based method for analysis of a better utilization of thermal-mineral spring in municipality of Kuršumlija (Serbia). Renewable and Sstainable Energy Reviews 9, pp. 948-957, https://doi.org/10.1016/j.rser.2018.05.005

Valjarević, A., Živković, D., Valjarević, D., Stevanović, & Golijanin, J. 2014. GIS analysis of land cover changes on the territory of the Prokplje municipality. The Scientific World Journal, 12, pp. 1-8, https://doi.org/10.1155/2014/805072.

Vogeltanz-Holm, N. & Schwartz, G. G. 2018. Radon and lung cancer: what does the public really know? J. Environ. Radioactiv. 192, pp. 26-31, DOI: 10.1016/j.jenvrad.2018.05.017

Vučković, B., Mrazovac Kurilić, S., Nikolić-Bujanović, Lj., Todorović, N., Nikolov, J., Živković Radovanović, J., Milošević, R. & Jokić, A. 2022. Radon in drinking water

from alternative sources of water supply in the north Kosovo, Radiation Protection Dosimetry, pp. 1-8, https://doi.org/10.1093/rpd/ncac222

WHO (2004). World Health Organisation Guidelines for drinking water quality. 3rd ed. WHO Press, Geneva (2004). https://www.who.int/water_sanitation_health/dwq/GDWQ2004web.pdf

Xinwei, L. 2006. Analysis of radon concentration in drinking water in Baoji (China) and the associated health effects, Radiation Protection Dosimetry, 121(4), pp. 452-455, https://doi.org/10.1093/rpd/ncl048

Zalewski, M., Karpinska, M., Mnich, Z., Kapala, J. & Zalewski, P. 2001. Study of 222Rn concentrations in drinking water in the north-eastern hydroregions of Poland.Journal of Environmental Radioactivity, 53(2), pp. 167-173, https://doi.org/10.1016/S0265-931X(00)00122-3

Available Online

This journal is available online. Please visit http://www.bulletinnsr.com to search and download published articles.